LAMINAR FLOW SEPARATION
IN
A CONSTRICTED CHANNEL

BY

Najdat Nashat Abdulla

A DISSERTATION

Submitted to
Michigan State University
in partial fulfillment of the requirement
for the degree of

DOCTOR OF PHILOSOPHY

Department of Mechanical Engineering

1987

ABSTRACT

LAMINAR FLOW SEPARATION IN A CONSTRICTED CHANNEL

By

Najdat Nashat Abdulla

The two-dimensional, incompressible, laminar flow in the entrance region of a channel with and without constrictions (in the form of forward, backward and finite steps) has been analyzed numerically for various step-to-channel height ratios, step lengths and step positions for Reynolds numbers up to 2000, based on the channel height.

A stream function-vorticity formulation is used in conjunction with a finite-difference, over-relaxation method utilizing accelerating parameters to solve the full Navier-Stokes equations which describe the steady flow. The power of the method is contained in the structure of the finite-difference equations, which, for all Reynolds numbers, yields a diagonally dominant system of linear, algebraic equations. This avoids the numerical instability of the finite-difference equations at high Reynolds numbers.

The stream function, vorticity, streamwise velocity and pressure are reported at each grid point. The inviscid-core region and profile-development region, which form the entrance length, are identified for various Reynolds numbers and inlet velocity profiles. In addition, separation and reattachment points are obtained for various step-to-channel height ratios, step lengths and positions for the constricted channel. Furthermore, the convergence domain for the successive over-relaxation method and the optimum values of

accelerating parameters, which minimize the computing time, are obtained.

The centerline velocity and entrance length for the channel without a constriction are compared with the results obtained by approximate techniques. Also, the separation and reattachment points for a constricted channel are compared with both numerical and experimental results.

A DEDICATION

This thesis is dedicated to my wife, Najah, who has displayed great patience and tolerance during the preparation of this study and without her encouragement and confidence this work would not have been completed. It is also dedicated to my son, Zayd and daughter, Noora.

ACKNOWLEDGMENT

The author wishes to express his sincere thanks to his major professor Dr. Merle C. Potter for his valuable guidance throughout this study. The author's graduate work has been made possible through his patience, understanding and personal interest.

Special thanks to Dr. Richard W. Bartholomew for his constructive comments about numerical technique used in this study.

Thankful acknowledgment is extended to Dr. John Lloyd, chairman, Mechanical Engineering Department and to other members of the Guidance Committee: Dr. Craig Somerton and Dr. Robert H. Wasserman.

Thanks are also extended to Carol Bishop for her accuracy and neatness in typing this dissertation.

TABLE OF CONTENTS

LIST OF TABLES

Table

[illegible]. We

[illegible]. We

[illegible]. We

[illegible]. Fa

Table		Page
32.	Weighting factor (KS) vs. computing time, h-1/20	94
33.	Weighting factor (KV) vs. computing time, h-1/15	95
34.	Weighting factor (KV) vs. computing time, h-1/20	95
35.	Factors of reduction in the computing time	96

LIST OF FIGURES

Figure | Page

Figure		Page

Figure Page

NOMENCLATURE

a	Step height
b	Dimensionless vertical coordinate
FS	Optimum value of the over-relaxation factor for stream function
FV	Optimum value of the over-relaxation factor for vorticity
g	Gravity
h	Mesh size equal in both X- and Y-directions
H	Channel height
K	Number of iterations
KS	Weighting factor for the stream function
KV	Weighting factor for the vorticity
L	Step position
p	Pressure
p_k	Dimensionless kinematic pressure
Re, $(Re)_H$	Reynolds number based on the channel height
$(Re)_a$	Reynolds number based on the step height
u	Dimensionless streamwise velocity component
u_c	Dimensionless centerline velocity
U_o	Average uniform velocity at channel inlet
v	Dimensionless normal velocity component
X	Streamwise coordinate
x	Dimensionless streamwise coordinate (X/H)
Xs	Upstream separation point

Xr	Downstream reattachment point
Y	Normal coordinate
y	Dimensionless normal coordinate (Y/H)
Ys	Downstream separation point
Yr	Upstream reattachment point
ψ	Dimensionless stream function
ω	Vorticity
ρ	Fluid density
ν	Fluid kinematic viscosity
ϵ	Difference between two values of stream function or vorticity

CHAPTER 1

INTRODUCTION

1.1 Background

The study of incompressible fluid flow through an entrance region of a pipe or a duct and through constricted channels is of considerable practical significance. The applications of such flows are quite numerous; they include fluid flows found in physiology (flow through blood vessels and lung airways, flow separation due to build-up of deposits on artery walls, and measurements of blood pressure using a cuff on the arm), and in machinery (flow in the vicinity of junctions and valves).

The Navier-Stokes equations, which are considered to describe the fluid motion of interest, are nonlinear. Because of this nonlinearity, some difficulties have arisen in numerical as well as in analytical studies. One of the greatest difficulties with the numerical studies is the problem of divergence of the iterative methods at high Reynolds numbers. Since an analytical solution of the actual problem is extremely difficult, if not impossible, a number of assumptions together with a numerical solution may be employed to obtain approximate results.

Since the pioneering work of Prandtl early in this century, boundary-layer theory has provided the principal basis for the theoretical analysis of laminar flow phenomena near solid boundaries.

It is now possible to conduct a more rigorous analysis of laminar flow; the development of high-speed computers and sophisticated numerical techniques permit the solution of the complete set of field equations describing a particular fluid motion.

1.2 Entrance Region of a Channel

In the entrance region of a channel, our primary concern is with changes in the streamwise velocity component. The entrance region extends a considerable distance downstream and may be quite significant in high Reynolds number flows. It may take up to 100 gap widths before a fully developed flow is produced. So, in any study of a high Reynolds number channel flow, the assumption of a fully developed velocity profile implicitly assumes a substantial length of entrance flow that must be accounted for. Many channels, ducts, or pipes are not sufficiently long to allow developed flow to occur. A variety of methods have been employed for the determination of the flow characteristics in the entrance region as reported in the large number of references in the literature.

1.3 Methods of Solving the Entrance Flow Problem

In general, four different methods have been applied to solve the entrance flow. These methods will be outlined in this section.

1.3.1 The Integral Method

An early analysis of the entrance region in a tube was presented by Schiller [1]. The entrance region was considered to be composed of two zones: a boundary layer developing on the wall and an inviscid core. The core flow terminated as the boundary layers merged resulting in a fully-developed parabolic profile. Subsequent

modifications to this integral method have been presented elsewhere [2,3].

Mohanty and Asthano [4] investigated the flow in the entrance region of a pipe. They solved the boundary-layer equations in the inlet region and the Navier-Stokes equations, with order-of-magnitude analysis, in the "filled region" using a fourth-degree velocity profile. This work was the first to recognize that the core region terminated with a non-parabolic profile; a "filled region" separated the core region from the developed flow region.

1.3.2 Axially Patched Solutions

In this method, initially used by Schlichting [5,6], the entrance region is divided into two regions. Near the entrance a boundary layer model is used and an approximate solution is obtained in terms of a perturbation of the Blasius boundary layer solution. In the region where the flow is nearly fully developed, the velocity profile is approximated in terms of a small perturbation to the fully developed parabolic profile. The two solutions are then matched at some approximate streamwise location.

Van Dyke [7] improved Schlichting's solution near the entrance by an upstream expansion whose first approximation is the leading edge solution for a semi-infinite plate, which had been presented by Davis [8]. The displacement effect of the boundary layer on the inviscid core is accounted for in this higher order approximation.

1.3.3 Linearization of the Momentum Equation

The nonlinear inertia terms in the x-component Navier-Stokes equations were linearized and the solution to the resulting equation found in a method proposed by Langhaar [9]. Sparrow, et.al. [10], who

followed the linearization method of Langhaar, solved both channel and circular pipe flow.

Lundgren [11] employed the linearized equations of motion to predict the incremental pressure drop due to the entrance region for ducts of arbitrary cross-section.

Morihara and Cheng [12] investigated the entrance flow in a channel between semi-infinite parallel plates using a quasi-linearization method.

Recent work by Du Plessis [13], who followed the linearization method of Lungren [11], solved a channel flow with an arbitrary inlet velocity profile.

1.3.4 Finite Difference Methods

The Navier-Stokes equations have been solved by finite difference methods for flow inside circular pipes and for parallel plate channels. In these solutions, the assumptions inherent in boundary-layer theory have been used; that is, both the streamwise velocity derivative $\partial^2 u/\partial x^2$ and the pressure gradient $\partial p/\partial y$ normal to the plate have been neglected.

In a pipe flow, Christiansen and Lemmon [14] numerically studied the flow in the entrance region of a circular pipe with a uniform inlet velocity profile. They solved boundary layer equations near the entrance and restricted the equations of motion in cylindrical coordinates to conditions such that the flow is independent of time, the radial component of the equations of motion is negligible, any angular motion is negligible, and the flow is independent of any existing body force field far from the entrance.

Robert W. Hornbeck [15] analyzed the laminar flow of an incompressible fluid in the inlet of a pipe up to Reynolds number of

1.3. He
equation
This is
marching
position
point.

magneto-
that.
conduct
that wa
usual b

region
to solv
neglect

differe
maintai
pressur
been li

the ste
distanc
inclin
paraboi
They ma
the ea
partic

0.9. He solved an approximate form of the governing differential equations by neglecting the axial molecular transport of momentum. This is accomplished numerically by means of a finite-difference marching procedure in which the velocities and pressure at any axial position in the pipe are determined by using values upstream from the point.

In a channel flow, Hwang and Fan [16] investigated a laminar magneto-hydrodynamic flow in the entrance region of a flat rectangular duct. They assumed that the duct walls are electrically non-conducting, with a uniform magnetic field imposed perpendicular to the duct walls. They employed a finite-difference method to solve the usual boundary-layer equations.

Bodia and Osterle [17] investigated the flow in the inlet region of a straight channel. They used finite-difference techniques to solve an approximate form of the governing differential equation by neglecting the axial diffusion of vorticity.

Several publications have described the use of finite difference methods to solve the full Navier-Stokes equations, maintaining the axial transport of vorticity terms as well as the pressure gradient terms in the radial direction; these however, have been limited to relatively low Reynolds numbers.

Vrentas, Duda and Bargeron [18] analyzed the development of the steady, laminar flow of an incompressible Newtonian fluid in the entrance of a circular tube at a Reynold number of 250. The circular conduit is considered to be infinite in extent with a fully developed parabolic velocity profile existing far downstream from the entrance. They numerically studied the effect of axial diffusion of vorticity on flow development in circular conduits, by solving the boundary-layer equations and the complete equations of motion.

F

Stokes eq

region of

numbers.

W

section o

the compl

new indep

exponenti

problem.

.. Sepa

T

Navier-St

have been

external

laminar f

placed in

velocity

I

concerns

fluids, n

obtained

I

near-fiel

channel r

A

now is i

ifica

Friedman, Gillis, and Liron [19] solved the complete Navier-Stokes equations for the steady-state, axisymmetric flow in the inlet region of a straight circular pipe at low and moderate Reynolds numbers.

Wang and Longwell [20] studied laminar flow in the inlet section of parallel plates at a Reynolds number of 300. They solved the complete Navier-Stokes equations. A transformation from x to a new independent variable η to make the boundaries finite and an exponential solution are used for a numerical treatment of the problem.

1.4 Separated Flows

There have been numerous computational studies made of the Navier-Stokes equations for laminar flow involving separation. These have been two-dimensional or axisymmetric steady flows in both external and internal flow situations at Reynolds numbers such that laminar flow exists. For constricted flows, constriction was always placed in the fully-developed flow region with an initial parabolic velocity profile upstream of the constriction.

In external flows, the most classical type of such problems concerns the fluid motion past a bluff body. For incompressible fluids, numerical solutions for the flow around bluff bodies have been obtained by many authors, over various ranges of Reynolds numbers.

In constricted flows, such as flow through a channel, the near-field motions due to a constriction or an enlargement of the channel resulting in a separated flow are of particular interest.

An understanding of laminar separation in a channel or pipe flow is incomplete at this time. Approximations have resulted in significant errors in the predicted flows.

1.5 Math

G

predictio

and react

sections.

1.5.1 M

limits o

consider

laminar.

the inne

valid ne

intermed

entrance

the for

the gove

boundary

position

of the b

structur

of an i

differen

with an

displace

separati

numerica

1.5 Methods of Solving the Constricted Flow Problem

Generally, three methods have been utilized to obtain predictions for the separated streamline shape and for the separation and reattachment points. Each method is discussed in the following sections.

1.5.1 Matched Asymptotic Expansions

Using the method of matched asymptotic expansions (MAX), two limits of the solutions to the Navier-Stokes equations may be considered as the Reynolds number becomes large while still remaining laminar. The outer solution describes the inviscid core flow, while the inner solution satisfies the surface boundary conditions and is valid near the wall. These two solutions are then matched in an intermediate range.

Using MAX, Smith [21] studied the influence of the uniform entrance conditions on a steady, laminar flow through a constricted tube for large Reynolds numbers. A linearized asymptotic solution of the governing equations of the inviscid core flow and the two viscous boundary layers is used to determine the influence of the size and position of the constriction. Effects of the constriction's position on the boundary layers were described.

In another study, Smith [22] constructed a triple-deck structure in the vicinity of the separation point for a laminar flow of an incompressible fluid streaming past a smooth surface. A finite-difference approach was used to solve the boundary layer equations with an elliptic relation between the unknown pressure and streamline displacement within the triple-deck structure. Comparisons with the separating fluid motion in a similarly constricted flow, determined numerically from an approximate form of the Navier-Stokes equations by the o

lower

towns

the ve

Dennis and Chang [23], and obtained experimentally by Dimopoulos and Hanratty [24], give some support to the triple-deck description.

In still another study, Smith [25] described the effects on the otherwise unidirectional flow field within a long, straight, rigid-wall channel suffering a severe asymmetric constriction at some downstream station. The flow is considered to be laminar, steady, and fully-developed with a large Reynolds number. A numerical approach, similar to that used by Smith and Stewartson [26], is adopted for the boundary layer equations which describe the nonlinear flow of the lower and upper viscous zones. Free streamline theory is used for the inviscid portion of the flow. Both upstream and downstream separation regions were found. The upstream separation point was found to move further upstream as the upstream slope of the constriction was increased.

In a fourth study, Smith [27], using free-stream theory, located the separation point in the axisymmetric flow of an incompressible fluid through a pipe suffering a severe constriction, with incoming Poiseuille flow. The upstream viscous separation, the downstream eddy, and the drag on the constriction were considered for the very severe constriction. The limiting solution in the upstream region was found using a numerical solution of Euler's equations of motion. Qualitatively, all the flow patterns given by the approximate solutions and the experimental data tend to support the limiting solution.

Smith and Duck [28] extended the study of laminar flow in a constricted channel by utilizing free streamline theory to describe separation and reattachment of a steady, plane flow at high Reynolds numbers through a channel suffering a severe non-symmetric constriction. A numerical approach is used to solve the non-linear equatio

separat

place a

the con

The fir

constri

second

constri

measure

1.5.2

used to

approxi

the Nav

dimensi

except

Reynolds

and far

Navier-S

component

vorticit

obtained

analytic

solution

restri

tensio

attach

equations, using a Runge-Kutta scheme, for the positions of the separation and reattachment points. The upstream separation takes place asymptotically far ahead of the constriction. The separation on the constriction is described by Smith's [22] triple-deck structure. The first reattachment, described by an inviscid process near the constriction surface, induces only small reversed velocities; the second reattachment takes place at a large distance downstream of the constriction. Discrepancies between these predictions and the measurements of Blowers [29] are noted.

1.5.2 Numerical Methods

On the numerical side, the Navier-Stokes equations have been used to describe the constricted flow, and have been solved approximately using numerical methods. Dennis and Smith [30] solved the Navier-Stokes equations numerically for the flow of a two-dimensional, laminar flow through a channel suffering an asymmetric abrupt decrease of its width in the form of a semi-infinite step, for Reynolds numbers up to 2000. Poiseuille flow is assumed far upstream and far downstream of the step. In the numerical technique, the Navier-Stokes equations are separated into two equations; by suitable exponential expansions, an approximate value for stream function and vorticity is obtained at internal grid points. Good agreement was obtained for the upstream separation and the wall vorticity with the analytical solutions of Smith [27].

Hung and Macagno [31] have obtained a finite-difference solution of the Navier-Stokes equations for flow in a channel with a symmetric sudden expansion. The velocity profile upstream of the expansion is taken to be parabolic. They found that the point of reattachment and the distance of the center of the eddy measured from the expa

Morihara

I

right-an

for the

A

a backst

out by N

I

finite-e

channel

as astea

difficul

equation

solution

the deta

agreemen

with con

was obtai

W

of stead

fluid tu

Stokes e

governing

that of (

constri

tube and

fields

deliber

the expansion are linear with Reynolds number. Results obtained by Morihara [32] for the above problem also show a linear trend.

Hurd and Peters [33] numerically studied the motion through a right-angle bend in a channel. They assumed an approximate solution for the Navier-Stokes equations.

A numerical investigation of separated flow in a channel with a backstep, or with single or multiple obstructions, has been carried out by Nallasamy [34].

Ralph [35] solved the Navier-Stokes equations using the finite-element method for a two-dimensional fluid flow in a straight channel for various contraction ratios up to Reynolds number of 100. An unsteady, quasi-linear approach is used to circumvent the difficulties associated with the nonlinearity of the governing equations. A steady-state solution is assumed when the time-dependent solution becomes convergent. The flow patterns and separation regions are detailed for a wide range of Reynolds numbers. Reasonable agreement with the results of Lee and Fung [36], who used a method which combines conformal mapping with a finite-difference technique, was obtained.

Deshpande, Giddens and Mabon [37] numerically solved the case of steady flow through a localized axisymmetric constriction in a rigid tube for Reynolds numbers up to 200. The continuity and Navier-Stokes equations, in cylindrical coordinates, are taken as the governing relations. The numerical scheme employed closely follows that of Gosman [38] with modifications to treat the curved boundaries; a constriction similar to that employed in the experimental study by Young and Tsai [39] is used. Separation regions were detailed up to a Reynolds number of 100. The results agreed well with those determined experimentally by Young and Tsai [39] for the separation location and

pressure drop across the constriction. The reattachment prediction was not in good agreement.

A more accurate solution of the Navier-Stokes equations is given by Greenspan [40] who numerically investigated a two-dimensional, laminar flow through a channel with a constriction formed by a finite step on one wall. Boundary conditions consisted of a parabolic velocity profile upstream, and a horizontal flow and constant pressure downstream. Upstream and downstream separation regions were detailed up to a Reynolds number of 1000. In this study, a coarse mesh size is used and consequently an upstream vortex for Reynolds numbers less than 200 was not observed. The problem is modified by eliminating the downstream step to reduce computing time.

Friedman [41] studied the same problem of Greenspan [40] but with a corrected sign in the downstream boundary condition. A numerical approach, similar to that developed by Greenspan [40], is used for the small Reynolds number analysis, and a linearized numerical technique for moderate and high Reynolds numbers reduces the computing time needed for convergence. A fine mesh size is used and the upstream vortex is detailed up to a Reynolds number of 500.

Andreas and Mark [42] examined the sudden expansion (symmetric) of a laminar flow in a two-dimensional channel in the limit of large Reynolds number. Boundary layer equations are solved numerically using a finite-difference technique for selected values of λ, the ratio of the upstream channel half-width to the step height. Velocity profiles, the streamline pattern and the wake length are found for values of λ in the range of (0.3-19) when the inlet velocity profile is parabolic.

Taylor and Ndefo [43] studied the viscous incompressible flow in a two-dimensional channel with a backstep (asymmetric) for Reynolds numbers

non-dime

coupled

profiles

and rea

consider

step he

incompre

dependen

with and

a Reynol

point mo

corner t

and desc

number

been obt

velocity

detailed

the dist

linearly

that a s

Newton's

solution

the sha

the obt

smaller

numbers up to 100 using a splitting method. In this technique, the two-dimensional, unsteady Navier-Stokes equations are reduced to a coupled set of one-dimensional, unsteady flow equations. Velocity profiles, streamline patterns, the pressure gradient and separation and reattachment points are obtained for the range of Reynolds numbers considered. The results show that separation occurs at about 2/3 the step height.

Roache and Mueller [44] obtained solutions for both incompressible and compressible laminar separated flows using time-dependent finite-difference equations. These include backstep flow with and without splitter plates, and flow over square cavities up to a Reynolds number of 100. The results indicate that the separation point moves down from the conjectured limit position at the sharp corner toward a Stokes flow limit as the Reynolds number is decreased.

Kitchens [45] solved the steady-state, Navier-Stokes equations and described the flow field near a square, two-dimensional protuberance immersed in a plane Couette flow. Numerical results have been obtained for Reynolds numbers between 1 and 200 based on plate velocity and protuberance height. The downstream separation region is detailed up to a Reynolds number of 200. The reattachment length and the distance of the center of the eddy from the protuberance vary linearly with the Reynolds number.

Recently, Frank and Andreas [46] studied steady, laminar flow past a sudden channel expansion at large Reynolds number. A global Newton's method was used to obtain accurate finite-difference solutions for uniform inflow to several sudden expansion geometries. Eddy shapes and length, the pressure gradient and streamline contours were obtained. The results suggest that for uniform inflows and smaller values of the expansion ratio, the eddy length will no longer increase linearly with Reynolds number when the latter is sufficiently large.

Kwon and Pletcher [47] studied the laminar and turbulent incompressible flow in a two-dimensional channel with a sudden expansion by using viscous-inviscid iteration techniques. The viscous flow solutions are obtained by solving the boundary-layer equations using a finite-difference scheme; the inviscid flow is computed by numerically solving the Laplace equation for the stream function using an Alternating-Direction Implicit Method (ADI). The viscous and inviscid solutions are matched interatively along displacement surfaces. The flow fields were detailed up to a Reynolds number of 500 and for a ratio of step height to channel inlet height of 0.0664.

1.5.3 Experimental Methods

On the experimental side, various experimental investigations were performed in a wind tunnel to obtain a better understanding of fluid flow following separation including reattachment and the redevelopment of the flow following reattachment in this regime. Several experimental investigations for the laminar separating flow over back steps have been reported.

Mueller and O'Leary [48] have done an experimental as well as a numerical study in a channel with a back step up to a Reynolds number of 200. Their results show that for Reynolds numbers in the range of 50 to 200, the reattachment length and the distance of the center of the eddy from the step vary linearly with the Reynolds number, confirming the numerical results presented earlier.

Goldstein, et.al., [49] investigated the flow over a back step with a laminar free shear layer until reattachment. The experiments include visual observations of smoke filaments. Velocity profiles,

reattachment points, and the momentum thickness are reported over a range of ratio of the step height to the wind tunnel height of 0.023 to 0.0625.

Honji [50] investigated the incompressible starting flow past a back step at Reynolds numbers less than 500 by means of flow visualization techniques. The distance between the step and the point of reattachment on the downstream wall was found to increase linearly with time at intermediate stages of the flow development.

Leal and Crivos [51] investigated the effect of base bleed on a recirculating wake behind a bluff body under conditions of a laminar shear layer at the separation point and a steady flow field. The streamline pattern in the wake region was observed photographically by means of a bubble-tracer technique; in addition, a number of quantities, such as the physical dimensions of the wake region, were measured.

Sinha, et.al., [52] investigated the incompressible laminar flow over back steps by flow visualization over a range of step to channel height ratios of 0.02 to 0.08. The flow fields were detailed up to a Reynolds number of 1000. The experimental results indicate that the reattachment length increases linearly with Reynolds number as long as the reattachment is laminar.

1.6 Description of the Present Work

The influence of a non-parabolic upstream velocity profile on the fluid motion in the vicinity of a step may be considerable in high Reynolds number motion. In many cases of high Reynolds number channel or pipe flow, the upstream assumption of a fully-developed velocity profile demands a substantial length and may render the study inapplicable in practice. In seeking to understand realistic situations there arose a need, therefore, for an investigation of the effects that the entrance conditions may have on the flow in the vicinity of a constriction.

In the entrance region the derivative $\partial^2u/\partial x^2$ is small relative to $\partial^2u/\partial y^2$ but it may influence the solution; the pressure gradient in the y-direction is also small but the y-component momentum equation may not be negligible. The solution of the complete set of the Navier-Stokes equations, without any simplifying assumption is desirable in the solution of the entrance flow problem.

The purposes of the present work are first, to numerically investigate the steady, two-dimensional, Newtonian, incompressible laminar flow in the entrance region of a channel using the full Navier-Stokes equations. The two regions making up the entrance region are to be quantified; these include the <u>inviscid-core region</u>, in which a viscous layer is assumed to exist on the wall, and the <u>profile-development region</u>, in which viscous effects completely dominate the channel, as shown in Figure 1. Second, a constriction in the form of a step, will be positioned in the inviscid core, in the profile-development region, and in the fully developed region of the channel flow, as shown in Figures 2 & 3. Both a finite step and a semi-infinite step will be considered. The resulting flow will be investigated numerically to identify the separation and reattachment points using the full Navier-Stokes equations. Various degrees of severity will be considered by using different heights for the step. A wide range of Reynolds numbers will be considered. The full Navier-Stokes equations will be expressed in terms of a stream function and the vorticity and solved by a finite-difference scheme. A numerical solution will be utilized which does not invoke the boundary-layer assumptions and therefore will represent an exact solution in the sense

negle

govern

which

equat

posse

spring

instal

optim

funct

minim

and th

sense that no terms in the x- and y-momentum equations will be neglected. Also, no approximations or exponential solutions for the governing equations are assumed. A vorticity-stream function scheme, which utilizes a finite-difference approximation to the Navier-Stokes equations and has second-order accuracy in the whole flow field, possessing conservative and transportive properties and utilizing upwind differencing for advection terms, avoids the numerical instability of an iterative solution at high Reynolds numbers. Third, optimum over-relaxation values and the weighting factors for stream function and vorticity values will be determined; these factors minimize the spectral radius of the over-relaxation iteration matrix and thereby maximize the rate of convergence of the method.

CHAPTER 2

MATHEMATICAL FORMULATION

2.1 Primary Flow

For duct flows, which are completely bounded by solid surfaces, the flow is assumed to be uniform at the duct entrance with average velocity U_0. Because of the no-slip condition, the velocity at the wall must be zero along the entire length of the duct. A boundary layer develops along the walls of the channel due to the retarding shear force of the solid surface on the flow; thus, the speed of the fluid in the neighborhood of the surface is reduced. At successive sections along the pipe the viscous effects of the solid surface diffuse farther and farther out into the flow.

Eventually, the viscous effects dominate the entire flow thereby terminating the inviscid core region. Viscous effects finally result in a fully developed velocity profile: a parabolic velocity profile in a pipe or a wide channel. This defines the end of the entrance region.

The velocity profiles of a laminar flow in a channel entrance, or in a channel with a constriction in the form of a step, undergo a change from an assumed uniform profile at the inlet to that of a fully-developed, parabolic profile at a location far downstream. Both a finite step (sudden contraction followed by a sudden expansion) and a semi-infinite step (sudden contraction or a sudden expansion) are consi

semi-

upstr

occur

while

downs

the R

steady

Newton

the d

Fluid

Chang

considered. The straight two-dimensional channel, and a channel with semi-infinite and finite steps, are shown in Figures 1, 2 and 3.

In the case of a sudden contraction, the flow separates upstream for sufficiently large Reynolds numbers. Flow separation occurs in the case of a sudden enlargement on the downstream side, while in the case of a finite step it may occur upstream as well as downstream. Basically, the size of the separation region depends on the Reynolds number Re, step height a, length w and position L.

2.2 Governing Equations

For the entrance configuration described above we consider the steady state, two-dimensional, incompressible, laminar flow of a Newtonian fluid with constant physical properties.

The dimensionless streamwise and normal velocity components (u,v) are referenced to the average velocity U_0 at the inlet, p_k is the dimensionless kinetic pressure referenced to $\rho U_0^2/2$, where ρ is the fluid density, and the streamwise and normal dimensionless coordinates (x,y) are normalized with H, the height of the channel. The dimensionless Navier-Stokes equations are

$$u \frac{\partial u}{\partial x} + v \frac{\partial u}{\partial y} = - \frac{\partial p_k}{\partial x} + \frac{1}{Re} \left(\frac{\partial^2 u}{\partial x^2} + \frac{\partial^2 u}{\partial y^2} \right) \tag{2.2.1}$$

$$u \frac{\partial v}{\partial x} + v \frac{\partial v}{\partial y} = - \frac{\partial p_k}{\partial y} + \frac{1}{Re} \left(\frac{\partial^2 v}{\partial x^2} + \frac{\partial^2 v}{\partial y^2} \right) \tag{2.2.2}$$

where the Reynolds number is represented by

$$Re = \frac{HU_0}{\nu} \tag{2.2.3}$$

In addition, the pressure term includes the body force term; that is

$$p_k = p + \frac{gH}{U_0^2} b \tag{2.2.4}$$

where b is a dimensionless vertical coordinate. The quantity (gH/U_0^2) will not play a role in this problem since there are no pressure boundary conditions that would demand the imposition of Eq. (2.2.4). The continuity equation is

$$\frac{\partial u}{\partial x} + \frac{\partial v}{\partial y} = 0 \tag{2.2.5}$$

Since it proves to be more convenient to work in terms of a stream function and vorticity, the dimensionless stream function $\psi(x,y)$ is introduced in the usual manner:

$$u = \frac{\partial \psi}{\partial y} \tag{2.2.6}$$

$$v = - \frac{\partial \psi}{\partial x} \tag{2.2.7}$$

It is evident from Eqs. (2.2.6) and (2.2.7) that the stream function satisfies the continuity equation identically. Furthermore, for this plane flow field, the only non-zero component of the vorticity is

$$\omega = \frac{\partial v}{\partial x} - \frac{\partial u}{\partial y} \tag{2.2.8}$$

Combining the definition of vorticity and the velocity components in terms of the stream function, and cross-differentiating the Navier-Stokes equations to reduce the number of equations and eliminate the pressure terms, a new set of equations is obtained with independent variables ψ and ω:

$$\frac{\partial^2\psi}{\partial x^2} + \frac{\partial^2\psi}{\partial y^2} = -\omega \tag{2.2.9}$$

$$\frac{\partial^2\omega}{\partial x^2} + \frac{\partial^2\omega}{\partial y^2} + \mathrm{Re}\left(\frac{\partial\psi}{\partial x}\frac{\partial\omega}{\partial y} - \frac{\partial\psi}{\partial y}\frac{\partial\omega}{\partial x}\right) = 0 \tag{2.2.10}$$

Equation (2.2.9) is a Poisson equation, an elliptic, partial differential equation. Equation (2.2.10), which represents the steady Navier-Stokes equations, is also an elliptic partial differential equation in terms of ω if the stream function terms are assumed to be known coefficients. The numerical solution technique selected treats the equations such that the stream function derivatives in Eq. (2.2.10) are known; hence, this equation will be considered to be elliptic in the vorticity ω. These two equations are to be solved in a given region subject to the condition that the values of the stream function and the vorticity, or their derivatives, are prescribed on the boundary of the domain.

2.3 Boundary Conditions

2.3.1 The Channel Entrance with no Constriction

The boundary condition for the two-dimensional channel, shown in Figure 1, are stated in the following:

1. The no-slip condition is applicable at the walls:

   lower wall AB: $u(x,0) = 0,\ v(x,0) = 0$ (2.3.1.1)

   upper wall CD: $u(x,1) = 0,\ v(x,1) = 0$ (2.3.1.2)

2. Two cases for the entrance velocity distribution are considered:

a) Uniform velocity profile:

$$u(0,y) = 1, \quad v(0,y) = 0 \qquad (2.3.1.3)$$

b) Actual velocity profile:

$$u(0,y) = f(y), \quad v(0,y) = 0 \qquad (2.3.1.4)$$

where f(y) is specified from actual data, as given in Table 1.

3. The flow approaches the fully-developed parabolic channel flow far downstream ($x>L_E$):

$$u(x,y) = 6y - 6y^2, \quad v(x,y) = 0 \qquad (2.3.1.5)$$

For the problem under consideration to be completely specified, the stream function and the vorticity must now be specified on all boundaries. For the channel with and without a constriction, a vorticity condition at the solid boundaries (AB, CD in Figure 1 and AB, BC, CD, DE, EF and GH in Figures 2 and 3) is determined by using a method presented by Thom [53]: if the subscript "0" represents a mesh point on a boundary and "1" represents a neighboring mesh point on the inward normal to "0" we expand in a Taylor series as

$$\psi_1 = \psi_0 + h \left(\frac{\partial\psi}{\partial y}\right)_0 + \frac{1}{2} h^2 \left(\frac{\partial^2\psi}{\partial y^2}\right)_0 + \frac{1}{6} h^3 \left(\frac{\partial^3\psi}{\partial y^3}\right)_0 \qquad (2.3.1.6)$$

neglecting terms of higher order. But,

$$\left(\frac{\partial\psi}{\partial y}\right)_0 = u = 0 \qquad (2.3.1.7)$$

According to Eq. (2.2.9),

$$\left(\frac{\partial^2\psi}{\partial y^2}\right)_0 = - \omega_0 - \frac{\partial}{\partial x} \left(\frac{\partial\psi}{\partial x}\right) = - \omega_0 \qquad (2.3.1.8)$$

Differentiating once again results in

$$\left(\frac{\partial^3\psi}{\partial y^3}\right)_0 = - \frac{\partial\omega_0}{\partial y} \cong - \left(\frac{\omega_1 - \omega_0}{h}\right) \qquad (2.3.1.9)$$

It follows from Eqs. (2.3.1.6), (2.3.1.8), and (2.3.1.9) that at the boundary, the vorticity is related to the stream function by

$$\omega_0 = \frac{3(\psi_0 - \psi_1)}{h^2} - \frac{\omega_1}{2} \qquad (2.3.1.10)$$

where h is the mesh size equal in both the x- and y-directions.

In terms of the stream function and vorticity, the boundary conditions used to solve Eqs. (2.2.9) and (2.2.10) are:

entrance AD: $\frac{\partial\psi}{\partial x}(0,y) = 0,\ \frac{\partial\psi}{\partial y}(0,y) = 1,\ \psi(0,y) = y,$

$$\omega(0,y) = 0 \qquad (2.3.1.11)$$

lower wall AB: $\frac{\partial\psi}{\partial x}(x,0) = 0,\ \frac{\partial\psi}{\partial y}(x,0) = 0,\ \psi(x,0) = 0,$

$$\omega(x,0) = \frac{3(\psi_0 - \psi_1)}{h^2} - \frac{\omega_1}{2} \qquad (2.3.1.12)$$

upper wall CD: $\frac{\partial\psi}{\partial x}(x,1) = 0,\ \frac{\partial\psi}{\partial y}(x,1) = 0,\ \psi(x,1) = 1,$

$$\omega(x,1) = \frac{3(\psi_0 - \psi_1)}{h^2} - \frac{\omega_1}{2} \qquad (2.3.1.13)$$

exit BC: $\psi(x,y) = 3y^2 - 2y^3,\ \omega(x,y) = 12y - 6$ for $x \geq L_E$ (2.3.1.14)

2.3.2. The Channel Entrance With a Constriction

The boundary conditions, in terms of the stream function and vorticity for the two-dimensional channel with a constriction in the form of both a finite step (sudden contraction and expansion) and a semi-finite step as shown in Figures 2 and 3, which are used to solve Eqs. (2.2.9) and (2.2.10) are:

entrance AG:

uniform flow $\psi(0,y) = y$

$$\omega(0,y) = 0 \qquad (2.3.2.1)$$

parabolic flow $\psi(0,y) = 3y^2 - 2y^3$

$$\omega(0,y) = 12y - 6 \qquad (2.3.2.2)$$

lower walls AB, BC, CF, FE, EF, GH:

$$\frac{\partial\psi}{\partial x}(x,0) = 0$$

$$\frac{\partial\psi}{\partial y}(x,0) = 0 \qquad (2.3.2.3)$$

$$\psi(x,0) = 0$$

$$\omega(x,0) = \frac{3(\psi_0 - \psi_1)}{h^2} - \frac{\omega_1}{2}$$

upper wall GH:

$$\frac{\partial\psi}{\partial x}(x,1) = 0$$

$$\frac{\partial\psi}{\partial y}(x,1) = 0 \qquad (2.3.2.4)$$

$$\psi(x,1) = 1$$

$$\omega(x,1) = \frac{3(\psi_0 - \psi_1)}{h^2} - \frac{\omega_1}{2}$$

exit FG: $\psi(x,y) = 3y^2 - 2y^3$ for $x \geq L_E$

$$(2.3.2.5)$$

$$\omega(x,y) = 12y - 6 \text{ for } x \geq L_E$$

CHAPTER 3

NUMERICAL METHODS

3.1 Introduction

Numerical methods have been developed to handle problems involving nonlinearities in the describing equations, or complex geometries involving complicated boundary conditions. A finite-difference method is commonly used to solve either ordinary or partial differential equations. The describing differential equations and the necessary boundary conditions form a boundary value problem.

Any finite-difference method, used to solve a boundary value problem, leads to a system of simultaneous algebraic, difference equations. Their number, however, depends on the number of nodal points which is generally very large and, for this reason, the solution becomes a major problem.

The matrices associated with the difference equations, approximating the partial differential equations, are either banded or not banded. Banded matrices (the coefficient matrix is dense) are matrices with non-zero elements lying between two sub-diagonals parallel to the main diagonal. Non-banded matrices (the coefficient matrix is sparse) are matrices in which the number of zero elements in the matrix is much greater than the number of non-zero elements.

The two commonly used methods of solving simultaneous algebraic equations include the direct method, that makes use of the

Gauss elimination or Gauss-Jordan elimination procedure, and the iterative method, that makes use of the Gauss-Seidel iteration or a successive over-relaxation procedure to solve the equations. These two methods will now be discussed in some detail.

3.1.1 Direct methods

Direct methods are used to solve the system of equations in a known number of arithmetic operations. The most elementary methods of solving simultaneous linear algebraic equations are Cramer's rule and the various forms of Gaussian elimination.

3.1.1.1 Cramer's Rule

This is one of the most elementary methods. Unfortunately the algorithm is immensely time consuming, the number of operations being approximately proportional to $(N+1)!$, where N is the number of unknowns. A number of horror stories have been told about the large computation time required to solve systems of equations by Cramer's rule. Even if time were available, the accuracy would be unacceptable due to round-off error.

3.1.1.2 Gaussian Elimination

This method is a very efficient tool for solving many systems of algebraic equations, particularly for the special case of a tridiagonal system of equations. However, the method is not as fast as some others to be considered for more general systems of algebraic equations. Approximately N^3 multiplications are required in solving N equations. Also, round-off errors, which can accumulate through the many algebraic operations, sometimes cause deterioration of accuracy when N is large. Actually the accuracy of a method depends on the

specific system of equations and the matter is too complex to resolve by a simple general statement.

Rearranging the equations to the extent possible, in order to locate the coefficients which are largest in magnitude on the main diagonal, will tend to improve accuracy; this is known as "pivoting". For a matrix that is not banded, standard Gaussian elimination is inefficient in that the band is filled with non-zero numbers that have to be stored in the computer and used at subsequent stages of the elimination process.

3.1.2 Iterative Methods

When large sets of equations with sparse, non-banded coefficient matrices are to be solved and if computer storage is critical, it is desirable to use a method that does not require a large storage capacity. An iterative method is suitable for such purposes. In this method an initial guess at the solution is improved with a second approximation, which in turn is improved with a third approximation, and so on. The iterative procedure is said to be convergent when the differences between the successive approximations tend to zero as the number of iterations increase. In general, the exact solution is never obtained in a finite number of steps, but this does not matter. What is important is that the successive iterations converge fairly rapidly to values that are within specified accuracy.

With iterative methods, however, no manipulations are associated with zero coefficients so considerably fewer numbers have to be stored in the computer memory. As a consequence, they can be used to solve systems of equations that require matrices which are too large when direct methods are used. Programming and data handling are also much simpler using iterative methods than when using direct methods, especially in the solution of sets of nonlinear equations. The efficient use of iterative methods is very dependent, however, upon the direct calculation or estimation of the value (or values) of some numerical parameter called an acceleration parameter, and upon the coefficient matrix being well-conditioned; otherwise, convergence will be slow and the volume of computations enormous. With optimum acceleration parameters the volume of computations, when using an iterative method with large sets of equations, may actually be less than the computations involved when using a direct method. Iterative methods need or require approximately N^2 operations. In addition, the coefficient matrix of the system which results from the finite difference approximation has many strategically placed zeroes. However, no special account of these zeroes is taken in most direct methods. It is reasonable to expect that a particular method, designed in accordance with the general structure of the coefficient matrix, could further reduce the number of operations. Many such special iteration schemes have been devised and conditions on the coefficient matrix have been established, which are sufficient to insure the convergence to an acceptable solution. However, there is no general procedure available to determine which of the many possible methods is "best" in a given case.

The most frequently used iterative method is the Gauss-Seidel iteration. One difficulty with the Gauss-Seidel method is that convergence is relatively slow. Convergence is improved when a successive over-relaxation method is used.

3.1.2.1 Gauss-Seidel Iteration

Although many different iterative methods have been suggested over the years, Gauss-Seidel iteration (often called Liebmann iteration when applied to the algebraic equations that results from the differencing of an elliptic, partial differential equation) is one of the most efficient and useful point-iterative procedures for large systems of equations. The method is extremely simple but converges only under certain conditions related to "diagonal dominance" of the matrix of coefficients. The method makes explicit use of the sparseness of the coefficient matrix.

3.1.2.2 Successive Over-Relaxation Method

Successive over-relaxation (SOR) is a technique which can be used in an attempt to accelerate any iterative procedure. Often, the number of iterations required to reduce the error, of an initial estimate of the solution of a system of equations, by a predetermined factor can be substantially reduced by a process of extrapolation from previous iterations of the Gauss-Seidel method. Actually, the solution of a system of simultaneous algebraic equations by Gauss-Seidel iteration requires numerous recalculation, or iterations before convergence to an acceptable solution is achieved. During this process there are changes in the values of the unknowns at each mesh point between two successive iterations; a correction of the values in the anticipated direction before the next iteration is necessary to accelerate convergence. The parameter which is used to accelerate the convergence is known as a relaxation factor. If the optimum relaxation factor is found, it is apparently possible to reduce the computation time in some problems by a factor of up to 30. It is obviously very important to find this optimum factor. Occasionally, successive over-relaxation may not be of much help in accelerating convergence, but it should be considered and evaluated. The potential for savings in computation time is simply too great to ignore.

3.2 Numerical Solutions

Because of the simplicity and effectiveness of an iterative technique in solving large sets of equations with sparse coefficient matrices, which result from the finite-difference approximations of the governing equations, an over-relaxation technique is used to solve the full Navier-Stokes equations which describe the steady flow.

In terms of the stream function ψ and the vorticity ω, the two dimensional, steady state Navier-Stokes equations are

$$\frac{\partial^2\psi}{\partial x^2} + \frac{\partial^2\psi}{\partial y^2} = -\omega \qquad (3.2.1)$$

$$\frac{\partial^2\omega}{\partial x^2} + \frac{\partial^2\omega}{\partial y^2} + \mathrm{Re}\left(\frac{\partial\psi}{\partial x}\frac{\partial\omega}{\partial y} - \frac{\partial\psi}{\partial y}\frac{\partial\omega}{\partial x}\right) = 0 \qquad (3.2.2)$$

It will be convenient to approximate these coupled equations by linear, elliptic difference equations; the numerical solution of such equations is well understood.

A square computational grid of size $\Delta x = \Delta y = h$ is selected, with a grid lines parallel to the x and y axes such that the grid fits exactly the geometry of the channel with and without a constriction. Around a typical internal grid point (x,y) we adopt the convention that quantities at (x,y), (x+h,y), (x,y+h), (x-h,y) and (x,y-h) are denoted by the subscripts 1, 2, 3, 4, 5, respectively, as shown in Figure 4.

Equation (3.2.1) which is an elliptic, partial differential equation is to be solved simultaneously with the nonlinear, partial differential equation (3.2.2) in a rectangular region subject to the condition that the values of the stream function and vorticity are prescribed on the boundary of that domain.

Eq. (3.2.1) can be approximated using central-difference at the representative interior point (x,y) by

$$\frac{\partial^2\psi}{\partial x^2} = \frac{1}{h^2}\,[\psi_2 + \psi_4 - 2\psi_1] \tag{3.2.3}$$

$$\frac{\partial^2\psi}{\partial y^2} = \frac{1}{h^2}\,[\psi_3 + \psi_5 - 2\psi_1] \tag{3.2.4}$$

with an error $O(h^2)$. Thus, Eq. (3.2.1) can be written for the square mesh as

$$\psi_1 = \frac{1}{4}\,[\psi_2 + \psi_3 + \psi_4 + \psi_5] + \frac{1}{4}\,h^2\omega_1 \tag{3.2.5}$$

We could also use a central-difference formulation for Eq. (3.2.2), but we anticipate that the problem will need to be solved for reasonably high values of Reynolds number; it is known that such a formulation may not be satisfactory owing to the loss of diagonal dominance in the sets of difference equations, with resulting difficulties in convergence when using an iterative procedure.

Eq. (3.2.2) can be approximated by a difference equation, using central-differences for the second derivatives and a forward-difference for the first derivatives; there results

$$(-4\omega_1 + \omega_2 + \omega_3 + \omega_4 + \omega_5)$$

$$+ \mathrm{Re}\left[\frac{\psi_2 - \psi_4}{2h}\cdot\frac{\omega_3 - \omega_5}{2h} - \frac{\psi_3 - \psi_5}{2h}\cdot\frac{\omega_2 - \omega_4}{2h}\right] = 0 \tag{3.2.6}$$

or, equivalently,

$$-4\omega_1 + \left[1 - \frac{Re}{4}(\psi_3 - \psi_5)\right]\omega_2 + \left[1 + \frac{Re}{4}(\psi_2 - \psi_4)\right]\omega_3$$

$$+ \left[1 + \frac{Re}{4}(\psi_3 - \psi_5)\right]\omega_4 + \left[1 - \frac{Re}{4}(\psi_2 - \psi_4)\right]\omega_5 = 0 \quad (3.2.7)$$

Eqs. (3.2.5) and (3.2.7) with the appropriate boundary conditions can be solved using the Gauss-Seidel scheme. The numerical solution for the stream function and the vorticity will be denoted by ψ^{k+1} and ω^{k+1}, where k is the number of iterations. This solution works relatively well but diverges for Reynolds numbers greater than 250 and h = 1/40. The reason for this divergence is that, for high Reynolds numbers, the terms $Re(\psi_3 - \psi_5)/4$ and $Re(\psi_2 - \psi_4)/4$ in Eq. (3.2.7) become so large that the matrix of the resulting system loses its diagonal dominance.

A forward-backward technique can be introduced to maintain the diagonal dominance coefficient of ω_1 in Eq. (3.2.2) which determines the main diagonal elements of the resulting linear system; this technique is outlined as follows:

Set

$$\alpha = \psi_2 - \psi_4 \quad (3.2.8)$$

$$\beta = \psi_3 - \psi_5 \quad (3.2.9)$$

Then approximate Eq. (3.2.2) by

$$-4\omega_1 + \omega_2 + \omega_3 + \omega_4 + \omega_5 + h^2 Re \left(\frac{\alpha}{2h}\frac{\partial\omega}{\partial y} - \frac{\beta}{2h}\frac{\partial\omega}{\partial x}\right) = 0 \quad (3.2.10)$$

Now , if

$$\alpha \geq 0, \quad \frac{\partial \omega}{\partial y} \simeq \frac{\omega_3 - \omega_1}{h}$$

$$\alpha < 0, \quad \frac{\partial \omega}{\partial y} \simeq \frac{\omega_1 - \omega_5}{h} \tag{3.2.11}$$

If

$$\beta \geq 0, \quad \frac{\partial \omega}{\partial x} \simeq \frac{\omega_2 - \omega_4}{h}$$

$$\beta < 0, \quad \frac{\partial \omega}{\partial x} \simeq \frac{\omega_4 - \omega_2}{h} \tag{3.2.12}$$

To assure the diagonal dominance of the coefficient matrix for ω_1, which depends on the sign of α and β, Eq. (3.2.2) is expressed in the following difference forms:

$$\left(-4 - \frac{\alpha Re}{2} - \frac{\beta Re}{2}\right) \omega_1 + \omega_2$$

$$+ \left(1 + \frac{\alpha Re}{2}\right) \omega_3 + \left(1 - \frac{\beta Re}{2}\right) \omega_4 + \omega_5 = 0 \quad (\alpha \geq 0,\ \beta \geq 0) \tag{3.2.13}$$

$$\left(-4 - \frac{\alpha Re}{2} + \frac{\beta Re}{2}\right) \omega_1 + \left(1 - \frac{\beta Re}{2}\right) \omega_2$$

$$+ \left(1 + \frac{\alpha Re}{2}\right) \omega_3 + \omega_4 + \omega_5 = 0 \quad (\alpha \geq 0,\ \beta < 0) \tag{3.2.14}$$

$$\left(-4 - \frac{\alpha Re}{2} - \frac{\beta Re}{2}\right) \omega_1 + \omega_2 + \omega_3$$

$$+ \left(1 + \frac{\beta Re}{2}\right) \omega_4 + \left(1 - \frac{\alpha Re}{2}\right) \omega_5 = 0 \quad (\alpha < 0,\ \beta \geq 0) \tag{3.2.15}$$

$$\left(-4 + \frac{\alpha Re}{2} + \frac{\beta Re}{2}\right) \omega_1 + \left(1 - \frac{\beta Re}{2}\right) \omega_2$$

$$+ \omega_3 + \omega_4 + \left[1 - \frac{\alpha Re}{2}\right] \omega_5 = 0 \quad (\alpha < 0, \ \beta < 0) \qquad (3.2.16)$$

It has been found that the new equations result in convergence for $0 \leq Re \leq 10^5$, $h = 1/15$ but diverge for $h < 1/15$.

Weighted averages can be introduced to avoid any possible divergence. A smoothing formula results which corrects the value of the vorticity in the interior region; that is, the vorticity is assumed to be

$$\omega^* = KV\ \omega^k + (1 - KV)\ \omega^{k+1} \qquad (3.2.17)$$

and the stream function

$$\psi^* = KS\ \psi^k + (1 - KS)\ \psi^{k+1} \qquad (3.2.18)$$

where ω^{k+1} and ψ^{k+1} are the calculated vorticity and stream function. The values of the weighted averages KS and KV are within the range of 0 to 1 and their determination will be discussed in more detail in the next chapter.

An over-relaxation technique can be applied to accelerate the convergence of Eqs. (3.2.5) and (3.2.13-3.2.16); the expressions are used in this technique presented in the following:

For Poisson's equation

$$\psi_1^{k+1} = (1 - FS)\ \psi_1^k$$

$$+ \frac{FS}{4} (\psi_2 + \psi_3 + \psi_4 + \psi_5 + h^2 \omega_1) \qquad (3.2.19)$$

For the vorticity equations

$$\omega_1^{k+1} = (1 - FV)\,\omega_1^k + FV \left\{ \left[\omega_2 + [1 + (\psi_2 - \psi_4)\,\frac{Re}{2}]\,\omega_3 + [1 + (\psi_3 - \psi_5)\,\frac{Re}{2}]\,\omega_4 + \omega_5 \right] \Big/ \left[4 + (\psi_2 - \psi_4)\,\frac{Re}{2} + (\psi_3 - \psi_5)\,\frac{Re}{2} \right] \right\} \quad (\alpha \geq 0,\ \beta \geq 0) \tag{3.2.20}$$

$$\omega_1^{k+1} = (1 - FV)\,\omega_1^k + FV \left\{ \left[[1 - (\psi_3 - \psi_5)\,\frac{Re}{2}]\,\omega_2 + [1 + (\psi_2 - \psi_4)\,\frac{Re}{2}]\,\omega_3 + \omega_4 + \omega_5 \right] \Big/ \left[4 + (\psi_2 - \psi_4)\,\frac{Re}{2} + (\psi_3 - \psi_5)\,\frac{Re}{2} \right] \right\} \quad \alpha \geq 0,\ \beta < 0 \tag{3.2.21}$$

$$\omega_1^{k+1} = (1 - FV)\,\omega_1^k + FV \left\{ \left[\omega_2 + \omega_3 + [1 + (\psi_3 - \psi_5)\,\frac{Re}{2}]\,\omega_4 + [1 - (\psi_2 - \psi_4)\,\frac{Re}{2}]\,\omega_5 \right] \Big/ \left[4 - (\psi_2 - \psi_4)\,\frac{Re}{2} + (\psi_3 - \psi_5)\frac{Re}{2} \right] \right\} \quad (\alpha < 0,\ \beta \geq 0) \tag{3.2.22}$$

$$\omega_1^{k+1} = (1 - FV)\,\omega_1^k + FV \left\{ \left[[1 - (\psi_3 - \psi_5)\,\frac{Re}{2}]\,\omega_2 + \omega_3 + \omega_4 + [1 - (\psi_2 - \psi_4)\,\frac{Re}{2}]\,\omega_5 \right] \Big/ \left[4 - (\psi_2 - \psi_4)\,\frac{Re}{2} + (\psi_3 - \psi_5)\frac{Re}{2} \right] \right\} \quad (\alpha < 0,\ \beta < 0) \tag{3.2.23}$$

In the above equations FS and FV are the relaxation factors for the stream function and vorticity, respectively. The values of these relaxation factors are in the range of 0 to 2 and the determination of their optimum values will be discussed in the next chapter.

A numerical solution of Eqs. (3.2.19-3.2.23) is carried out be an iterative procedure according to the following steps:

(1) Initial values of $\omega_{i,j}$ and $\psi_{i,j}$ are assumed at all mesh points. Here $\omega_{i,j}$ represents the vorticity at x = ih and y = jh.

(2) Calculate the values of the vorticity on the boundary using Eq. (2.3.1.10).

(3) Successively calculate for every mesh point:

   a. the values of the stream function and vorticity from Eqs. (3.2.19) and (3.2.20-3.2.23).

   b. corrected the values $\psi_{i,j}$ using Eq. (3.2.18).

   c. corrected the values $\omega_{i,j}$ using Eq. (3.2.17).

(4) Except for the points where $\omega_{i,j} = \psi_{i,j} = 0$, continue the iteration until the following error criterion is satisfied:

$$\left|\frac{f_{i,j}^{k+1} - f_{i,j}^{k}}{f_{i,j}^{k+1}}\right| \leq 10^{-6} \tag{3.2.24}$$

Here $f_{i,j}$ represents either $\omega_{i,j}$ or $\psi_{i,j}$. When the above is satisfied the iteration is terminated, k being the number of iterations. If this relation is not satisfied for some preselected maximum number of iterations, then return to step (2) and repeat the process.

The computer time is significantly reduced by using the optimal over-relaxation factors.

CHAPTER 4

CONVERGENCE CRITERIA AND THE NAVIER-STOKES EQUATIONS

4.1 Introduction

The numerical solution of boundary value problems for partial differential equations usually requires the solution of large systems of linear algebraic equations. The order N of such systems is generally equal to the number of mesh points in the domain under consideration. Since direct inversion procedures require the order of N^3 operations they are not practical, even when using high speed digital computers, for reasonable mesh size in two dimensions. Thus, iterative methods for solving linear systems are of interest as they usually require an order of N^2 operations. In addition, the coefficient matrix of the system, which results from the finite difference approximations, has many strategically placed zeroes. However, no special account of these zeroes is taken in most direct inversions. It is reasonable to expect that a particular method, designed in accordance with the general structure of the coefficient matrix, could further reduce the number of operations. Because of simplicity and effectiveness, the successive over-relaxation method has been the most popular of the iterative methods for solving a large system of linear algebraic equations possessing a sparse, non-banded coefficient matrix.

In this chapter, our main objective is to determine optimum values of the over-relaxation and weighting factors that maximize the rate of convergence of the successive over-relaxation method.

4.2 The Problem Under Consideration

The two-dimensional, incompressible, laminar flow in the entrance region of a channel is investigated numerically. The non-dimensional Navier-Stokes equations in terms of a stream function ψ and vorticity ω as the governing equations are

$$\frac{\partial^2 \psi}{\partial x^2} + \frac{\partial^2 \psi}{\partial y^2} = - \omega \tag{4.2.1}$$

$$\frac{\partial^2 \omega}{\partial x^2} + \frac{\partial^2 \omega}{\partial y^2} + \text{Re} \left(\frac{\partial \psi}{\partial x} \frac{\partial \omega}{\partial y} - \frac{\partial \psi}{\partial y} \frac{\partial \omega}{\partial x} \right) = 0 \tag{4.2.2}$$

In a finite-difference form, using over-relaxation factors, the equations take the forms

$$\psi_1^{k+1} = (1\text{-FS})\, \psi_1^k + \frac{\text{FS}}{4} (\psi_2 + \psi_3 + \psi_4 + \psi_5 + h^2 \omega_1^2) \tag{4.2.3}$$

$$\begin{aligned} \omega_1^{k+1} = (1\text{-FV})\, \omega_1^k + \frac{\text{FV}}{4} \Big\{ &\left[1 - \frac{\text{Re}}{2} (\psi_3 - \psi_5)\right] \omega_2 + \\ &\left[1 + \frac{\text{Re}}{4} (\psi_2 - \psi_4)\right] \omega_3 + \left[1 + \frac{\text{Re}}{4} (\psi_3 - \psi_5)\right] \omega_4 + \\ &\left[1 - \frac{\text{Re}}{4} (\psi_2 - \psi_4)\right] \omega_5 \Big\} \end{aligned} \tag{4.2.4}$$

Using smoothing formulas they become

$$\psi^* = \text{KS}\, \psi^k + (1 - \text{KS})\, \psi^{k+1} \quad 0 \le \text{KS} \le 1 \tag{4.2.5}$$

$$\omega^* = KV\ \omega^k + (1 - KV)\ \omega^{k+1} \quad (0 \le KV \le 1) \qquad (4.2.6)$$

where FS and FV are optimum over-relaxation factors for Poisson's and the vorticity equations, respectively; KS and KV are weighted averages for the stream function and vorticity, respectively.

With rectangular field boundaries represented by $i = 0,\ I + 1$, and $j = 0,\ J + 1$, each of these difference Eqs. (4.2.3) and (4.2.4) represents a set of J x J equations, so that there are 2I x J algebraic equations to be solved simultaneously.

4.3 Convergence Conditions

The question of stability and convergence of any iterative procedure can only be answered completely by a consideration of Eqs. (4.2.3) and (4.2.4), one of which is nonlinear. However, Poisson's equation is known to have excellent convergence properties when solved along. Therefore, it is reasonable to assume that the convergence of the simultaneous solution of the nonlinear vorticity Eq. (4.2.4) and the Poisson Eq. (4.2.3), for the stream function will be most affected by the convergence properties of the nonlinear equation. Since equations (4.2.3) and (4.2.4) are coupled in ψ and ω, the accelerating parameters, which are optimum for the Poisson's Eq. (4.2.3) when solved alone with ψ constant during the iteration, may not accelerate the convergence of the simultaneous solution of Eqs. (4.2.3) and (4.2.4).

For the general solution of the simultaneous Eqs. (4.2.3) and (4.2.4), the iteration will be continued until the relative error criterion

$$\left|\frac{f_{i,j}^{k+1} - f_{i,j}^{k}}{f_{i,j}^{k+1}}\right| \le 10^{-6}$$

is satisfied. Here, $f_{i,j}$ represents either $\omega_{i,j}$ or $\psi_{i,j}$ and k will be the number of iterations.

4.3.1 Sufficient Conditions for Convergence of the Successive Over-Relaxation Method

The general linear algebraic system of N equations in the N unknowns $\psi_1, \psi_2, \ldots, \psi_N$ or $\omega_1, \omega_2, \ldots, \omega_N$ can be written in the form

$$a_{11}\psi_1 + a_{12}\psi_2 + a_{13}\psi_3 + \ldots + a_{1N}\psi_N = b_1$$

$$a_{21}\psi_1 + a_{22}\psi_2 + a_{23}\psi_3 + \ldots + a_{2N}\psi_N = b_2$$

$$a_{N1}\psi_1 + a_{N2}\psi_2 + a_{N3}\psi_3 + \ldots + a_{NN}\psi_N = b_N \qquad (4.3.1.1)$$

If the matrices ψ, b and A are defined by

$$\psi = \begin{pmatrix} \psi_1 \\ \psi_2 \\ \vdots \\ \psi_N \end{pmatrix}, \quad b = \begin{pmatrix} b_1 \\ b_2 \\ \vdots \\ b_N \end{pmatrix}, \quad A = \begin{pmatrix} a_{11} & a_{12} & \cdots & a_{1N} \\ a_{21} & a_{22} & \cdots & a_{2N} \\ \vdots & \vdots & & \vdots \\ a_{N1} & a_{N2} & & a_{NN} \end{pmatrix} \qquad (4.3.1.2)$$

Then

$$A\psi = b \qquad (4.3.1.3)$$

Let us assume that A is nonsingular so that for a given A and b, ψ exists and is unique. In order to provide a compact notation, we will order the equations, if possible, so that the coefficient largest in magnitude in each row is on the diagonal. Then if the system is irreducible (cannot be arranged so that some of the unknowns can be determined by solving less than N equations) and if

$$|a_{ii}| \geq \sum_{\substack{j=1 \\ j \neq i}}^{N} |a_{ij}| \tag{4.3.1.4}$$

for all i and if for at least one i,

$$|a_{ii}| > \sum_{\substack{j=1 \\ j \neq i}}^{N} |a_{ij}| \tag{4.3.1.5}$$

then the over-relaxation iteration will converge. This is a sufficient condition which means that convergence may sometimes be observed when the above condition is not met. A necessary condition can be stated but it is impractical to evaluate.

The sufficient condition can be interpreted as requiring for each equation that the magnitude of the coefficient on the diagonal be greater than or equal to the sum of the magnitudes of the other coefficients in the equation with the "greater than" holding for at least one (usually corresponding to a point near a boundary for a physical problem) equation. The matrix which satisfies this condition is called a diagonal dominant matrix. Therefore, for convergence, the matrix of the resulting system must be diagonally dominant.

Perhaps we should relate the above iterative convergence criteria to the system of equations which results from a finite-difference approximation of Poisson's and the vorticity equations.

Consider that at any point in our iteration our intermediate values of stream function ψ's and vorticity ω's are the exact solution plus some tolerance ϵ, i.e., $\psi_1 = (\psi_1)_{exact} + \epsilon$ and $\omega_1 = (\omega_1)_{exact} + \epsilon$; then our condition of diagonal dominance is forcing the ϵ's to become smaller and smaller as the iteration is repeated cyclically.

For a general system of equations, the multiplications per iteration could be as great as N^2 but could be much less if the matrix is sparse. This is the case in our system of equations.

4.4 Accelerating Parameters

For different flow situations (i.e., different Reynolds numbers) and mesh size h, the values of FS, FV, KS and KV in Eqs. (4.2.3-4.2.6) have a significant effect on the convergence of the solution as well as the computing time. These parameters are called accelerating factors and they play an important role in the solution.

The successive over-relaxation (SOR) method can be used in an attempt to accelerate any iterative procedure but we will propose it here primarily as a refinement to the Gauss-Seidel method (unaccelerated method). With the determination of optimized accelerating parameters, it is possible to reduce the required number of overall iterations in the solution by more than an order of magnitude from that required by Gauss-Seidel iteration; in addition, we may remove the restriction placed on the maximum size of the space step imposed by the Gauss-Seidel technique. The general idea of accelerating the solution is well known; however, the determination of the optimum acceleration parameter for, and the application to, this nonlinear set of simultaneous equations has not heretofore been given. Therefore, a search must be made for the optimum acceleration parameters.

The optimum value of the over-relaxation factor FS for the Poisson equation depends on the mesh size, the shape of domain, and the boundary conditions. For the problem in a rectangular domain of size $(I-1)\Delta x$ by $(J-1)\Delta y$ with constant Δx and Δy, it has been shown [54] that

$$FS = \frac{8-4\sqrt{4-\gamma^2}}{\gamma^2} \qquad (4.4.1)$$

with $\gamma = \cos(\pi/M) + \cos(\pi/N)$, where M and N are, respectively, the total number of increments into which the horizontal and vertical sides of the rectangular region are divided.

The optimum value of the over-relaxation factor FV for the vorticity equation depends on the Reynolds number, which identifies the coefficient of the matrix which results from the finite-difference form of the governing equations; the mesh size also plays a role.

In addition, the values of the weighting factor KS for the stream function and KV or the vorticity are determined by experimentation; the values that fall within the range of 0 to 1 will accelerate the convergence of the solution; this results due to the different percent of the old and the new values of stream function and vorticity used during the matrix iteration.

The main idea behind the convergence of the solution is that the matrix that results from the finite-difference equations must be diagonally dominant; this is the case for low Reynolds number flows. For high Reynolds number flows, the matrix of the resulting system loses its diagonal dominance. A forward-backward technique can be introduced to maintain the diagonal dominance and, consequently, convergence will also be maintained. Actually, the optimum value of

FV minimizes the spectral radius (i.e., results in the smallest magnitude of the maximum eigenvalue of matrix A, Eq. (4.3.1.3)) of the over-relaxation iteration matrix and thereby maximizes the rate of convergence of the method.

CHAPTER 5

RESULTS, DISCUSSION AND CONCLUSIONS

5.1 Background

The numerical solution of the full Navier-Stokes equations, for the entrance flow and constricted flow problems, has been obtained using a successive over-relaxation technique. In the development of a numerical scheme, one is never sure of the accuracy of the numerical solution obtained. At times, convergence in an iterative procedure may not mean that the solution is convergent to the solution of the differential equations. Comparing the numerical results with a known analytical solution is one possibility, but on the other hand, analytical solutions that are available use either simplified Navier-Stokes equations or an assumption is made concerning the approximate form of the solution. Alternatives are to compare the results with other numerical or experimental studies and to perform a grid-independency test for confidence in the numerical results.

Numerous solutions to the entrance flow problem have been reported in the literature. All of those available, both analytical and numerical, report methods that solve boundary-layer equations or simplified versions of the Navier-Stokes equations (for Reynolds numbers up to 2000), or full Navier-Stokes equations with a transformation and an exponential solution for numerical treatment (for Reynolds numbers up to 300). Solutions to the full Navier-Stokes equations in the entrance region, with and without constrictions for Reynolds numbers based on the channel height up to 2000, have not been presented in the literature.

The laminar incompressible flow in the entrance region of a high aspect-ratio, plane channel with and without constriction in the form of a step (forward, backward, and finite) has been analyzed using the full Navier-Stokes equations.

The stream function, vorticity, and streamwise velocity are reported at each grid point for Reynolds numbers up to 2000 for various step-to-channel height ratios and step lengths for the constricted channel. In addition, separation and reattachment points are obtained by fitting a polynomial to the separated streamline coordinates. An actual profile, obtained by fitting a polynomial near the wall to a uniform central section, using velocity measurements from a hot wire annometer, as shown in Table 1, is also used.

The convergence domain for the successive over-relaxation method and the optimum values of over-relaxation and weighting factors, often referred to as accelerating parameters, required by the numerical scheme, are utilized to maximize the rate of convergence thereby minimizing the computing time.

The first case solved is for a Reynolds number of 20, based on channel height, with a mesh size of 0.091 by 0.091, eleven elements normal to the flow and a sufficient number of elements in the flow direction to allow a fully-developed flow to occur. Several other Reynolds numbers are used up to 2000, the limit for laminar flows of interest. In order to improve the accuracy of the solution and to avoid excessive computing time, a mesh size of 0.05 by 0.05 is used for subsequent cases. Using the 0.05 mesh size, the majority of the calculations are performed by the VAX-11/750 VMS 4 computer. In addition, however, mesh sizes in the range of 0.02 to 0.1 are used at selected Reynolds numbers to check the validity of the numerical work, i.e., that the solution is independent of the mesh size.

5.2 Results for the Channel Entrance with no Constriction

Table 2 summarizes the cases considered providing each Reynolds number, inlet condition, mesh size, number of iterations, and the time needed for convergence.

The velocity profiles for the cases Re=20, 200, 500, and 2000 are shown in Figures 5-8, assuming a uniform velocity inlet profile. It is noted that for only very small X, in fact, at only the first X-step, the velocity profiles include a minimum on the axis and symmetrically located maxima on either side of the centerline, where the maximum velocity is 0.05% higher than that at the centerline. This contradicts the results obtained by other authors [12, 55, 56], in which these local maxima are much more pronounced over significant downstream distances.

The centerline velocity for Reynolds numbers of 200 and 2000 is shown in Figure 9 along with those obtained by other researchers [6, 12, 56, 63]. Their values are generally smaller than those obtained in the present study; however the velocity distributions are similar in shape.

Near the entrance where the velocity gradients are large near the wall, large viscous stresses develop. Therefore, the streamwise pressure gradient dp/dx is largest near the entrance. Also, the normal pressure gradient dp/dy, neglected in other studies, is quite significant near the wall for small X. These characteristics are more pronounced for the high Reynolds number cases. A typical normalized pressure gradient, for Reynolds number 20 and 200, is plotted versus

X/Re in Figures 10 and 11, respectively. It approaches unity asymptotically as X/Re become large.

The streamwise pressure gradient along the wall and centerline is always negative and [-(dp/dx)(Re/12)] is large near the entrance and decreases asymptotically to unity. This contradicts the result obtained by Morihara and Cheng [12], in which a localized adverse pressure gradient resulted due to the maximas in the velocity profile. This is undoubtedly due to the approximate form of the governing equations used in the solution.

The entrance length L_E, which is defined as the distance from the inlet to the point where the centerline velocity reaches 99% of the parabolic centerline velocity, is calculated using both the uniform profile and the actual profile. The velocity profiles that develop from an actual inlet profile are shown in Figures 12 and 13. The entrance length is found to be insensitive to the inlet velocity distribution, as shown in Table 3. It is noted that the entrance length increases slightly as the inlet velocity gradient at the wall decreases.

The entrance length calculated in this study is compared with that of other researchers [6, 12, 16, 17, 55, 57] in the Table 4. No significant difference is noted.

The entrance region in a channel is analyzed suggesting the existence of two distinct regions: the inviscid-core region and the profile-development region. The lengths of these regions and their ratios are obtained for various Reynolds numbers as presented in Table 5.

The end of the inviscid-core region occurs when the boundary layer thickness becomes equal to half of the channel height. This is determined numerically to occur when the velocity at the centerline exceeded the velocity at the first node above the centerline. The inviscid-core region is observed to be approximately one-fifth of the entrance length, a much shorter length than has been reported by Mohanty and Asthana [58] for a pipe flow.

Finally, the vorticity distribution in the entrance region of a straight channel at different locations X/Re for Reynolds number 200, is given in Table 6.

5.3 Results for the Channel Entrance with a Constriction

5.3.1 Forward Step

Solutions of the finite-difference equations are obtained for flow through a channel whose width is altered sharply, asymmetrically and by a finite amount of 0.4 of the channel height (a forward step). This step is positioned at various locations in the entrance region, and Reynolds numbers based on the channel height up to 2000 are considered. Table 7 summarizes the cases considered and their Reynolds number, step height and position, computational domain, purpose and computing time. Streamlines in the vicinity of the step are shown in Figures 14-16 for Reynolds numbers $(Re)_H$=20, 200, and 2000, for a step located in the profile-development region. Also, the Y-values for selected streamlines for the entire flow field are given in Tables 8-10 for $(Re)_H$=20, 200, and 2000, respectively. The streamline plots give a qualitative picture of the flow solutions; quantitative information is presented in Figures 17-23. The numerical results show that there is a detectable eddy of recirculating fluid upstream of the step for Re=50; as the Reynolds number increases the size of the eddy increases. The step's position has no observable effect on the reattachment point, as shown in Figures 17 and 18.

Increasing the height of the step forces the separation point further upstream and reattachment point upward in a linear nature as shown in Figures 19 and 20 for $(Re)_H$=200 and 1000, respectively. The streamline separates ahead of the step at a distance approximated by 0.0215 $(Re)^{.4319}$ and reattaches to the vertical face of the step at a height of 0.0282 $(Re)^{.2572}$. This separation of the streamline is observed at Re=50, while, in Greenspan's study [40], it is observed at Re=2000, due to a coarse mesh size used. Figures 21-23 show the separation and reattachment points as a function of step height and Reynolds number.

The separation point, which is predicted as Xs=0.0215 $(Re)^{.2572}$ in this study, is compared in Figure 24 with that found in Smith's asymptotic theory [27] for a channel with an asymmetric constriction in the form of a semi-infinite step and Dennis and Smith's numerical solution [30] for a channel with a symmetric contraction. The trend of the results is consistent with Dennis and Smith [30] for low Reynolds numbers and with Smith [27] for high Reynolds numbers. Also, the reattachment point is compared with Dennis and Smith [30] in Figure 25. Their values are relatively higher than the present work, however, the trends are the same.

On the qualitative side, asymmetric or symmetric constrictions produce a sizeable upstream adjustment of the flow when the Reynolds number is large. As the Reynolds number increases, the size of the separation region grows. Also, the dividing streamline upstream, reported by Greenspan [40] and Smith [27], exhibits the concave-upwards behavior for all values of Reynolds numbers, in agreement with the results displayed in Figure 17 for low Reynolds number and Figure 18 for high Reynolds number.

5.3.2 Backward Step

In this section, the numerical results for incompressible flow past a backward step will be presented and discussed. The ratio of step height to channel downstream height is 0.2. The step is positioned at various locations in the entrance region and Reynolds numbers $(Re)_H$, based on the downstream channel height, up to 2000 are considered. The presence of the step is observed to induce a noticeable acceleration in the flow near the step. The general features of the flow are separation of a shear layer from the vertical face of the step and its reattachment to the surface of the downstream lower wall, resulting in the formation of a separation region immediately behind the step.

The cases are summarized in Table 11; their Reynolds numbers, step height, position, computational domain, purpose and computing time are listed.

The numerical results show that the step's position has little effect on the separation point; it is more pronounced for a high step-to-channel ratio and high Reynolds number, as shown in Figures 26-30. Although, the reattachment points are different for the step in the different positions, the trend of the results is the same. Therefore, the streamline patterns are shown for selected positions. In Figures 31-33 the streamline patterns are shown for Reynolds numbers $(Re)_H=20$, 200 and 2000, for flow in the vicinity of a backward step located in the profile-development region. Also, the Y-values are given for selected streamlines for the entire flow field, in Tables 12-14.

Figures 34-36 show the effect of step height on the separation region for $(Re)_H=20$, 200 and 500 for a step located in the inviscid-core region. The results show both separation and reattachment points are sensitive to the step height. The separation point moves upward as the step height increases in a nonlinear manner and approaches the top of the step for high step height and Reynolds number as shown in Figure 37. In addition, the step height has significant effect on the reattachment point; as the step height increases, the reattachment point moves further downstream in a linear fashion, as shown in Figure 38, for Reynolds numbers 20, 200 and 500.

Increasing Reynolds number $(Re)_H$ forces the separation point further upward, as shown in Figure 39 for the step height 0.3H and Reynolds numbers up to 500, and in Figure 40 for the step height of 0.2H and Reynolds numbers up to 2000, for the step in the inviscid-core region.

The location of the separation point, Ys/a, for the step height 0.2H, is plotted versus Reynolds numbers in Figure 41. The separation point does not show the linear variation with Reynolds numbers as found by Kawaguti [59] and by Macagno and Hung [60] in channels with a sudden expansion. It approaches asymptotically to unity (i.e., the top of the step) as Reynolds number becomes large. The present nonlinear trend is probably due to the influence of the upper wall. A similar nonlinear trend is found by Roache and Mueller [44] for a backward step.

To compare the numerical results of this study with the theoretical and experimental results of others, the Reynolds number $(Re)_a$ is based on the step height "a" rather than the channel downstream height.

The numerical results indicate separation occurring at about 2/3 the step height for low step height and Reynolds number. This is consistent with the numerical results obtained by Taylor [43] for low Reynolds number [$(Re)_a$=4]; it is not a constant value for Reynolds numbers higher than 4, as Taylor [43] claimed. For Reynolds numbers in the range of 20 to 40, separation occurs in the range of 90% to 95% of the step height, which is found to be consistent with the numerical results of Roache and Mueller [44], Kitchens [45] and Mueller and O'Leary [48]. For high Reynolds numbers $(Re)_a$ of 100 to 400 the streamline separates at the top of the step. A similar trend is clearly seen for large Reynolds numbers in an experimental study by Honji [50] for the backward step, and in a numerical study by Kummar and Yajnih [61] for a sudden expansion in a channel flow.

The numerical results also show that, for low Reynolds numbers [$(Re)_a$ below 100], the reattachment point is a nonlinear function of Reynolds number, while, for high Reynolds numbers [$(Re)_a$ 100 to 400], it is a linearly increasing function of Reynolds number.

Convergence could not be obtained using the iterative procedure as reported by Kitchens [45] for Reynolds number higher than 200. This is probably caused by the local mesh size and related to the numerical stability problems encountered by Macagno and Hung [60]. Nonconvergence is also noted by Mueller and O'Leary [48] and Roache and Mueller [44] for Reynolds number higher than 100 (based on step height and free stream velocity). In this work, convergence is obtained for mesh sizes of 0.05 and 0.07 for all Reynolds numbers (up to 400); this is because upwind differencing is used for the advection terms in the Navier-Stokes equations. This avoids the numerical instability of an iterative solution at high Reynolds numbers; in addition, optimum accelerating parameters are used to accelerate the solution.

For low Reynolds number range, the reattachment points compare favorably with the theoretical results obtained by Roache and Mueller [44] and Mueller and O'Leary [48], as shown in Figure 42. Also, the reattachment points for high Reynolds numbers in the range of 100 to

400, are in good agreement with experimental data obtained by Sinha, et.al. [52], Leal and Acrivos [51], and Goldstein [49] as shown in Figure 43. Furthermore, the trend of the results is consistent with the numerical results of Kumar and Yajnih [61], Andreas and Mark [42] and Schrader [62] for flow through a sudden expansion at large Reynolds numbers.

5.3.3 Finite Step

The numerical results of the steady-state, Navier-Stokes equations for the flow field near a finite step immersed in a two-dimensional channel entrance region are described in this section. The qualitative features of the separation phenomena induced by the finite step are expected to be similar to those found in the forward and backward step cases. The cases are summarized in Table 15 by listing the Reynolds number, step height, length and position, computational domain, purpose and computing time. Numerical results are obtained for Reynolds numbers between 20 and 1300 based on the channel height and average velocity.

The numerical solutions for a finite step immersed in the channel entrance flow show a very small separated flow region upstream of the step, with separation region length and height almost independent of Reynolds number, for $(Re)_H$ between 200 and 1300. Recall that for the same range of Reynolds numbers, a significant upstream separation region is found for the forward step case. A similar upstream influence of the finite step is reported by Kitchens [45] and Greenspan [40]. Obviously, the downstream region is significantly influencing the upstream separation region.

On the other hand, the numerical results show that the downstream separation region introduced by the backward step, extends further downstream than that associated with the finite step; this effect increases as the Reynolds number increases.

The numerical results show that channel length downstream of the step, the step length, and the position of the step have an insignificant effect on the downstream separation region for the cases considered, as given in Tables 16-20 and shown in Figures 44 and 45. Therefore, the streamline patterns are shown for a selected position of the finite step.

Streamlines in the vicinity of the finite step are shown in Figures 46-48 for $(Re)_H$ of 20, 200 and 1300, for a step in the profile-development region. The Y-values for selected streamlines for the entire flow field are given in Tables 21-23 for various Reynolds numbers.

The effect of the step height on the downstream separation region is shown in Figures 49 and 50. As in a backward step, the downstream separation point moves upward toward the top of the step as the step height increases, in a nonlinear manner, and approaches the top of the step for high step height and Reynolds numbers as shown in Figure 51. Also, as the step height increases, the downstream reattachment point moves further downstream in a linear fashion, as shown in Figure 52, for $(Re)_H$=20 and 200. The locations of the downstream separation point and reattachment point with $(Re)_H$ are shown in Figure 53 for the step located in the inviscid-core region, with height of 0.3H and $(Re)_H$ up to 1300. The linear relationship of the downstream reattachment point as a function of Reynolds numbers based on the step height, in the range of 60 up to 390 is shown in Figure 54. A similar trend was obtained numerically by Kitchens [45] for flow past square protuberance.

As a special case, a finite step with one mesh size (0.05) of length (called a single step) is investigated up to $(Re)_H$=500. The cases are summarized in Table 24. As in a finite step, a single step causes a very small separated flow region upstream of the step for high Reynolds number. The numerical results show that for low $(Re)_H$ up to 20, the step position has a significant effect on the downstream separation region due to the short distance of the inviscid-core region, as shown in Figure 55. This effect is diminished as the Reynolds number increases, as shown in Figure 56.

Streamlines in the vicinity of the single step, located in the inviscid-core region, are shown in Figures 57 and 58 for (Re)=20 and 200. The Y-values for selected streamlines for the entire flow field are given in Tables 25 and 26 for $(Re)_H$=20 and 200, respectively. For $(Re)_H$ greater than 20, the streamlines separate from the top of the single step, as shown in Figures 59 and 60. The step height, for $(Re)_H$ greater than 20, has no effect on the downstream separation points; however, it does effect the downstream reattachment point which increases linearly with step height, as shown in Figure 61. Furthermore, as $(Re)_H$ increases, the downstream reattachment point moves further downstream and increases almost linearly with Reynolds number, as shown in Figure 62. A similar trend is also shown for flow past a square protuberance in a Couette flow studied by Kitchens [45].

The downstream reattachment points for the flow past a finite and a single step, are compared with the numerical results of Kitchens [45] for a square protuberance in Figure 63. His values are relatively higher than the present work. However, the trends are similar. In addition, the comparison of downstream separation and reattachment points for different steps located in the inviscid-core region, and for the Reynolds numbers considered, are shown in Figures

64 and 65. The trend of the downstream separation and reattachment points is similar for the different steps.

5.4 Optimum Over-Relaxation and Weighting Factors

The starting point of the numerical analysis is the consideration of the full Navier-Stokes equations and Poisson equation in the entrance region of the unconstricted channel. The rate of convergence to the solution of the above equations, using a finite-difference scheme, can be significantly increased by using the optimum values of the over-relaxation factors (FV) for the Navier-Stokes equations and (FS) for the Poisson equation, and the optimum values of the weighting factors (KS) for the stream function and (KV) for the vorticity.

The purpose of this section is to report the optimum values of the over-relaxation and weighting factors, often referred to as accelerating parameters. These parameters depend on the mesh size and the Reynolds number and significantly minimize the computing time for the simultaneous solution of Eqs. (4.2.3) and (4.2.4). They are determined primarily by computer experimentation.

A large number of combinations for Reynolds numbers and mesh sizes are attempted using different values for the accelerating parameters (1 to 1.9 for FS and FV and 0 to 1 for KS and KV). Convergent results are obtained with a relative error criterion of ϵ=10^{-6}, for $(Re)_H$=20, 50, 100, 200, 500, 1000 and 2000 with a mesh size of h=1/15 and h=1/20. Tables 27 and 28 give the computing time required for convergence for the range of the Reynolds numbers and different mesh sizes considered over a range of values of FS. The numerical results show that the optimum value of FS depend on the mesh size (assumed equal in the X- and Y-direction) of the computational domain. It is noted that the computing time decreases as FS increases until a minimum computing time is achieved; further increases in the value of FS result in an increase in the computing time. At the minimum computing time, FS represents the optimum value. The variation in computing time is more pronounced for high Reynolds numbers, as shown in Tables 27 and 28.

Reduction in computing time, at least by factor of 2, is obtained by using the optimum value of the over-relaxation factor FS. Reducing FS below unity significantly increases the computing time. It is also found that the results converge most rapidly when FS is given by Eq. (4.4.1).

Tables 29 and 30 show the effect of the relaxation factor FV on the computing time for various Reynolds numbers and mesh sizes. It is noted that as FV increases for a certain value of Reynolds number, the computing time decreases until a minimum computing time is reached at the optimum FV value; further increases in the FV value cause the computing time to increase for low Reynolds numbers of 100 or below. However, the value of FV is equal to unity for Reynolds numbers of 200 or higher; the numerical solution does not converge for values of FV slightly greater than unity.

The influence of the weighting factors KS and KV, defined in Eqs. (4.2.5) and (4.2.6), respectively, which allow for a different percent of the old and the new values of the stream function and vorticity during the matrix iteration, are given in Tables 31-34 for various Reynolds numbers and mesh sizes. It is noted that the computing time decreases as KS decreases to zero for low Reynolds numbers (Re=20, 50 and 100). It has a value in the range of 0.1 to 0.3 for Reynolds numbers in the range of 200 to 2000 for minimum computing time. Also, as the value of KV increases, the computing time decreases until a minimum computing time is obtained at an optimum value of KV; further increases in the value of KV beyond this optimum value result in an increase in the computing time, as shown in Tables 33 and 34. A reduction in computing time by a factor of 2 to 4 is possible using the optimum values of the weighting factors KS and KV.

Finally, for each Reynolds number and mesh size there is an optimum combination of the values for FS, FV, KS and KV to minimize computing time. The optimum values, as a function of Reynolds number, are shown in Figures 66 and 67 for the two different mesh sizes considered. It may be noted that the optimum value of FS increases as Reynolds number increases up to 50 for $h=1/20$ and 500 for $h=1/15$; for higher Reynolds numbers, it approaches a constant value of 1.8, as shown in Figure 68. On the other hand, the optimum value of FV is large at low Reynolds number and decreases asymptotically to unity for high Reynolds numbers, for both mesh sizes, as shown. The optimum values of KS is nearly zero for Reynolds numbers up to 100 and increases as Re increases.

The Figures also show that the optimum value of the weighting factor KV increases as the Reynolds number increases for the range of the Reynolds numbers considered. For the range of the mesh size considered, it is noted that for low Reynolds numbers, the over-relaxation factors FS and FV are a function of Re, while they approach constant values of 1.8 and 1, respectively, for high Re as shown in Figure 68. Furthermore, the weighting factors KS and KV have relatively high values for the smaller mesh grid than larger grid as shown in Figure 69. This Figure also shows that KV has a constant value for high Re, while KS has a constant value for low Re.

For a channel with a constriction in the form of a step (forward, backward and finite) several runs are also performed using different values of the accelerating parameters. The numerical results show that the optimum values of the accelerating parameters, which are used to reduce the computing time for the channel flow without a constriction, also represent the optimum values for the channel flow with a constriction in the form of a step.

In summary, a reduction in computing time, by factors of 1.5 to 4 for mesh size h=1/15 and factors of 2 to 6.6 for h=1/20, is obtained by using the optimum values of the accelerating parameters FS, FV, KS and KV as compared with the unaccelerated case (FS=FV=1 and KS=KV=0); this is shown in Table 35.

5.5 Conclusions

A successive over-relaxation method, utilizing optimum accelerating parameters, is numerically stable for all Reynolds numbers, step-to-channel ratios and mesh sizes considered. The entrance region in a rectangular channel with and without a constriction has been studied using a grid size of 0.05 by 0.05. The following conclusions are based on the results presented earlier.

Channel Entrance Region

1. By solving the full Navier-Stokes equations, it is found that the local maxima in the velocity profiles are essentially non-existent; they are apparently the result of solving modified Navier-Stokes equations with certain terms neglected or they are a manifestation of the numerical algorithms.

2. The results show that an actual inlet profile with velocity gradients near the two walls does not influence the flow in the entrance region significantly.

3. The inviscid-core region for the channel flow is approximately one-fifth of the entrance length, substantially shorter than that reported for pipe flow. The profile-development region makes up the remaining four-fifths of the entrance region.

Forward Step

1. For the downstream region of the step, at least 0.55 of the channel height is needed using the selected algorithm to satisfy the fully-developed flow downstream boundary conditions for the stream function and vorticity. This is true for all Reynolds numbers considered. Therefore, a step height of 0.4 is used for the analysis of the flow.

2. Separation occurs for Reynolds numbers greater than 20; no separation occurs for a step height of 0.2 of the channel height for the range of Reynolds numbers considered.

3. No separation of the fluid downstream of the step is observed at any Reynolds number; use of very fine grids would be necessary to obtain this separation and recover the true flow situation in the region immediately downstream of the step.

Backward Step

1. The location of the separation point from the vertical face is a nonlinear function of step height. The location of the reattachment point on the lower surface is a linear function of the step height.

2. The step location has negligible effect on the separation point, however, it does effect the reattachment point and is more pronounced for high step-to-channel ratios and Reynolds numbers. For example, for Re=400 (based on step height), the reattachment point for the step located in the profile-development region is further downstream than the reattachment point for the step in the inviscid-core region by 42.5% and 8% further downstream than the reattachment point for the step in the fully-developed region.

3. The separation point approaches the top of the step for high Reynolds numbers.

4. The reattachment point is a nonlinear function of Reynolds numbers (based on the step height) up to 100 and a linear function for high Reynolds number of 100 to 400.

Finite Step

1. Both the finite and single step possess a very small upstream separated region, with length and height almost independent of Reynolds number, quite unlike the forward step.

2. The finite step position and length, and the length of the channel downstream of the step have negligible effect on the downstream separation region.

3. The location of the downstream separation point is a nonlinear function of the finite step height and a constant value for the single step. The downstream reattachment point is a linear function of step height for both finite and single steps.

4. For a single step, the streamlines separate from the top of the step for all Reynolds numbers (based on the downstream channel height) greater than 20. This is not the case for backward and finite steps.

5. The location of the downstream reattachment point is a nonlinear function of Reynolds numbers, based on the step height, up to 60 for a finite step and 15 for a single step, and a linear function of Reynolds number for higher values.

6. Generally, the upstream and downstream separation regions introduced by the finite step are smaller than those associated with the forward and the backward step cases.

Optimum Accelerating Parameters

1. Generally, for a uniform grid size in a rectangular domain, the iterated results converge most rapidly when FS is defined by Eq. (4.4.1) for the range of Reynolds numbers considered. For fine

mesh, or high Reynolds number, FS is constant and equal to 1.808 as predicted by Eq. (4.4.1).

2. The fastest rate of convergence of the Navier-Stokes equations is obtained when FV-1, for high Reynolds number (200 or greater), and in the range of 1.1 to 1.5 for low Reynolds number.

3. The values of weighting factors KS and KV for mesh size h-1/20 are slightly greater than for mesh size h-1/15.

4. Using optimum values of the accelerating parameters, the maximum reduction in computing time is a factor of 4 for h-1/15 and a factor of 6.6 for h-1/20.

5. The optimum values of the accelerating parameters FS, FV, KS and KV, which are found in this study for the channel flow without a constriction, are also applicable for a channel flow with a constriction in the form of a step.

6. The optimum values of the four accelerating parameters should serve as a guide to reduce the computing time for other flow situations which use this system of equations.

TABLES

Table 1. Actual inlet velocity profile

Normal distance Y	Velocity u/U_0	Stream function ψ
0.00	0.000	0.0000
0.05	0.725	0.0300
0.10	0.875	0.0725
0.15	0.975	0.1175
0.20	1.075	0.1700
0.25	1.100	0.2250
0.30	1.100	0.2800
0.35	1.100	0.3350
0.40	1.100	0.3900
0.45	1.100	0.4450
0.50	1.100	0.5000
0.55	1.100	0.5550
0.66	1.100	0.6100
0.65	1.100	0.6650
0.70	1.100	0.7200
0.75	1.100	0.7750
0.80	1.075	0.8300
0.85	0.975	0.8825
0.90	0.875	0.9275
0.95	0.725	0.9700
1.00	0.000	1.0000

Table 2. Summary of entrance flow problems studied

$(Re)_H$	Inlet velocity profile	Mesh size	No. of iterations	CPU time
5	Uniform velocity	0.0833	44	0 00:02:35.19
20	Uniform velocity	0.0500	75	0 00:06:10.17
20	Actual velocity	0.0500	64	0 00:05:42.03
50	Uniform velocity	0.0500	96	0 00:20:03.55
50	Actual velocity	0.0500	94	0 00:19:48.42
100	Uniform velocity	0.0500	131	0 00:27:10.24
100	Actual velocity	0.0500	118	0 00:22:03.35
200	Uniform velocity	0.0500	143	0 01:20:13.69
200	Actual velocity	0.0500	136	0 01:13:43.36
500	Uniform velocity	0.0500	210	0 04:46:31.47
500	Actual velocity	0.0500	190	0 04:04:14.62
1000	Uniform velocity	0.0500	233	0 10:50:31.09
2000	Uniform velocity	0.0500	592	1 05:54:53.35

Table 3. Entrance length L_E

$(Re)_H$	Inlet velocity profile	L_E	$L_E/H\ Re$
5	Uniform velocity	0.83	0.1666
20	Uniform velocity	0.90	0.0450
20	Actual velocity	1.05	0.0525
50	Uniform velocity	2.20	0.0440
50	Actual velocity	2.40	0.0480
100	Uniform velocity	4.40	0.0440
100	Actual velocity	4.60	0.0460
200	Uniform velocity	8.85	0.0442
200	Actual velocity	9.10	0.0455
500	Uniform velocity	22.15	0.0443
500	Actual velocity	22.55	0.0451
1000	Uniform velocity	44.25	0.0442
2000	Uniform velocity	88.55	0.0443

L_E is the distance at which the velocity at the centerline reaches 99 percent of the fully developed value.

Table 4. Comparison of $2L_E/H$ and L_E/H Re with other researchers

$(Re)_H$	Morihara & Cheng	Schlichting	Gillis, et al.	Present work
	$2L_E/H$			
5				0.33
20	2.24	1.60	2.26	1.80
50				4.40
100				8.80
200	18.06	16.00	18.23	17.70
500				44.30
1000				88.50
2000	171.60	160.00		177.10
	L_E/H Re			
5				0.1666
20	0.0559	0.0400	0.0565	0.0450
50		0.0400		0.0440
100		0.0400		0.0440
200	0.0452	0.0400	0.0456	0.0442
500		0.0400		0.0443
1000		0.0400		0.0442
2000	0.0429	0.0400		0.0443

At large Re limit

Researcher	L_E/H Re
Present work	0.0443
Schlichting	0.0400
Hwang and Fan	0.0422
Morihara and Cheng	0.0423
Bodoia and Osterle	0.0440
Gillis, et al.	0.0442
Roidt and Cess	0.0454

Table 5. The inviscid-core length, the profile-development length, and the entrance length for various Reynolds numbers

Re	L_i	L_d	L_E	L_E/H Re	L_i/H Re	L_d/H Re	L_i/L_E
20	0.18	0.72	0.9	0.0450	0.0090	0.0360	0.200
50	0.44	1.76	2.2	0.0440	0.0088	0.0352	0.1999
100	0.88	3.52	4.4	0.0440	0.0088	0.0352	0.2000
200	1.75	7.1	8.85	0.0442	0.0087	0.0355	0.1977
500	4.43	17.72	22.15	0.0443	0.0088	0.0354	0.2000
1000	8.8	35.45	44.25	0.0442	0.0088	0.0354	0.1990
2000	17.5	71.05	88.55	0.0447	0.0087	0.0355	0.1978

L_i - Inviscid-core length
L_d - Profile-development length
L_E - Entrance length

Table 6. **Vorticity values in the entrance region of a straight channel, Re=200**

Y \ X|Re	0.00025	0.005	0.00875	0.02	0.05
0.00	-43.814	-13.967	-13.316	-11.633	-11.470
0.05	- 9.629	- 6.574	- 6.233	- 5.507	- 5.435
0.10	- 2.635	- 5.608	- 5.295	- 4.861	- 4.820
0.15	- 0.683	- 4.336	- 4.263	- 4.207	- 4.202
0.20	- 0.164	- 2.903	- 3.172	- 3.550	- 3.583
0.25	- 0.036	- 1.664	- 2.137	- 2.896	- 2.965
0.30	- 0.007	- 0.819	- 1.288	- 2.259	- 2.354
0.35	- 0.001	- 0.348	- 0.690	- 1.650	- 1.751
0.40	- 0.000	- 0.127	- 0.325	- 1.074	- 1.159
0.45	0.000	- 0.038	- 0.122	- 0.528	- 0.576
0.50	0.000	0.000	0.000	0.000	0.000
0.55	0.000	0.038	0.122	0.528	0.576
0.60	0.000	0.127	0.325	1.074	1.159
0.65	0.001	0.348	0.690	1.650	1.751
0.70	0.007	0.819	1.288	2.259	2.354
0.75	0.036	1.664	2.137	2.896	2.965
0.80	0.164	2.903	3.172	3.550	3.583
0.85	0.683	4.336	4.263	4.207	4.202
0.90	2.635	5.608	5.295	4.861	4.820
0.95	9.629	6.574	6.233	5.507	5.435
1.00	43.814	13.967	13.316	11.633	11.470

Table 7. Summary of cases studied for forward step

$(Re)_H$	Step height	Step position	Computational domain	purpose	CPU time
20	0.40H	Inviscid-core	1.5H		0 00:01:40.27
20	0.40H	Profile-dev	2.0H		0 00:02:55.10
20	0.40H	Fully-dev	2.5H	Effect	0 00:05:37.22
50	0.40H	Inviscid-core	3.0H	of	0 00:12:57.57
50	0.40H	Profile-dev	4.0H	step	0 00:15:26.18
50	0.40H	Fully-dev	6.0H	position	0 00:14:17.52
200	0.40H	Inviscid-core	10.5H	on the	0 00:13:16.79
200	0.40H	Profile-dev	15.0H	separation	0 00:30:21.31
200	0.40H	Fully-dev	12.0H	region	0 01:09:14.29
2000	0.40H	Inviscid	110.0H		0 08:25:49.09
2000	0.40H	Profile-dev	130.0H		0 10:32:07.14
2000	0.40H	Fully-dev	110.0H		1 07:03:24.28
200	0.45H	Inviscid-core	10.5H		0 01:52:25.10
200	0.40H	Inviscid-core	10.5H		0 00:13:16.79
200	0.35H	Inviscid-core	10.5H		0 00:14:06.21
200	0.30H	Inviscid-core	10.5H	Effect	0 00:14:42.46
200	0.25H	Inviscid-core	10.5H	of	0 00:15:10.48
200	0.20H	Inviscid-core	10.5H	step	0 00:15:58.90
1000	0.45H	Inviscid-core	60.0H	height	0 15:20:42.20
1000	0.40H	Inviscid-core	60.0H	on the	0 05:01:07.95
1000	0.35H	Inviscid-core	60.0H	separation	0 04:59:12.72
1000	0.30H	Inviscid-core	60.0H	region	0 04:51:41.50
1000	0.25H	Inviscid-core	60.0H		0 04:20:55.28
1000	0.20H	Inviscid-core	60.0H		0 04:01:11.37
50	0.40H	Inviscid-core	3.0H		0 00:12:57.57
100	0.40H	Inviscid-core	6.5H		0 00:06:55.01
200	0.40H	Inviscid-core	10.5H		0 00:13:16.79
500	0.40H	Inviscid-core	32.5H		0 01:42:27.66
1000	0.40H	Inviscid-core	60.0H		0 05:01:07.95
2000	0.40H	Inviscid-core	110.0H		0 08:25:49.09
50	0.40H	Profile-dev	4.0H	Effect	0 00:15:26.18
100	0.40H	Profile-dev	8.0H	of	0 00:11:44.22
200	0.40H	Profile-dev	15.0H	Reynolds	0 00:30:21.31
500	0.40H	Profile-dev	38.5H	number	0 02:08:35.41
1000	0.40H	Profile-dev	70.0H	on	0 08:58:23.21
2000	0.40H	Profile-dev	130.0H	separation	0 10:32:07.14
50	0.40H	Fully-dev	6.0H	region	0 00:14:17.52
100	0.40H	Fully-dev	12.0H		0 00:53:59.04
200	0.40H	Fully-dev	20.0H		0 01:09:14.29
500	0.40H	Fully-dev	50.0H		0 05:27:02.47
1000	0.40H	Fully-dev	100.0H		1 01:25:49.72
2000	0.40H	Fully-dev	110.0H		1 07:03:24.28

Table 8. **The Y-values for selected streamlines for the flow past a forward step located in the profile-development region,** $(Re)_H$=20

X	ψ = 0.005	ψ = 0.1	ψ = 0.2	ψ = 0.5	ψ = 0.7	ψ = 0.8
0.05	.0090	.1320	.2370	.5312	.7106	.8000
0.10	.0160	.1643	.2754	.5585	.7196	.8000
0.15	.0280	.1986	.3158	.5824	.7280	.8000
0.20	.0470	.2365	.3584	.6040	.7363	.8010
0.25	.0591	.2821	.4030	.6233	.7446	.8056
0.30	.0807	.3385	.4467	.6408	.7528	.8106
0.35	.1208	.4016	.4843	.6564	.7607	.8157
0.40	.2130	.4650	.5153	.6698	.7680	.8206
0.45	.4050	.4811	.5380	.6809	.7744	.8250
0.50	.4080	.4996	.5535	.6898	.7794	.8317
0.55	.4111	.5090	.5635	.6966	.7838	.8340
0.60	.4130	.5153	.5703	.7018	.7870	.8355
0.65	.4142	.5190	.5748	.7054	.7893	.8360
0.70	.4147	.5212	.5776	.7079	.7903	.8365
0.75	.4148	.5223	.5792	.7093	.7916	.837
0.80	.4147	.5227	.5798	.7100	.7918	.8371
0.85	.4146	.5226	.5800	.7101	.7918	.8369
0.90	.4144	.5222	.5796	.7099	.7914	.8364
0.95	.4142	.5217	.5790	.7093	.7908	.8359
1.00	.4140	.5210	.5783	.7086	.7901	.8352
1.10	.4138	.5203	.5775	.7077	.7893	.8345
1.15	.4136	.5197	.5767	.7068	.7885	.8338
1.20	.4135	.5191	.5759	.7060	.7877	.8324
1.25	.4132	.5180	.5745	.7043	.7864	.8319
1.30	.4131	.5176	.5739	.7036	.7857	.8315
1.35	.4130	.5171	.5733	.7029	.7851	.8311
1.40	.4128	.5167	.5728	.7024	.7847	.8308
1.45	.4127	.5163	.5722	.7018	.7843	.8305
1.50	.4124	.5158	.5716	.7014	.7841	.8302
1.55	.4122	.5151	.5710	.7010	.7840	.8302
1.60	.4120	.5144	.5704	.7000	.7839	.8302
1.65	.4120	.5142	.5703	.7000	.7839	.8302
1.70	.4120	.5142	.5703	.7000	.7839	.8302

Table 9. The Y-values for selected streamlines for the flow past a forward step located in the profile-development region, $(Re)_H = 200$

X	$\psi = 0.005$	$\psi = 0.1$	$\psi = 0.2$	$\psi = 0.5$	$\psi = 0.6$	$\psi = 0.8$
0.05	.0070	.1169	.2110	.5000	.5960	.7880
0.20	.0190	.1486	.2363	.5000	.5888	.7637
0.30	.0240	.1591	.2461	.5000	.5852	.7539
0.50	.0270	.1691	.2570	.5000	.5802	.7430
0.75	.0280	.1742	.2618	.5000	.5785	.7374
1.00	.0280	.1767	.2660	.5000	.5770	.7342
1.50	.0290	.1803	.2703	.5000	.5754	.7303
2.00	.0302	.1830	.2740	.5000	.5742	.7270
2.50	.0316	.1866	.2770	.5020	.5740	.7262
3.00	.0330	.1907	.2820	.5059	.5760	.7264
3.20	.0341	.1930	.2846	.5070	.5779	.7277
3.40	.0357	.1964	.2882	.5102	.5807	.7299
3.60	.0384	.2008	.2932	.5149	.5850	.7333
3.80	.0417	.2065	.3005	.5218	.5915	.7385
4.00	.0480	.2150	.3104	.5320	.6010	.7460
4.20	.0527	.2283	.3256	.5476	.6158	.7583
4.40	.0595	.2511	.3502	.5705	.6371	.7751
4.60	.0670	.2660	.3893	.6040	.6512	.7850
4.80	.0130	.3660	.4000	.6480	.7040	.8212
4.90	.2240	.4410	.5090	.6710	.7230	.8322
4.95	.4041	.4730	.5300	.6812	.7312	.8366
5.05	.4105	.5040	.5570	.6975	.7445	.8360
5.15	.4166	.5174	.5714	.7084	.7535	.8490
5.25	.4190	.5240	.5790	.7150	.7590	.8510
5.35	.4190	.5274	.5835	.7185	.7619	.8527
5.45	.4180	.5280	.5855	.7190	.7630	.8520
5.55	.4169	.5276	.5819	.7195	.7622	.8508
5.65	.4159	.5260	.5840	.7180	.7614	.8490
5.75	.4151	.5248	.5826	.7171	.7593	.8472
5.85	.4142	.5230	.5812	.7150	.7572	.8450
5.95	.4140	.5219	.5798	.7139	.7558	.8434
6.05	.4136	.5210	.5785	.7120	.7540	.8420
6.25	.4132	.5190	.5764	.7099	.7514	.8391
6.55	.4129	.5175	.5745	.7062	.7485	.8363
6.75	.4128	.5169	.5738	.7054	.7472	.8351
6.95	.4127	.5167	.5732	.7050	.7453	.8342
7.25	.4127	.5167	.5730	.7050	.7434	.8332
7.75	.4127	.5167	.5730	.7050	.7435	.8310
8.05	.4127	.5167	.5730	.7030	.7435	.8310
9.05	.4127	.5167	.5730	.7030	.7435	.8310
10.05	.4127	.5167	.5730	.7030	.7435	.8310
11.05	.4127	.5167	.5730	.7030	.7435	.8310
12.05	.4127	.5167	.5730	.7030	.7435	.8310
13.05	.4127	.5167	.5730	.7030	.7435	.8310
14.05	.4127	.5167	.5730	.7030	.7435	.8310
14.95	.4127	.5167	.5730	.7030	.7435	.8310

Table 10. **The Y-values for selected streamlines for the flow past a forward step located in the profile-development region, $(Re)_H = 2000$**

X	ψ=0.005	ψ=0.1	ψ=0.2	ψ=0.5	ψ=0.6	ψ=0.8
0.05	.0230	.1600	.2482	.5000	.5831	.7520
2.00	.0242	.1639	.2518	.5000	.5826	.7482
4.00	.0247	.1672	.2557	.5000	.5811	.7443
6.00	.0256	.1702	.2590	.5000	.5798	.7410
8.00	.0264	.1727	.2618	.5000	.5786	.7382
10.00	.0271	.1748	.2642	.5000	.5776	.7358
12.00	.0277	.1767	.2664	.5000	.5767	.7336
14.00	.0283	.1783	.2681	.5000	.5759	.7319
16.00	.0288	.1798	.2698	.5000	.5751	.7302
18.00	.0292	.1811	.2713	.5000	.5745	.7288
20.00	.0298	.1826	.2729	.5004	.5743	.7279
22.00	.0324	.1868	.2773	.5038	.5770	.7298
23.00	.0399	.1967	.2875	.5134	.5861	.7378
23.25	.0448	.2017	.2929	.5186	.5899	.7421
23.50	.0507	.2082	.3006	.5260	.5981	.7482
23.75	.0544	.2156	.3086	.5341	.6083	.7572
24.00	.0606	.2324	.3265	.5517	.6227	.7697
24.20	.0700	.2506	.3449	.5688	.6388	.7829
24.40	.0906	.2739	.3703	.5923	.6604	.7990
24.60	.1187	.3122	.4093	.6243	.6890	.8205
24.70	.1470	.3407	.4367	.6439	.7058	.8317
24.80	.1787	.3815	.4724	.6651	.7235	.8427
24.90	.2473	.4450	.5149	.6861	.7405	.8531
24.95	.4042	.4762	.5354	.6957	.7483	.8579
25.05	.4115	.5073	.5625	.7118	.7616	.8659
25.15	.4225	.5229	.5787	.7236	.7716	.8719
25.25	.4347	.5329	.5891	.7316	.7785	.8760
25.35	.4449	.5394	.5958	.7368	.7829	.8785
25.45	.4500	.5432	.5999	.7400	.7856	.8799
25.55	.4470	.5451	.6017	.7416	.7869	.8805
25.75	.4388	.5456	.6022	.7414	.7865	.8796
25.95	.4325	.5423	.5994	.7388	.7839	.8776
26.25	.4257	.5367	.5934	.7340	.7796	.8740
26.55	.4220	.5313	.5884	.7363	.7764	.8718
26.75	.4205	.5290	.5865	.7289	.7751	.8709
27.05	.4192	.5275	.5853	.7279	.7741	.8700
27.55	.4181	.5268	.5848	.7271	.7733	.8689
28.05	.4172	.5263	.5844	.7266	.7726	.8679
29.05	.4161	.5254	.5836	.7252	.7709	.8658
30.05	.4149	.5213	.5788	.7211	.7670	.8622
40.00	.4087	.5005	.5559	.7028	.7500	.8618
50.00	.4080	.5000	.5500	.7000	.7500	.8616
60.00	.4077	.5000	.5500	.7000	.7500	.8612
70.00	.4072	.5000	.5500	.7000	.7500	.8608
90.00	.4050	.5000	.5500	.7000	.7500	.8600
110.00	.4050	.5000	.5500	.7000	.7500	.8600
130.00	.4050	.5000	.5500	.7000	.7500	.8600

Table I

$(Re)_H$
20
20
20
20
20
20
20
20
20
200
200
200
2000
2000
2000
20
20
20
20
200
200
200
200
500
500
500
20
50
100
200
500
20
50
100
200
500
[illegible]
[illegible]
20
50
100
200
500
[illegible]
[illegible]

Table 11. Summary of cases studied for backward step

$(Re)_H$	Step height	Step position	Computational domain	purpose	CPU time
20	0.2H	Inviscid-core	2.2H		0 00:04:43.21
20	0.2H	Profile-dev	2.6H		0 00:10:08.95
20	0.2H	Fully-dev	2.2H		0 00:08:10.08
20	0.3H	Inviscid-core	2.2H	Effect	0 00:07:45.44
20	0.3H	Profile-dev	2.6H	of	0 00:18:20.34
20	0.3H	Fully-dev	2.2H	step	0 00:18:19.98
20	0.4H	Inviscid-core	2.2H	position	0 00:09:07.74
20	0.4H	Profile-dev	2.6H	on	0 00:14:48.01
20	0.4H	Fully-dev	2.2H	separation	0 00:12:50.17
200	0.4H	Inviscid-core	11.0H	region	0 02:40:35.81
200	0.4H	Profile-dev	14.0H		0 04:59:37.56
200	0.4H	Fully-dev	12.0H		0 03:12:28.17
2000	0.2H	Inviscid-core	110.0H		1 20:21:31.61
2000	0.2H	Profile-dev	130.0H		4 06:51:40.12
2000	0.2H	Fully-dev	110.0H		2 23:32:51.82
20	0.2H	Inviscid-core	2.2H		0 00:04:43.21
20	0.3H	Inviscid-core	2.2H		0 00:07:45.44
20	0.4H	Inviscid-core	2.2H	Effect	0 00:09:07.74
20	0.5H	Inviscid-core	2.2H	of	0 00:10:47.43
200	0.2H	Inviscid-core	11.0H	step	0 00:49:04.14
200	0.3H	Inviscid-core	11.0H	height	0 01:15:36.18
200	0.4H	Inviscid-core	11.0H	on	0 02:40:35.81
200	0.5H	Inviscid-core	11.0H	separation	0 04:10:14.78
500	0.2H	Inviscid-core	32.5H	region	0 06:26:52.48
500	0.3H	Inviscid-core	32.5H		0 10:47:03.67
500	0.4H	Inviscid-core	32.5H		1 03:50:45.79
20	0.3H	Fully-dev	2.2H	Effect of	0 00:18:19.98
50	0.3H	Fully-dev	4.0H	Reynolds	0 00:44:33.64
100	0.3H	Fully-dev	8.0H	number on	0 00:24:51.98
200	0.3H	Fully-dev	12.0H	separation	0 02:08:35.05
500	0.3H	Fully-dev	32.5H	region	0 10:47:03.67
20	0.2H	Inviscid-core	2.2H		0 00:04:43.21
50	0.2H	Inviscid-core	3.4H		0 00:11:00.81
100	0.2H	Inviscid-core	6.5H		0 00:31:52.23
200	0.2H	Inviscid-core	11.0H	Effect	0 00:49:04.14
500	0.2H	Inviscid-core	32.5H	of	0 06:26:52.48
1000	0.2H	Inviscid-core	55.0H	Reynolds	0 12:52:31.50
2000	0.2H	Inviscid-core	110.0H	number on	1 20:21:31.61
20	0.2H	Profile-dev	2.2H	separation	0 00:08:10.08
50	0.2H	Profile-dev	6.0H	and	0 00:35:28.24
100	0.2H	Profile-dev	8.5H	reattachment	0 01:01:18.85
200	0.2H	Profile-dev	14.0H	points	0 02:02:19.48
500	0.2H	Profile-dev	38.5H		0 09:35:33.49
1000	0.2H	Profile-dev	70.0H		1 01:05:31.14
2000	0.2H	Profile-dev	130.0H		4 06:51:40.12

Table 11 (cont'd.)

20	0.2H	Fully-dev	2.2H	0 00:08:10.08
50	0.2H	Fully-dev	4.0H	0 00:13:55.13
100	0.2H	Fully-dev	6.5H	0 00:52:20.60
200	0.2H	Fully-dev	12.0H	0 01:29:09.86
500	0.2H	Fully-dev	32.5H	0 06:24:38.59
1000	0.2H	Fully-dev	55.0H	0 14:36:38.03
2000	0.2H	Fully-dev	110.0H	2 23:32:51.82

Table 12. **The Y-values for selected streamlines for the flow past a backward step in the profile-development region, $(Re)_H$=20**

X	ψ=0.05	ψ=0.1	ψ=0.2	ψ=0.5	ψ=0.7	ψ=0.8
0.00	.2050	.3000	.3750	.5985	.7475	.8220
0.05	.2066	.3011	.3760	.5976	.7463	.8210
0.10	.2100	.3156	.3882	.5954	.7350	.8058
0.15	.2130	.3254	.3969	.5934	.7258	.7940
0.20	.2154	.3317	.4027	.5914	.7184	.7850
0.25	.2166	.3355	.4060	.5892	.7123	.7779
0.30	.2169	.3371	.4074	.5869	.7072	.7723
0.35	.2163	.3366	.4071	.5843	.7027	.7675
0.40	.2143	.3340	.4053	.5814	.6986	.7634
0.45	.2111	.3291	.4019	.5782	.6949	.7597
0.50	.1812	.3217	.3969	.5746	.6914	.7562
0.55	.1529	.3125	.3903	.5706	.6879	.7528
0.60	.1206	.3025	.3828	.5663	.6843	.7500
0.65	.1017	.2900	.3746	.5617	.6808	.7466
0.70	.0795	.2776	.3663	.5569	.6771	.7438
0.75	.0672	.2664	.3581	.5520	.6734	.7409
0.80	.0649	.2565	.3502	.5471	.6699	.7381
0.85	.0558	.2473	.3417	.5422	.6664	.7353
0.90	.0528	.2381	.3340	.5375	.6629	.7326
0.95	.0508	.2304	.3271	.5329	.6596	.7300
1.00	.0479	.2241	.3209	.5287	.6564	.7276
1.05	.0447	.2188	.3155	.5247	.6534	.7253
1.10	.0423	.2144	.3108	.5210	.6506	.7232
1.15	.0404	.2108	.3067	.5176	.6482	.7213
1.20	.0389	.2077	.3031	.5145	.6460	.7195
1.25	.0378	.2052	.3001	.5118	.6440	.7179
1.30	.0369	.2031	.2972	.5093	.6423	.7165
1.35	.0361	.2014	.2947	.5072	.6408	.7153
1.40	.0356	.2000	.2926	.5054	.6394	.7143
1.45	.0351	.1985	.2909	.5037	.6383	.7134
1.50	.0348	.1974	.2895	.5024	.6373	.7126
1.55	.0345	.1964	.2883	.5012	.6365	.7120
1.60	.0343	.1957	.2874	.5002	.6359	.7116
1.65	.0342	.1951	.2866	.5000	.6354	.7112
1.70	.0340	.1947	.2860	.4988	.6350	.7109
1.75	.0340	.1943	.2856	.4984	.6347	.7108
1.80	.0340	.1941	.2853	.4980	.6346	.7107
1.85	.0340	.1939	.2850	.4978	.6345	.7107
1.90	.0340	.1938	.2848	.4976	.6344	.7107
1.95	.0340	.1938	.2848	.4975	.6344	.7107
2.00	.0340	.1938	.2848	.4975	.6344	.7107
2.05	.0340	.1938	.2848	.4975	.6344	.7107
2.10	.0340	.1938	.2848	.4975	.6344	.7107
2.15	.0340	.1938	.2848	.4975	.6344	.7107
2.20	.0340	.1938	.2848	.4975	.6344	.7107
2.25	.0340	.1938	.2848	.4975	.6344	.7107
2.30	.0340	.1938	.2848	.4975	.6344	.7107
2.35	.0340	.1938	.2848	.4975	.6344	.7107

Table 13. **The Y-values for selected streamlines for the flow past a backward step in the inviscid core region, $(Re)_H=200$**

X	ψ=0.005	ψ=0.1	ψ=0.2	ψ=0.5	ψ=0.7	ψ=0.8
0.05	.2119	.3222	.3930	.6000	.7380	.8065
0.20	.2139	.3232	.3940	.6000	.7378	.8059
0.40	.2178	.3357	.4063	.6000	.7286	.7936
0.80	.2184	.3420	.4133	.6000	.7230	.7866
1.20	.2189	.3449	.4164	.6000	.7203	.7835
1.80	.2196	.3480	.4196	.5998	.7173	.7800
2.40	.2201	.3500	.4216	.5994	.7146	.7773
3.00	.2201	.3503	.4219	.5979	.7119	.7742
3.50	.2191	.3477	.4190	.5933	.7049	.7692
3.60	.2187	.3464	.4177	.5916	.7033	.7669
3.70	.2180	.3445	.4158	.5894	.7017	.7646
3.80	.2171	.3419	.4133	.5867	.7001	.7623
3.90	.2152	.3380	.4098	.5834	.6968	.7599
3.95	.2134	.3353	.4077	.5815	.6951	.7582
4.00	.2085	.3320	.4052	.5794	.6932	.7564
4.05	.2039	.3285	.4025	.5771	.6913	.7545
4.10	.2000	.3245	.3994	.5747	.6892	.7525
4.15	.1867	.3204	.3958	.5721	.6870	.7503
4.20	.1771	.3160	.3920	.5713	.6877	.7482
4.25	.1683	.3116	.3881	.5666	.6823	.7461
4.30	.1603	.3071	.3840	.5637	.6799	.7441
4.35	.1529	.3025	.3800	.5607	.6773	.7420
4.40	.1403	.2974	.3759	.5577	.6748	.7398
4.45	.1268	.2917	.3718	.5547	.6722	.7375
4.50	.1165	.2862	.3677	.5516	.6696	.7354
4.60	.1017	.2758	.3598	.5456	.6644	.7311
4.70	.0814	.2665	.3524	.5397	.6593	.7269
4.80	.0693	.2581	.3447	.5341	.6545	.7227
4.90	.0623	.2507	.3375	.5289	.6500	.7185
5.00	.0577	.2427	.3311	.5242	.6463	.7153
5.20	.0524	.2299	.3205	.5161	.6395	.7090
5.40	.0489	.2210	.3125	.5098	.6355	.7050
5.60	.0443	.2148	.3066	.5056	.6315	.7023
5.80	.0417	.2105	.3024	.5023	.6293	.7009
6.00	.0402	.2076	.2995	.5001	.6277	.6993
6.40	.0386	.2044	.2952	.4988	.6273	.6998
6.80	.0378	.2029	.2940	.4985	.6283	.7016
7.40	.0375	.2018	.2932	.5000	.6305	.7040
7.60	.0371	.2012	.2929	.5000	.6317	.7053
8.20	.0368	.2006	.2921	.5000	.6326	.7066
8.60	.0364	.2001	.2913	.5000	.6334	.7080
9.20	.0360	.1992	.2903	.5000	.6342	.7096
10.00	.0357	.1982	.2894	.5000	.6350	.7107
10.60	.0357	.1976	.2892	.5000	.6356	.7113
11.20	.0357	.1976	.2892	.5000	.6350	.7116
12.20	.0357	.1976	.2892	.5000	.6350	.7121
12.80	.0357	.1976	.2892	.5000	.6350	.7121
13.40	.0357	.1976	.2892	.5000	.6350	.7121
14.00	.0357	.1976	.2892	.5000	.6350	.7121

Table 14

X
0.00
.55
1.05
1.55
2.05
4.05
6.05
8.05
9.05
9.55
9.65
9.75
9.85
9.95
.00
.10
.20
.30
.40
.50
.60
.80
.20
.40
.60
.80
.00
.50
.00
.50
.00
.50
.00
.50
.00
.50
.00
.00
.00
.00
.00
.00
.00
.00
.00
.00
.00
.00

Table 14. The Y-values for selected streamlines for the flow past a backward step in the profile-development region, $(Re)_H$=2000

X	ψ=0.005	ψ=0.1	ψ=0.2	ψ=0.5	ψ=0.7	ψ=0.8
0.00	.2220	.3310	.4000	.6000	.7330	.7991
0.55	.2200	.3320	.4019	.6000	.7320	.7981
1.05	.2173	.3324	.4030	.6000	.7310	.7970
1.55	.2162	.3326	.4034	.6000	.7308	.7967
2.05	.2162	.3329	.4040	.6000	.7302	.7959
4.05	.2167	.3360	.4074	.6000	.7276	.7925
6.05	.2173	.3385	.4100	.5998	.7253	.7897
8.05	.2174	.3399	.4114	.5989	.7225	.7865
9.05	.2168	.3388	.4103	.5955	.7193	.7833
9.55	.2157	.3365	.4080	.5933	.7156	.7796
9.65	.2154	.3356	.4072	.5922	.7145	.7785
9.75	.2150	.3346	.4062	.5910	.7132	.7773
9.85	.2145	.3334	.4050	.5896	.7117	.7758
9.95	.2137	.3318	.4035	.5879	.7100	.7742
10.00	.2133	.3309	.4026	.5870	.7091	.7733
10.10	.2122	.3287	.4006	.5850	.7070	.7714
10.20	.2096	.3260	.3982	.5827	.7049	.7692
10.30	.2064	.3230	.3953	.5801	.7022	.7668
10.40	.2032	.3197	.3921	.5773	.6995	.7642
10.50	.2005	.3160	.3881	.5742	.6966	.7614
10.60	.1921	.3122	.3849	.5710	.6935	.7584
10.80	.1768	.3039	.3769	.5639	.6869	.7518
11.20	.1528	.2833	.3597	.5484	.6725	.7385
11.40	.1330	.2730	.3509	.5405	.6651	.7316
11.60	.1161	.2633	.3416	.5327	.6578	.7249
11.80	.1040	.2544	.3329	.5254	.6508	.7185
12.00	.0859	.2455	.3251	.5186	.6445	.7125
12.50	.0604	.2270	.3099	.5051	.6322	.7004
13.00	.0528	.2166	.3008	.4969	.6277	.6938
13.50	.0502	.2117	.2961	.4932	.6216	.6912
14.00	.0492	.2100	.2948	.4927	.6216	.6916
14.50	.0494	.2102	.2953	.4950	.6232	.6935
15.00	.0497	.2105	.2964	.4955	.6252	.6958
15.50	.0497	.2110	.2974	.4970	.6268	.6978
16.00	.0492	.2116	.2980	.4982	.6285	.6995
16.50	.0483	.2109	.2980	.4987	.6292	.7005
17.00	.0472	.2105	.2981	.4993	.6300	.7016
18.00	.0451	.2092	.2973	.4994	.6306	.7026
19.00	.0433	.2079	.2963	.4996	.6308	.7032
20.00	.0422	.2067	.2955	.4998	.6310	.7038
25.00	.0380	.2030	.2925	.5000	.6320	.7058
30.00	.0370	.2007	.2910	.5000	.6320	.7078
40.00	.0360	.1984	.2895	.5000	.6320	.7090
50.00	.0350	.1975	.2881	.5000	.6320	.7100
60.00	.0350	.1965	.2878	.5000	.6320	.7100
70.00	.0348	.1962	.2876	.5000	.6320	.7100
80.00	.0347	.1959	.2872	.5000	.6320	.7100
90.00	.0346	.1959	.2868	.5000	.6320	.7100

Table 15. Summary of cases studied for a finite step

$(Re)_H$	Step height	Step position	Step length	Computational domain	purpose	CPU time
20	0.3H	Fully-dev	1.H	2.9H	Effect of	0 00:32:27.79
20	0.3H	Fully-dev	1.H	4.4H	downstream	0 01:04:01.78
200	0.3H	Inviscid-core	1.H	15.5H	length on	0 02:39.36.21
200	0.3H	Inviscid-core	1.H	18.0H	separation	0 03:25:55.59
					region	
20	0.3H	Fully-dev	2.H	3.9H	Effect of	0 00:27:14.46
20	0.3H	Fully-dev	1.H	2.9H	step	0 00:22:45.18
200	0.3H	Inviscid-core	1.H	15.5H	length on	0 02:39:36.21
200	0.3H	Inviscid-core	2.H	16.5H	separation	0 02:47:54.68
200	0.3H	Inviscid-core	4.H	18.5H	region	0 03:40:00.39
20	0.3H	Inviscid-core	1.H	2.6H		0 00:16:34.08
20	0.3H	Profile-dev	1.H	3.1H		0 00:22:45.18
20	0.3H	Fully-dev	1.H	2.9H	Effect of	0 00:32:27.79
200	0.3H	Inviscid-core	1.H	15.5H	step	0 02:39:36.21
200	0.3H	Profile-dev	1.H	17.2H	position	0 03:08:48.26
200	0.3H	Fully-dev	1.H	16.2H	on	0 04:02:22.66
500	0.3H	Inviscid-core	1.H	36.5H	separation	0 11:36:29.60
500	0.3H	Profile-dev	1.H	45.0H	region	0 13:17:28.62
500	0.3H	Fully-dev	1.H	39.0H		0 18:30:30.93
20	0.2H	Inviscid-core	1.H	2.6H		0 00:15:33.99
20	0.3H	Inviscid-core	1.H	2.6H		0 00:16:34.08
20	0.4H	Inviscid-core	1.H	2.6H		0 00:18:41.81
20	0.5H	Inviscid-core	1.H	2.6H	Effect of	0 00:23:12.63
200	0.2H	Inviscid-core	1.H	15.5H	step	0 03:43:51.59
200	0.3H	Inviscid-core	1.H	15.5H	height	0 02:39:36.21
200	0.4H	Inviscid-core	1.H	15.5H	on	0 08:51:26.13
200	0.5H	Inviscid-core	1.H	15.5H	separation	0 14:42:32.75
500	0.2H	Inviscid-core	1.H	36.5H	region	0 17:22:51.43
500	0.3H	Inviscid-core	1.H	36.5H		0 11:36:29.60
500	0.4H	Inviscid-core	1.H	36.5H		1 06:12:04.45
20	0.3H	Inviscid-core	1.H	2.6H		0 00:16:34.08
50	0.3H	Inviscid-core	1.H	4.8H		0 00:53:41.08
100	0.3H	Inviscid-core	1.H	8.4H		0 02:23:27.22
200	0.3H	Inviscid-core	1.H	15.5H		0 02:39:36.21
500	0.3H	Inviscid-core	1.H	36.5H		0 11:36:29.60
1000	0.3H	Inviscid-core	1.H	72.5H	Effect of	2 01:37:59.41
1300	0.3H	Inviscid-core	1.H	88.5H	Reynolds	3 02:49:26.68
20	0.3H	Profile-dev	1.H	2.9H	number	0 00:22:45.18
50	0.3H	Profile-dev	1.H	5.8H	on	0 01:06:13.55
100	0.3H	Profile-dev	1.H	10.1H	separation	0 02:44:28.51
200	0.3H	Profile-dev	1.H	17.2H	region	0 03:08:48.26
500	0.3H	Profile-dev	1.H	45.0H		0 13:17:28.62
1000	0.3H	Profile-dev	1.H	87.2H		2 11:06:04.09
1300	0.3H	Profile-dev	1.H	103.5H		3 14:56:18.67

Table 15 (cont'd.)

20	0.3H	Fully-dev	1.H	2.9H	0 00:32:27.79
50	0.3H	Fully-dev	1.H	5.3H	0 01:33:37.90
100	0.3H	Fully-dev	1.H	9.6H	0 03:44:45.73
200	0.3H	Fully-dev	1.H	16.2H	0 04:02:22.66
500	0.3H	Fully-dev	1.H	39.0H	0 18:30:30.93
1000	0.3H	Fully-dev	1.H	77.2H	3 01:42:19.25
1300	0.3H	Fully-dev	1.H	88.5H	4 07:18:20.88

Table 16. **Effect of downstream length on the downstream separation streamline Y-coordinate for the finite step of 0.3H located in the fully-developed region, $(Re)_H = 20$**

X	Length=1.35H	Length=2.85H
0.00	0.2200 (Ys)	0.2200 (Ys)
0.05	0.2190	0.2190
0.10	0.2021	0.2020
0.15	0.1665	0.1664
0.20	0.1284	0.1283
0.25	0.0774	0.0771
0.26 (Xr)	0.0000	0.0000

Table 17. **Effect of downstream length on the downstream separation streamline Y-coordinate for the finite step of 0.3H located in the inviscid-core region, $(Re)_H = 200$**

X	length=13.25H Y	length=17.75H Y
0.00	0.2788 (Ys)	0.2788 (Ys)
0.05	0.2785	0.2785
0.15	0.2769	0.2768
0.25	0.2692	0.2692
0.35	0.2594	0.2593
0.45	0.2471	0.2471
0.55	0.2257	0.2257
0.65	0.2078	0.2077
0.75	0.1825	0.1825
0.85	0.1575	0.1574
0.95	0.1212	0.1211
1.05	0.0813	0.0812
1.21 (Xr)	0.0000	0.0000

Table 18. Effect of step length on the downstream separation streamline Y-coordinate for the finite step of height of 0.3H located in the inviscid-core region, $(Re)_H$=20

X	Step length=2H Y	Step length=1H Y
0.00	0.2205 (Ys)	0.2202 (Ys)
0.05	0.2203	0.2190
0.10	0.2029	0.2019
0.15	0.1685	0.1656
0.20	0.1325	0.1284
0.25	0.0844	0.0791
0.26 (Xr)	0.0000	0.0000

Table 19. Effect of step position on the downstream separation streamline Y-coordinate for the finite step of height 0.3H, $(Re)_H$=20

X	Inviscid-core Y	Profile-development Y	Fully-developed Y
0.00	0.2200 (Ys)	0.2200 (Ys)	0.2200 (Ys)
0.05	0.2190	0.2192	0.2191
0.10	0.2019	0.2020	0.2019
0.15	0.1665	0.1666	0.1665
0.20	0.1284	0.1285	0.1284
0.25	0.0771	0.0772	0.0771
0.26 (Xr)	0.0000	0.0000	0.0000

Table 20. Effect of step position on the downstream separation streamlines Y-coordinate for the finite step of height 0.3H, **$(Re)_H$**=200

X	Inviscid-core	Profile-development	Fully-developed
0.00	0.2800 (Ys)	0.2805 (Ys)	0.2810 (Ys)
0.05	0.2794	0.2797	0.2794
0.15	0.2780	0.2789	0.2781
0.25	0.2705	0.2707	0.2706
0.35	0.2608	0.2610	0.2609
0.45	0.2500	0.2508	0.2502
0.55	0.2286	0.2291	0.2287
0.65	0.2100	0.2109	0.2105
0.75	0.1872	0.1880	0.1878
0.85	0.1611	0.1613	0.1612
0.95	0.1279	0.1284	0.1282
1.05	0.1001	0.1010	0.1006
1.15	0.0508	0.0520	0.0516
1.30 X(r)	0.0000	0.0000	0.0000

Table 21

X
0.05
0.10
0.20
0.25
0.30
0.35
0.40
0.45
0.50
0.55
0.60
0.65
0.70
0.75
0.80
0.85
0.90
0.95
1.00
1.20
1.40
1.50
1.55
1.60
1.65
1.70
1.75
1.80
1.85
1.90
1.95
2.00
2.10
2.20
2.30
2.40
2.50
2.60
2.80
3.00

Table 21. The Y-values for selected streamlines for the flow past a finite step located in the profile-development region, $(Re)_H$=20

X	ψ=0.005	ψ=0.1	ψ=0.2	ψ=0.5	ψ=0.7	ψ=0.8
0.05	.0101	.1627	.2411	.5387	.7008	.7801
0.10	.0159	.1800	.2847	.5594	.7054	.7820
0.20	.0413	.2182	.3278	.5706	.7124	.7833
0.25	.0552	.2532	.3597	.5843	.7169	.7843
0.30	.0708	.2919	.3905	.5971	.7218	.7863
0.35	.1067	.3336	.4186	.6086	.7268	.7890
0.40	.1766	.3700	.4430	.6189	.7318	.7919
0.45	.3061	.3971	.4619	.6279	.7364	.7948
0.50	.3099	.4126	.4757	.6355	.7406	.7975
0.55	.3130	.4214	.4848	.6414	.7438	.7987
0.60	.3162	.4298	.4935	.6467	.7470	.8020
0.65	.3173	.4341	.4982	.6504	.7488	.8032
0.70	.3185	.4377	.5025	.6534	.7510	.8049
0.75	.3187	.4391	.5044	.6551	.7518	.8057
0.80	.3189	.4407	.5060	.6565	.7528	.8060
0.85	.3188	.4409	.5062	.6569	.7537	.8059
0.90	.3187	.4410	.5066	.6571	.7538	.8057
0.95	.3185	.4405	.5061	.6564	.7524	.8051
1.00	.3183	.4398	.5056	.6560	.7514	.8043
1.20	.3168	.4348	.5004	.6500	.7459	.7990
1.40	.3137	.4248	.4886	.6390	.7370	.7915
1.50	.3009	.4134	.4778	.6308	.7304	.7862
1.55	.2718	.4044	.4703	.6259	.7266	.7831
1.60	.2429	.3915	.4616	.6203	.7224	.7797
1.65	.2112	.3763	.4518	.6142	.7179	.7761
1.70	.1807	.3613	.4400	.6077	.7130	.7722
1.75	.1538	.3459	.4277	.6007	.7078	.7680
1.80	.1221	.3283	.4155	.5934	.7024	.7637
1.85	.1029	.3127	.4037	.5859	.6970	.7592
1.90	.0828	.2986	.3910	.5785	.6918	.7546
1.95	.0702	.2830	.3787	.5711	.6866	.7501
2.00	.0627	.2699	.3675	.5638	.6814	.7461
2.10	.0545	.2500	.3478	.5501	.6715	.7386
2.20	.0503	.2313	.3303	.5377	.6626	.7317
2.30	.0440	.2190	.3170	.5273	.0548	.7258
2.40	.0399	.2106	.3072	.5188	.6485	.7210
4.50	.0374	.2048	.3000	.5142	.6438	.7205
2.60	.0358	.2024	.2950	.5120	.6412	.7190
2.80	.0356	.2000	.2900	.5100	.6400	.7180
3.00	.0356	.2000	.2900	.5100	.6400	.7180

Table 22. The Y-values for selected streamlines for the flow past a finite step located in the profile-development region, $(Re)_H=200$

X	$\psi=0.05$	$\psi=0.1$	$\psi=0.2$	$\psi=0.5$	$\psi=0.7$	$\psi=0.8$
0.05	.0677	.1170	.2116	.5001	.6931	.7885
0.25	.1048	.1549	.2422	.5006	.6735	.7587
0.55	.1172	.1738	.2596	.5013	.6618	.7427
0.75	.1198	.1756	.2644	.5020	.6590	.7391
1.05	.1225	.1798	.2695	.5037	.6575	.7368
1.25	.1245	.1825	.2727	.5054	.6576	.7365
1.55	.1283	.1876	.2787	.5094	.6594	.7375
1.75	.1320	.1925	.2841	.5138	.6623	.7397
2.05	.1411	.2032	.2966	.5248	.6705	.7465
2.55	.1768	.2459	.3438	.5664	.7028	.7740
2.75	.2207	.2921	.3876	.5961	.7237	.7904
2.85	.2706	.3352	.4197	.6126	.7344	.7985
2.95	.3509	.3875	.4531	.6281	.7427	.8061
3.00	.3655	.4036	.4656	.6349	.7485	.8095
3.05	.3753	.4139	.4755	.6409	.7524	.8124
3.15	.3883	.4272	.4894	.6503	.7586	.8169
3.25	.3957	.4348	.4979	.6565	.7627	.8196
3.35	.3990	.4387	.5024	.6601	.7647	.8208
3.45	.3997	.4401	.5043	.6616	.7652	.8205
3.55	.3985	.4397	.5045	.6615	.7643	.8192
3.65	.3963	.4382	.5034	.6601	.7623	.8170
3.75	.3934	.4356	.5013	.6577	.7595	.8140
3.85	.3898	.4323	.4980	.6543	.7558	.8105
3.95	.3849	.4277	.4934	.6501	.7515	.8062
4.05	.3772	.4213	.4875	.6450	.7466	.8013
4.15	.3680	.4136	.4805	.6391	.7412	.7963
4.35	.3481	.3948	.4639	.6254	.7289	.7853
4.55	.3203	.3710	.4447	.6098	.7150	.7729
4.65	.3075	.3594	.4338	.6015	.7076	.7663
4.85	.2773	.3336	.4124	.5845	.6928	.7525
5.05	.2507	.3091	.4022	.5681	.6789	.7402
5.15	.2352	.2981	.3913	.5603	.6722	.7345
5.45	.2019	.2658	.3808	.5395	.6543	.7192
5.75	.1758	.2437	.3547	.5238	.6414	.7076
6.25	.1562	.2209	.3337	.5084	.6297	.6978
6.75	.1489	.2120	.3133	.5025	.6265	.6965
7.05	.1465	.2095	.3045	.5015	.6269	.6977
8.05	.1429	.2060	.2999	.5021	.6311	.7039
9.05	.1403	.2034	.2956	.5024	.6338	.7080
10.05	.1382	.2012	.2930	.5020	.6350	.7099
11.05	.1367	.1996	.2911	.5015	.6357	.7111
12.05	.1357	.1983	.2987	.5011	.6362	.7118
13.05	.1350	.1976	.2888	.5009	.6365	.7123
14.05	.1346	.1970	.2881	.5006	.6366	.7127
15.05	.1340	.1963	.2877	.5000	.6367	.7129
16.05	.1339	.1960	.2874	.5000	.6368	.7130
17.25	.1338	.1955	.2868	.5000	.6369	.7132

Table 23. The Y-values for selected streamlines for the flow past a finite step located in the profile-development region, $(Re)_H = 1300$

X	$\psi=0.05$	$\psi=0.1$	$\psi=0.2$	$\psi=0.5$	$\psi=0.7$	$\psi=0.8$
0.05	.0658	.1146	.2095	.5000	.6943	.7904
0.55	.1117	.1620	.2485	.5000	.6679	.7579
1.05	.1126	.1646	.2520	.5000	.6651	.7480
1.55	.1123	.1652	.2531	.5000	.6643	.7470
2.05	.1128	.1663	.2545	.5001	.6634	.7457
4.05	.1165	.1717	.2607	.5013	.6607	.7417
6.05	.1319	.1904	.2809	.5176	.6723	.7512
7.05	.1945	.2585	.3539	.5815	.7232	.7951
7.15	.2114	.2765	.3720	.5950	.7328	.8029
7.25	.2363	.3032	.3961	.6100	.7429	.8112
7.35	.2780	.3406	.4250	.6255	.7530	.8190
7.45	.3509	.3884	.4561	.6402	.7620	.8261
7.50	.3666	.4023	.4683	.6467	.7666	.8292
7.60	.3840	.4249	.4861	.6575	.7735	.8342
7.70	.3964	.4341	.4976	.6652	.7783	.8376
7.80	.4026	.4411	.5045	.6702	.7812	.8392
8.00	.4057	.4463	.5095	.6737	.7822	.8385
8.20	.4033	.4441	.5082	.6717	.7788	.8343
8.40	.3977	.4385	.5037	.6669	.7733	.8284
8.50	.3932	.4350	.5008	.6638	.7700	.8252
8.55	.3908	.4334	.4991	.6622	.7683	.8235
8.65	.3860	.4292	.4954	.6587	.7646	.8200
8.75	.3810	.4250	.4914	.6550	.7610	.8164
8.85	.3760	.4206	.4871	.6511	.7572	.8126
8.95	.3709	.4160	.4827	.6471	.7532	.8088
9.05	.3658	.4114	.4782	.6430	.7492	.8049
9.15	.3608	.4067	.4736	.6387	.7451	.8008
9.25	.3558	.4019	.4688	.6343	.7410	.7969
9.45	.3438	.3900	.4592	.6254	.7326	.7892
9.65	.3300	.3780	.4506	.6161	.7239	.7812
9.85	.3175	.3665	.4380	.6066	.7150	.7729
10.05	.3057	.3552	.4273	.5969	.7058	.7643
10.55	.2723	.3250	.3995	.5722	.6829	.7426
11.15	.2307	.2850	.3665	.5443	.6570	.7189
12.05	.1882	.2497	.3316	.5147	.6302	.6935
13.05	.1693	.2316	.3173	.5035	.6209	.6860
14.05	.1676	.2306	.3176	.5061	.6250	.6911
15.05	.1678	.2312	.3197	.5104	.6239	.6973
16.05	.1659	.2302	.3194	.5119	.6230	.7005
17.05	.1626	.2269	.3171	.5112	.6224	.7015
18.05	.1594	.2235	.3144	.5099	.6219	.7017
20.05	.1549	.2185	.3103	.5081	.6212	.7026
30.05	.1434	.2066	.2995	.5044	.6192	.7076
40.05	.1386	.2017	.2937	.5026	.6180	.7103
50.05	.1363	.2008	.2906	.5016	.6171	.7117
60.05	.1351	.2000	.2889	.5010	.6165	.7125
70.05	.1350	.2000	.2889	.5010	.6165	.7124
78.45	.1350	.2000	.2889	.5010	.6165	.7124

Table 24. Summary of cases studied for a single step

$(Re)_H$	Step height	Step position	Step length	Computational domain	purpose	CPU time
20	0.3H	Inviscid-core	0.05H	1.7H	Effect	0 00:11:54.09
20	0.3H	Profile-dev	0.05H	2.0H	of step	0 00:13:02.56
20	0.3H	Fully-dev	0.05H	3.0H	position on	0 00:30:17.42
200	0.3H	Invisicid-core	0.05H	14.6H	separation	0 02:45:51.50
200	0.3H	Profile-dev	0.05H	15.6H	region	0 05:16:37.31
200	0.3H	Fully-dev	0.05H	14.6H		0 04:51:57.80
200	0.1H	Inviscid-core	0.05H	14.6H	Effect	0 01:07:47.32
200	0.2H	Inviscid-core	0.05H	14.6H	of step	0 01:24:55.30
200	0.3H	Inviscid-core	0.05H	14.6H	height on	0 02:45:51.50
200	0.4H	Inviscid-core	0.05H	14.6H	separation	0 05:45:15.46
200	0.5H	Inviscid-core	0.05H	14.6H	region	0 09:54:12.91
20	0.3H	Inviscid-core	0.05H	1.7H	Effect	0 00:11:54.09
50	0.3H	Inviscid-core	0.05H	3.9H	of Reynolds	0 00:39:08.59
100	0.3H	Inviscid-core	0.05H	7.5H	number on	0 02:06:07.06
200	0.3H	Inviscid-core	0.05H	14.6H	separation	0 02:45:51.50
500	0.3H	Inviscid-core	0.05H	36.3H	region	0 20:00:59.71

Table 25.

I	ϕ
0.05	.
0.10	.
0.15	.
0.20	.
0.25	.
0.30	.
0.35	
0.40	.
0.45	
0.50	
0.55	
0.60	
0.65	
0.70	
0.75	
0.80	
0.85	
0.90	
1.00	
1.10	
1.20	
1.30	
1.40	
1.50	
1.60	
1.80	
2.00	

Table 25. The Y-values for selected streamlines for the flow past a single step located in the inviscid core region, $(Re)_H$=20

X	ψ=0.05	ψ=0.1	ψ=0.2	ψ=0.5	ψ=0.7	ψ=0.8
0.05	.0988	.1802	.3139	.5637	.7231	.8046
0.10	.2430	.3206	.4032	.6036	.7385	.8084
0.15	.3497	.3867	.4531	.6299	.7492	.8119
0.20	.3757	.4177	.4828	.6477	.7570	.8151
0.25	.3975	.4377	.5026	.6596	.7625	.8176
0.30	.4079	.4509	.5141	.6673	.7660	.8192
0.35	.4127	.4562	.5204	.6716	.7679	.8199
0.40	.4128	.4573	.5224	.6733	.7682	.8196
0.45	.4089	.4547	.5211	.6728	.7671	.8184
0.50	.4020	.4489	.5170	.6704	.7649	.8164
0.55	.3896	.4389	.5107	.6665	.7616	.8133
0.60	.3748	.4271	.5027	.6613	.7573	.8096
0.65	.3594	.4142	.4921	.6549	.7523	.8052
0.70	.3412	.4006	.4801	.6477	.7467	.8002
0.75	.3206	.3831	.4677	.6396	.7408	.7954
0.80	.3020	.3664	.4550	.6310	.7344	.7904
0.85	.2695	.3406	.4310	.6220	.7278	.7850
0.90	.2501	.3170	.4100	.6080	.7209	.7795
1.00	.2237	.3000	.4002	.5943	.7067	.7680
1.10	.1973	.2716	.3737	.5761	.6930	.7565
1.20	.1754	.2503	.3521	.5593	.6804	.7460
1.30	.1613	.2316	.3327	.5440	.6689	.7370
1.40	.1518	.2183	.3174	.5307	.6587	.7291
1.50	.1437	.2086	.3055	.5192	.6498	.7225
1.60	.1377	.2015	.2954	.5092	.6429	.7172
1.80	.1370	.2013	.2951	.5090	.6423	.7169
2.00	.1370	.2013	.2951	.5090	.6423	.7169

Table

X
0.0
0.20
0.4
0.60
0.8
1.0
1.1
1.1
1.2
1.2
1.3
1.4
1.5
1.6
1.7
1.8
1.9
2.0
2.2
2.4
2.6
2.8
3.0
3.5
4.0
4.5
5.0
6.0
7.0
8.0
9.0
10.0
11.0
12.0
13.0
14.0
15.0

Table 26. The Y-values for selected streamlines for the flow past a single step located in the inviscid-core region, $(Re)_H=200$

X	ψ=0.05	ψ=0.1	ψ=0.2	ψ=0.5	ψ=0.7	ψ=0.8
0.05	.0688	.1189	.2144	.5036	.6963	.7913
0.20	.1058	.1574	.2479	.5137	.6891	.7745
0.40	.1286	.1855	.2772	.5273	.6893	.7690
0.60	.1382	.1979	.3020	.5439	.6974	.7737
0.80	.1690	.2201	.3317	.5662	.7111	.7836
1.00	.2140	.2830	.3789	.5955	.7288	.7963
1.10	.2644	.3279	.4025	.6112	.7379	.8028
1.15	.3081	.3570	.4299	.6187	.7421	.8058
1.20	.3452	.3809	.4457	.6256	.7460	.8087
1.25	.3579	.3948	.4575	.6317	.7494	.8111
1.30	.3657	.4046	.4664	.6369	.7524	.8131
1.40	.3766	.4161	.4785	.6446	.7568	.8159
1.50	.3826	.4220	.4849	.6489	.7589	.8169
1.60	.3839	.4236	.4872	.6500	.7588	.8162
1.70	.3811	.4218	.4862	.6492	.7569	.8139
1.80	.3753	.4172	.4824	.6460	.7533	.8102
1.90	.3671	.4103	.4765	.6412	.7484	.8053
2.00	.3574	.4018	.4689	.6350	.7426	.7995
2.20	.3298	.3774	.4503	.6196	.7286	.7869
2.40	.3006	.3518	.4268	.6019	.7127	.7727
2.60	.2657	.3223	.4038	.5834	.6962	.7578
2.80	.2342	.2967	.3806	.5658	.6811	.7438
3.00	.2079	.2719	.3608	.5500	.6675	.7321
3.50	.1654	.2167	.3249	.5217	.6432	.7111
4.00	.1509	.2146	.3079	.5083	.6329	.7024
4.50	.1448	.2082	.3012	.5036	.6305	.7015
5.00	.1426	.2058	.2986	.5034	.6315	.7038
6.00	.1405	.2036	.2960	.5033	.6345	.7084
7.00	.1385	.2016	.2936	.5030	.6359	.7107
8.00	.1369	.2002	.2918	.5023	.6364	.7117
9.00	.1359	.1989	.2901	.5017	.6367	.7123
10.00	.1352	.1976	.2894	.5013	.6368	.7127
11.00	.1347	.1972	.2884	.5009	.6369	.7129
12.00	.1343	.1962	.2875	.5007	.6370	.7131
13.00	.1341	.1962	.2866	.5005	.6370	.7130
14.00	.1339	.1960	.2857	.5000	.6370	.7130
15.00	.1339	.1960	.2857	.5000	.6370	.7130

Table 2

Relaxat factc
0.90
1.00
1.1
1.20
1.3
1.40
1.5
1.6
1.6
1.7
1.7
1.8
1.8
1.9

Table

Relaxa fact
0.9
1.0
1.1
1.2
1.3
1.4
1.5
1.5
1.5
1.7
1.7
1.8
1.8
1.9

[a] Comp

[b] The

Table 27. Relaxation factor (FS) vs. computing time*, h-1/15

Relaxation factor	Reynolds number 20	50	100	200	500	1000	2000
0.90	2.20	16.90	16.90	49.10	98.40	+	+
1.00	1.90	13.71	14.30	40.72	78.00	+	+
1.10	1.75	11.23	13.19	33.81	75.00	+	+
1.20	1.64	10.55	12.17	29.20	72.00	+	+
1.30	1.60	9.92	10.78	27.50	69.00	333.60	+
1.40	1.51	9.43	9.62	24.90	64.80	283.80	+
1.50	1.44	8.53	8.30	22.03	63.60	235.20	1087.20
1.60	1.40	8.35	7.91	19.38	60.60	192.00	909.60
1.65	1.28	8.14	7.10	16.97	56.40	175.20	806.40
1.70	1.37	7.40	7.06	16.76	55.20	163.20	774.00
1.75	1.40	7.48	7.30	16.90	54.60	150.60	582.60
1.80	1.44	7.60	7.50	17.48	79.20	144.00	381.60
1.85	1.50	8.92	8.20	22.82	86.40	157.80	418.80
1.90	1.60	10.10	8.60	25.05	100.20	177.00	490.80

Table 28. Relaxation factor (FS) vs. computing time*, h-1/20

Relaxation factor	Reynolds number 20	50	100	200	500	1000	2000
0.90	9.96	45.00	74.60	186.60	+	+	+
1.00	7.97	39.85	62.16	164.40	+	+	+
1.10	7.47	38.50	54.18	159.60	+	+	+
1.20	7.09	37.74	50.73	150.00	+	+	+
1.30	6.64	35.05	45.63	135.00	625.80	+	+
1.40	6.20	32.30	39.35	120.00	529.20	904.80	+
1.50	5.91	30.29	34.61	112.80	439.80	792.60	3314.40
1.60	5.40	29.50	31.96	93.60	372.00	688.80	2529.00
1.65	5.22	29.00	29.03	85.20	336.00	620.40	2012.00
1.70	5.11	28.24	28.70	79.80	303.00	577.80	1870.80
1.75	5.05	27.05	28.05	76.20	283.20	541.80	1716.00
1.80	5.30	31.50	27.40	72.00	252.60	504.00	1530.00
1.85	5.50	32.80	29.70	97.20	269.40	513.00	1752.60
1.90	5.90	36.20	32.20	112.80	326.40	528.00	2206.80

* Computing time is measured in minutes.
+ The run wasn't attempted, because the trend was obvious.

Table 29

Relaxat factor
0.90
1.00
1.05
1.10
1.15
1.20
1.25
1.30
1.35
1.40
1.45
1.50
1.65
1.70
1.85
1.90

Table

Relaxa fact
0.9
1.0
1.0
1.1
1.1
1.2
1.2
1.3
1.3
1.4
1.4
1.5
1.6
[illegible]
1.8
1.

Comp

The

Table 29. Relaxation factor (FV) vs. computing time*, h=1/15

Relaxation factor	Reynolds number 20	50	100	200	500	1000	2000
0.90	1.70	16.90	9.30	37.00	76.80	228.00	442.80
1.00	1.30	13.00	7.13	16.60	61.80	144.00	381.60
1.05	1.20	8.22	6.06	17.12	+	+	+
1.10	1.11	5.80	4.12	17.76	+	+	+
1.15	1.04	5.03	6.72	+	+	+	+
1.20	1.00	4.66	7.50	+	+	+	+
1.25	0.84	5.12	10.11	+	+	+	+
1.30	0.78	5.66	13.76	+	+	+	+
1.35	0.76	6.16	+	+	+	+	+
1.40	0.74	7.46	+	+	+	+	+
1.45	0.81	9.20	+	+	+	+	+
1.50	0.92	10.65	+	+	+	+	+
1.60	1.23	16.10	+	+	+	+	+
1.70	1.80	30.10	+	+	+	+	+
1.80	2.60	67.05	+	+	+	+	+
1.90	3.55	73.78	+	+	+	+	+

Table 30. Relaxation factor (FV) vs. computing time*, h=1/20

Relaxation factor	Reynolds number 20	50	100	200	500	1000	2000
0.90	6.20	34.20	34.80	83.60	354.00	642.00	1878.00
1.00	5.01	26.60	26.83	67.30	282.20	504.00	1530.00
1.05	4.94	24.30	24.04	80.30	+	+	+
1.10	4.88	22.05	20.33	99.20	+	+	+
1.15	4.39	19.80	19.02	+	+	+	+
1.20	4.15	17.66	20.90	+	+	+	+
1.25	3.77	15.55	26.54	+	+	+	+
1.30	3.40	13.60	35.10	+	+	+	+
1.35	2.92	17.38	+	+	+	+	+
1.40	2.66	23.05	+	+	+	+	+
1.45	2.48	26.90	+	+	+	+	+
1.50	2.35	30.00	+	+	+	+	+
1.60	3.01	34.50	+	+	+	+	+
1.70	4.50	40.50	+	+	+	+	+
1.80	8.01	50.00	+	+	+	+	+
1.90	8.60	52.90	+	+	+	+	+

* Computing time is measured in minutes.
\+ The numerical solution did not converge for these entries.

Table 3

Weighti factc
0.00
0.05
0.10
0.15
0.25
0.25
0.30
0.40
0.50
0.60
0.70
0.80
0.90
1.00

Table 3

Weighti facto
0.00
0.05
0.10
0.15
0.20
0.25
0.30
0.40
0.50
0.60
0.70
0.80
0.90
1.00

[a] Comp
[b] The r

Table 31. Weighting factor (KS) vs. computing time*, h=1/15

Weighting factor	Reynolds number 20	50	100	200	500	1000	2000
0.00	0.80	4.30	4.60	19.75	72.60	184.20	408.00
0.05	0.81	4.50	4.83	17.89	70.80	172.80	390.00
0.10	0.82	4.60	5.13	18.05	69.00	152.40	381.00
0.15	0.84	4.82	5.28	18.30	72.60	129.60	376.80
0.25	0.86	5.05	5.46	18.90	75.60	135.65	367.80
0.25	0.87	5.29	5.59	20.02	76.82	147.58	301.80
0.30	0.88	5.42	5.70	21.00	79.80	180.00	325.80
0.40	0.95	5.78	6.62	22.00	91.85	252.60	367.80
0.50	0.99	6.00	7.02	24.35	99.60	304.80	444.00
0.60	1.05	6.46	7.76	26.52	105.55	+	+
0.70	1.30	7.86	8.70	34.55	+	+	+
0.80	1.75	10.03	11.76	43.65	+	+	+
0.90	1.91	16.25	17.10	60.66	+	+	+
1.00	2.35	24.89	26.90	89.20	+	+	+

Table 32. Weighting factor (KS) vs. computing time*, h=1/20

Weighting factor	Reynolds numbers 20	50	100	200	500	1000	2000
0.00	2.25	14.90	32.70	60.00	291.00	1251.00	1974.00
0.05	1.79	14.30	25.41	49.20	288.60	1024.80	1850.40
0.10	1.20	14.00	20.91	46.30	283.80	922.20	1746.00
0.15	1.32	14.80	21.80	49.80	276.60	643.20	1679.40
0.20	1.50	16.00	22.38	57.00	319.80	564.00	1637.40
0.25	1.55	16.30	22.72	58.20	330.60	829.80	1590.00
0.30	1.65	16.80	23.26	59.40	349.20	1143.60	1573.20
0.40	2.05	20.95	23.56	63.00	381.70	1645.80	2430.60
0.50	2.50	21.00	26.70	64.80	469.20	2412.00	3133.80
0.60	3.10	21.66	31.23	67.20	580.20	+	+
0.70	3.47	25.98	36.03	69.60	+	+	+
0.80	4.15	34.90	42.31	93.00	+	+	+
0.90	4.96	52.33	59.95	115.20	+	+	+
1.00	6.05	73.55	80.70	138.90	+	+	+

* Computing time is measured in minutes.
+ The run wasn't attempted, because the trend was obvious.

Table 3

Weighti factor
0.10
0.15
0.20
0.25
0.30
0.35
0.40
0.45
0.50
0.55
0.60
0.65
0.70
0.75
0.80
0.85
0.90
1.00

Table 34

Weightin factor
0.10
0.15
0.20
0.25
0.30
0.35
0.40
0.45
0.50
0.55
0.60
0.65
0.70
0.75
0.80
0.85
0.90
1.00

Computi

The nur

Table 33. Weighting factor (KV) vs. computing time*, h=1/15

Weighting factor	Reynolds number 20	50	100	200	500	1000	2000
0.10	+	+	+	+	+	+	+
0.15	+	+	+	+	+	+	+
0.20	+	+	+	+	+	+	+
0.25	+	+	+	+	+	+	+
0.30	1.48	6.20	+	+	+	+	+
0.35	1.15	5.90	+	+	+	+	+
0.40	0.60	5.50	8.42	20.36	+	+	+
0.45	0.62	3.31	7.38	18.27	+	+	+
0.50	0.65	3.57	6.26	17.51	72.60	219.60	429.00
0.55	0.77	3.72	7.71	16.90	66.60	174.00	385.20
0.60	0.86	3.93	8.98	17.71	58.20	135.00	303.00
0.65	0.87	4.14	9.20	17.92	61.20	139.20	438.00
0.70	0.88	4.38	9.60	18.03	64.80	147.00	492.00
0.75	0.91	5.21	10.10	20.56	70.80	160.80	543.00
0.80	0.93	5.96	10.50	23.66	75.00	169.80	618.00
0.85	1.40	6.87	10.80	27.72	106.80	225.60	756.00
0.90	1.80	7.55	11.05	33.30	150.00	289.80	948.00
1.00	2.52	8.78	14.05	39.24	215.80	390.40	1205.00

Table 34. Weighting factor (KV) vs. computing time*, h=1/20

Weighting factor	Reynolds number 20	50	100	200	500	1000	2000
0.10	+	+	+	+	+	+	+
0.15	+	+	+	+	+	+	+
0.20	+	+	+	+	+	+	+
0.25	+	+	+	+	+	+	+
0.30	+	+	+	+	+	+	+
0.35	+	+	+	+	+	+	+
0.40	2.30	14.05	+	+	+	+	+
0.45	2.01	10.20	+	+	+	+	+
0.50	2.19	6.05	17.35	49.20	+	+	+
0.55	2.25	7.90	13.41	40.25	+	+	+
0.60	2.30	10.01	14.80	34.80	252.00	1173.00	1536.00
0.65	2.33	11.40	15.20	37.20	238.20	822.00	1422.00
0.70	3.37	12.05	17.03	39.00	223.80	564.00	1344.00
0.75	4.70	14.81	19.15	43.80	276.00	912.00	1506.00
0.80	5.41	18.52	20.83	46.80	348.00	1251.60	1782.00
0.85	7.90	25.70	34.50	66.00	363.00	1362.00	1968.00
0.90	9.25	32.80	46.40	73.80	385.80	1494.00	2232.00
1.00	14.70	40.15	60.05	86.92	412.70	1710.00	2668.00

* Computing time is measured in minutes.
\+ The numerical solution did not converge for these entries.

Table 1

Mesh size h
1.25
1.20

Table 35. Factors of reduction in the computing time

Mesh size h	Reynolds number 20	50	100	200	500	1000	2000
1/15	3.0	4.0	3.5	2.5	1.5	2.5	3.6
1/20	6.6	6.6	2.0	4.6	2.8	2.0	2.5

FIGURES


Uniform
Velocity
Profile

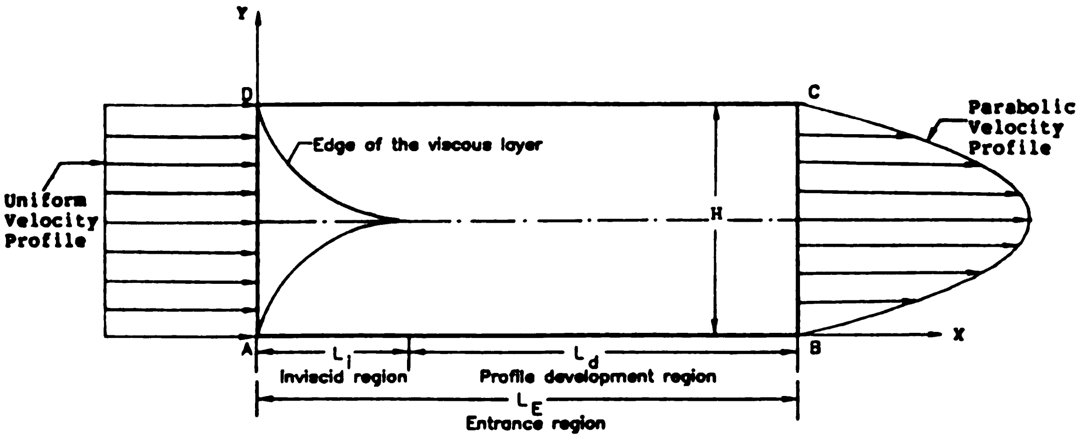

Figure 1. The two–dimensional channel.

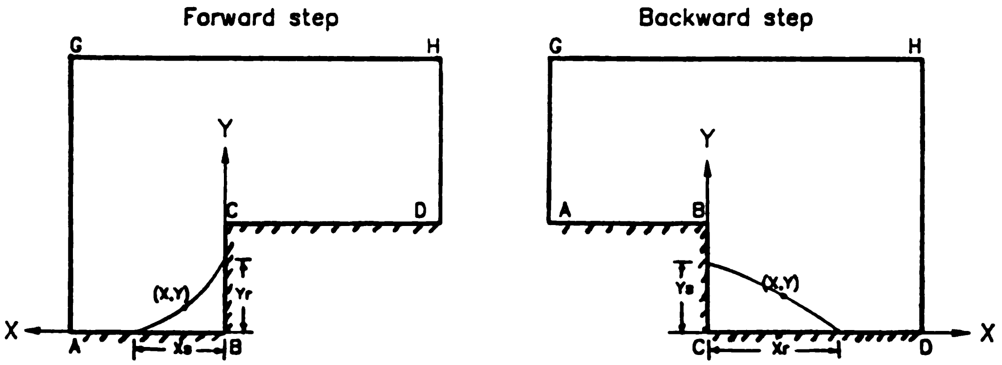

Figure 2. Forward and backward steps with notations.

lure

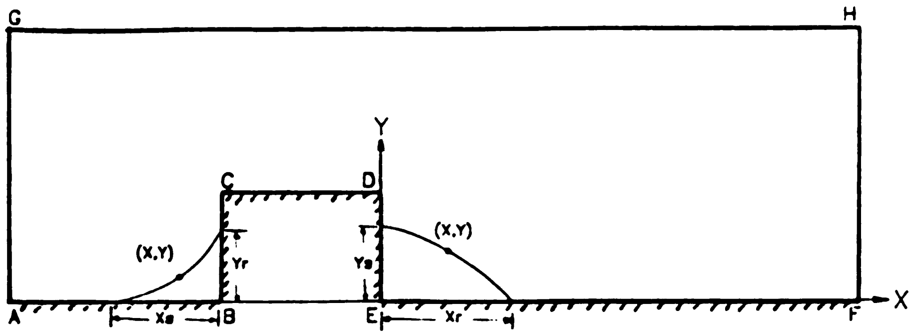

Figure 3. Finite step with notations.

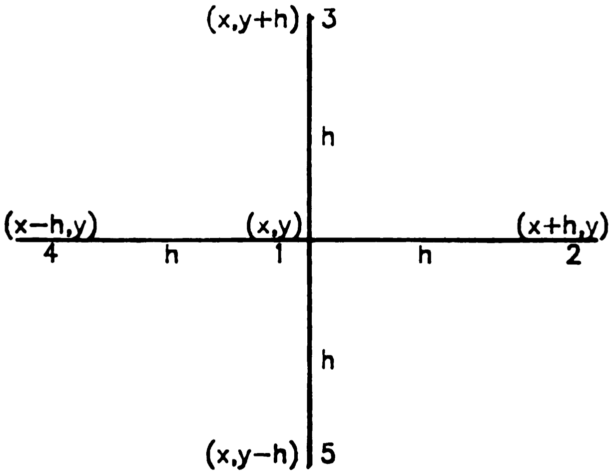

Figure 4. Finite difference representation of basic equations.


1.0

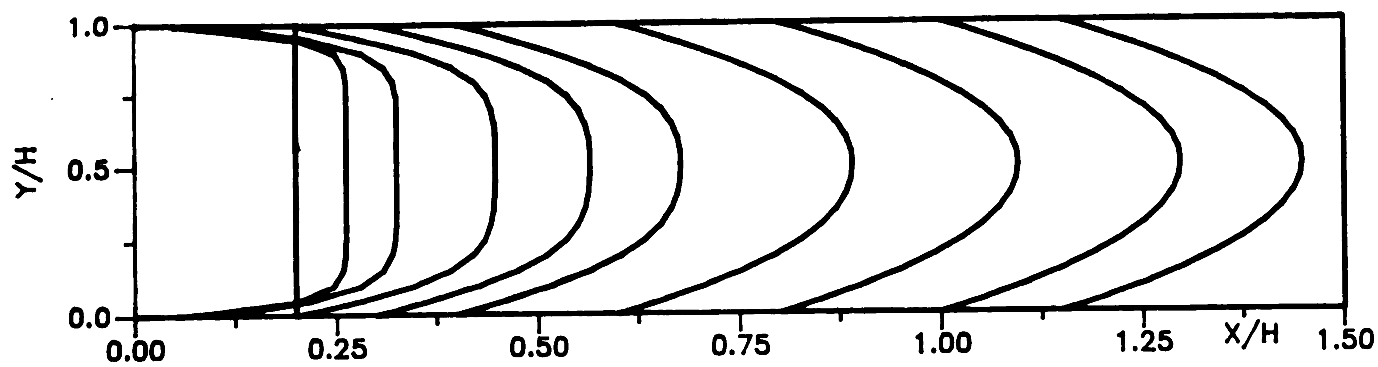

Figure 5. Flow development in the inlet region of a straight channel with uniform inlet velocity profile, $(Re)_H$=20.

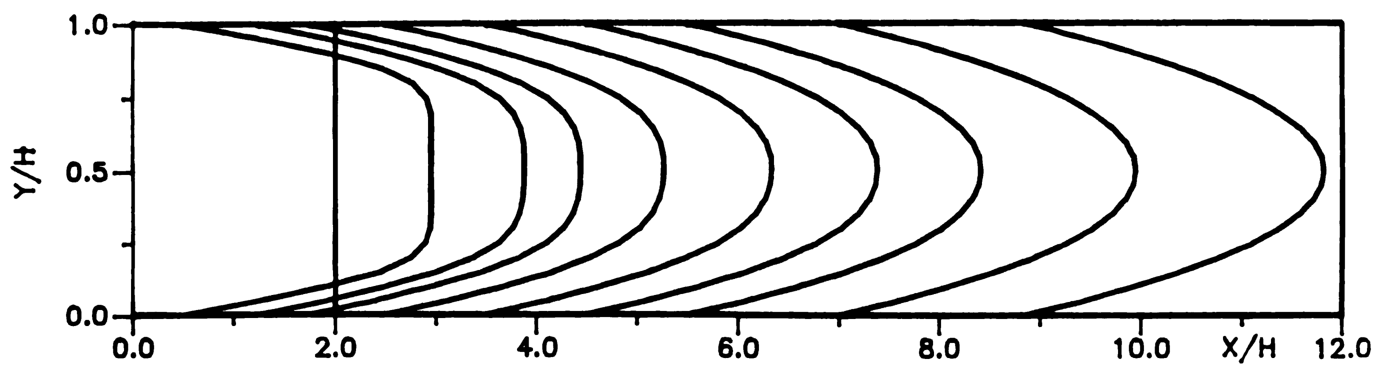

Figure 6. Flow development in the inlet region of the a straight channel with uniform inlet velocity profile, $(Re)_H$=200.

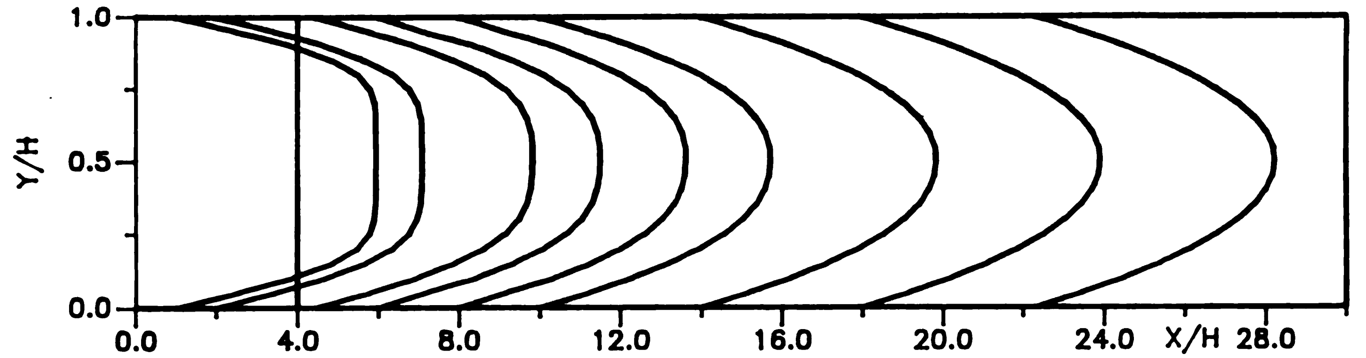

Figure 7. Flow development in the inlet region of a straight channel with uniform inlet velocity profile, $(Re)_H=500$.

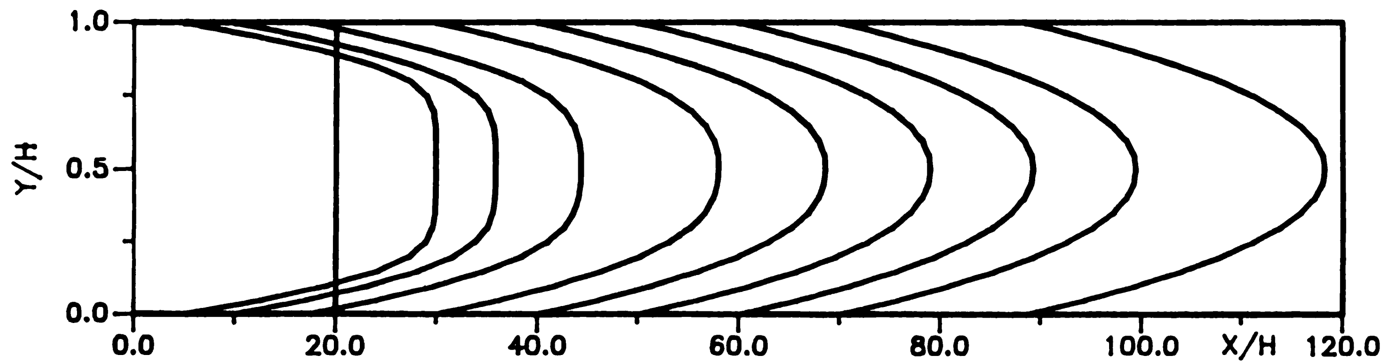

Figure 8. Flow development in the inlet region of a straight channel with uniform inlet velocity profile, $(Re)_H=2000$.

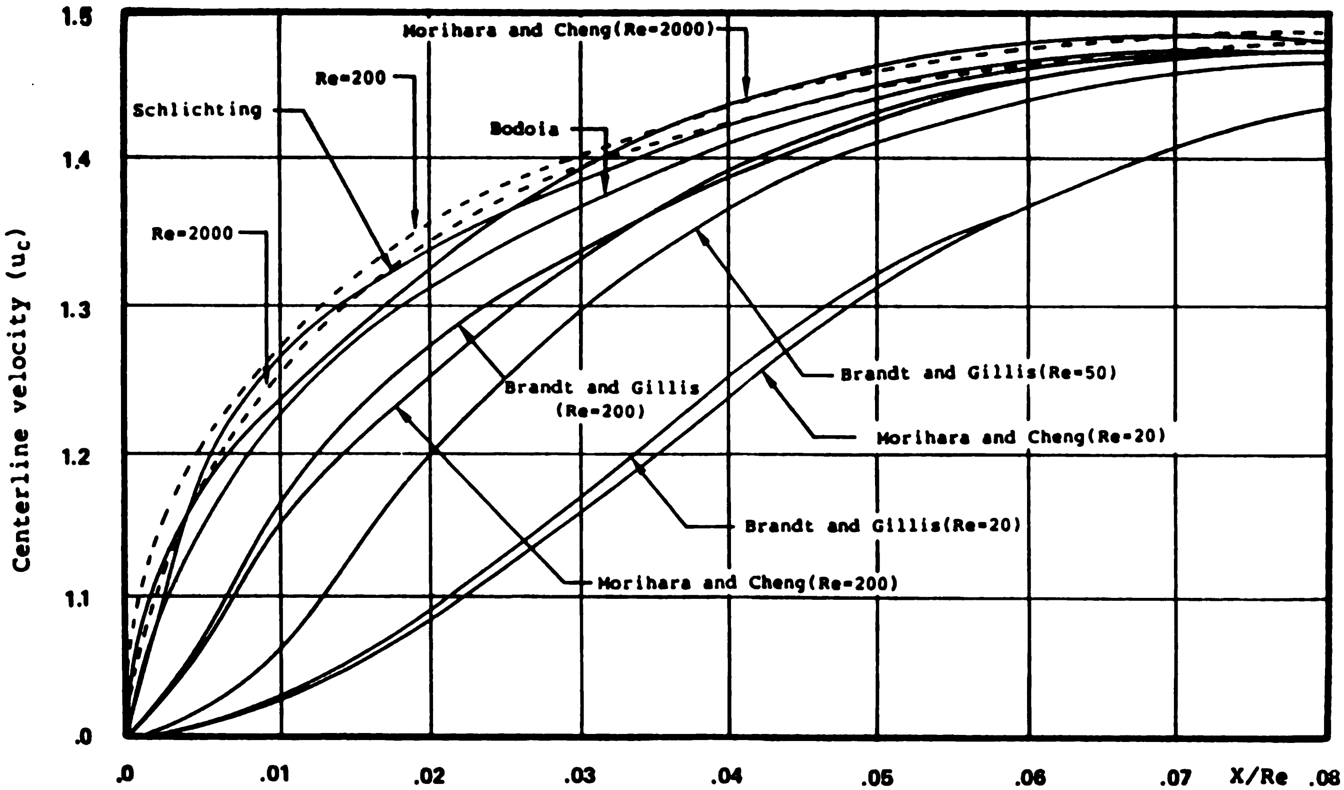

Figure 9. Comparison of centerline velocities.

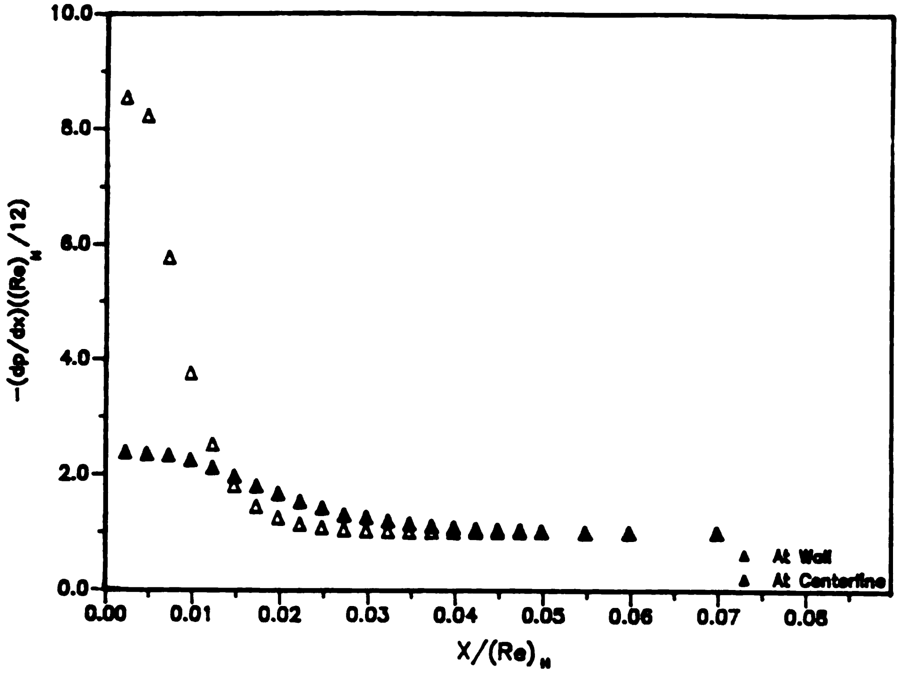

Figure 10. The streamwise pressure gradient, $(Re)_H=20$.

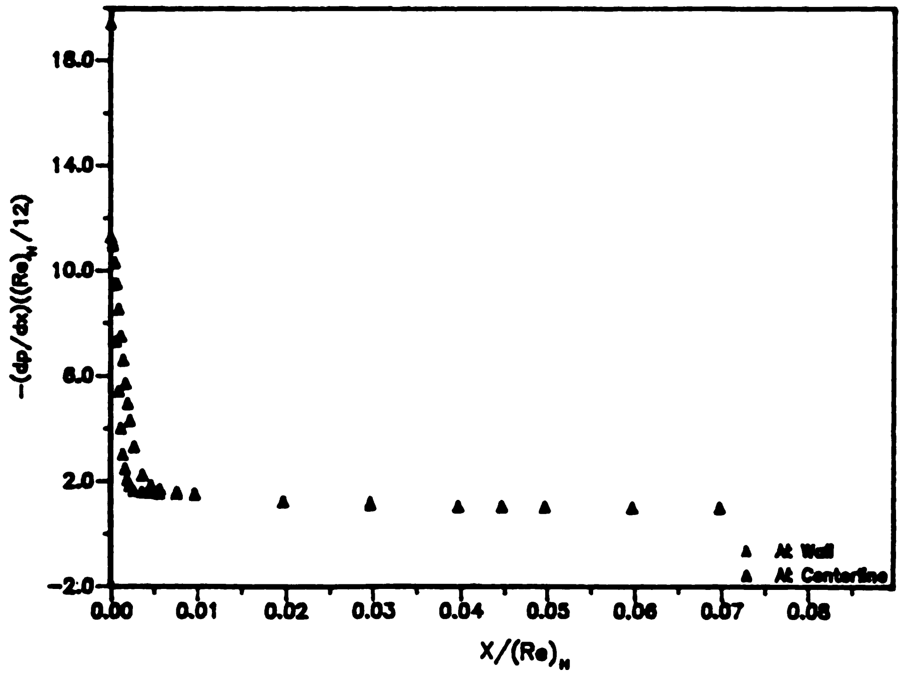

Figure 11. The streamwise pressure gradient, $(Re)_H=200$.

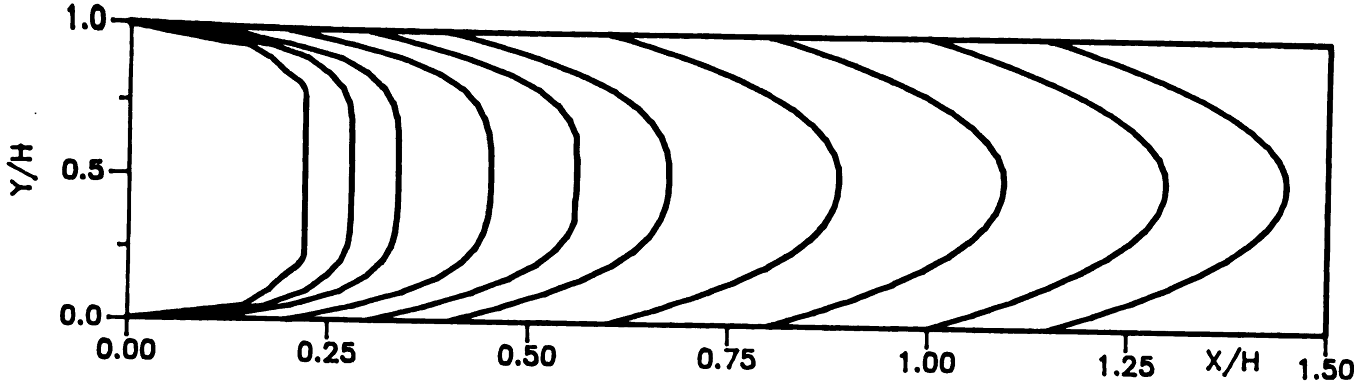

Figure 12. Flow development in the inlet region of a straight channel with an actual inlet velocity profile, $(Re)_H = 20$.

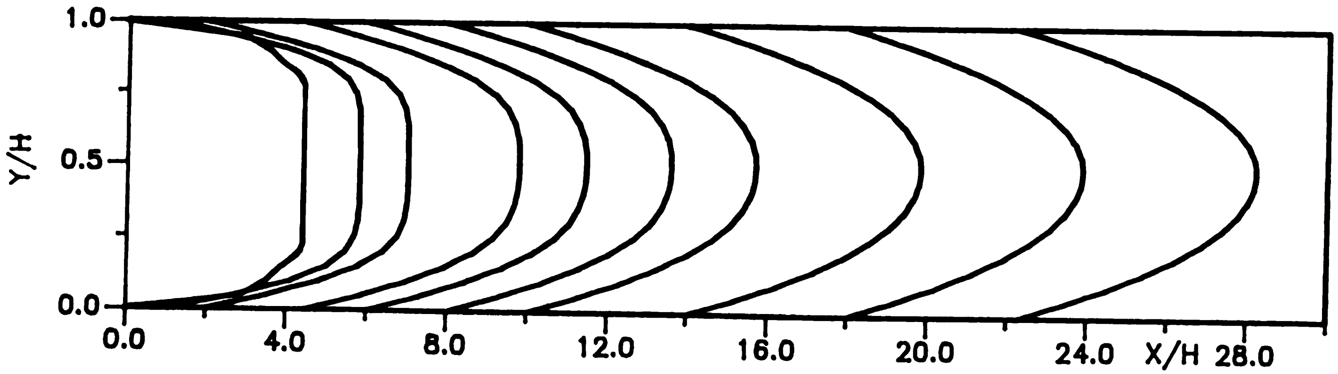

Figure 13. Flow development in the inlet region of a straight channel with an actual inlet velocity profile, $(Re)_H = 500$.

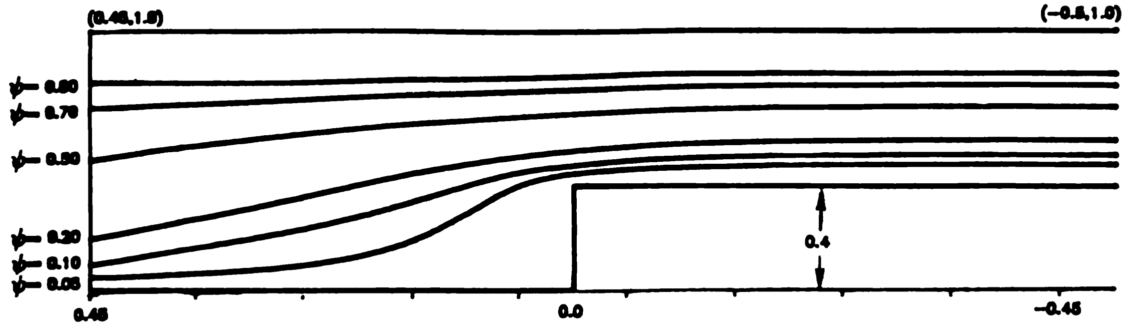

Figure 14. Streamlines in the vicinity of the forward step located in the profile-development region, $(Re)_H=20$.

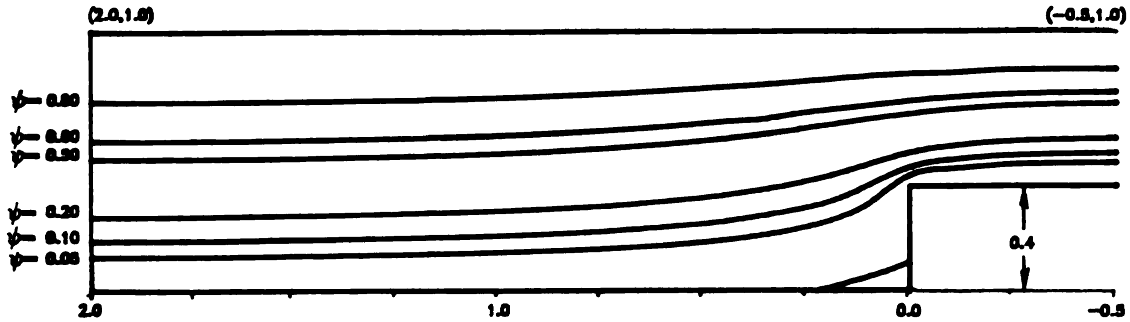

Figure 15. Streamlines in the vicinity of the forward step located in the profile-development region, $(Re)_H=200$.

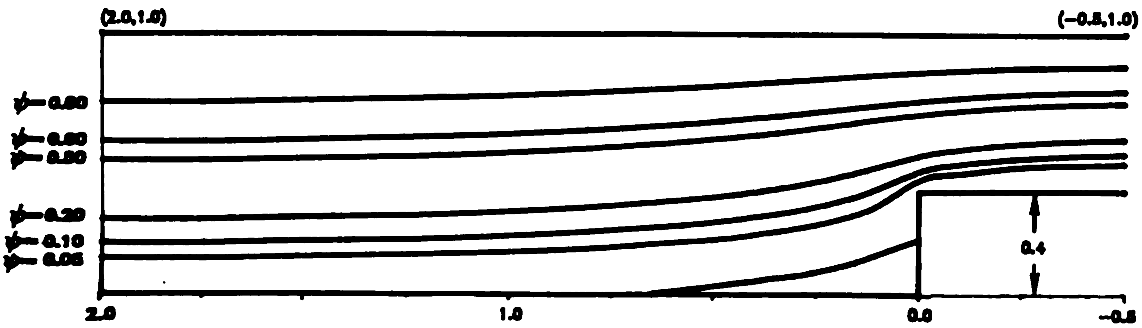

Figure 16. Streamlines in the vicinity of the forward step located in the profile-development region, $(Re)_H=2000$.

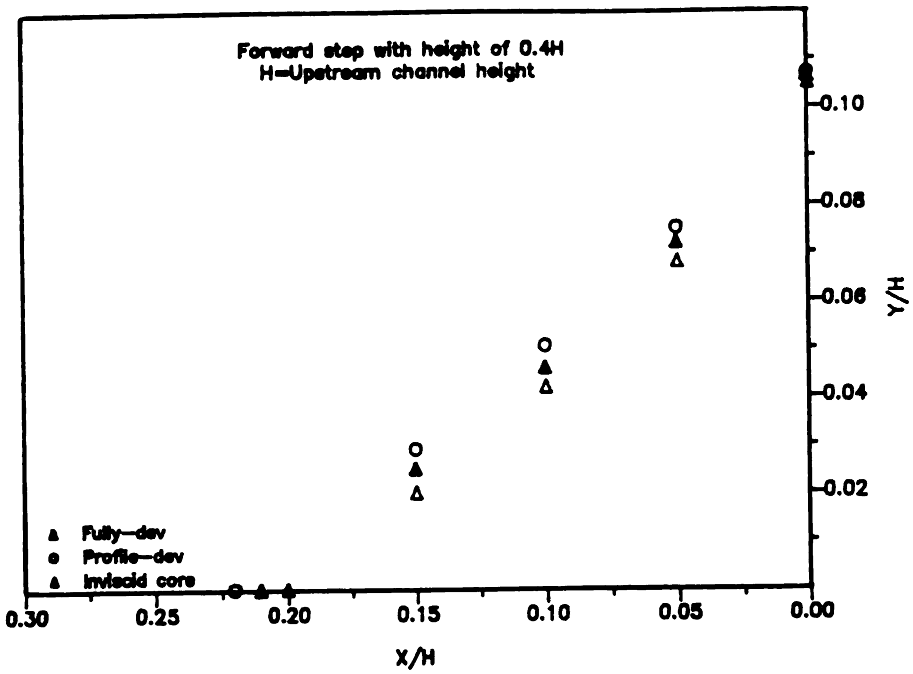

Figure 17. Effect of step position on separation region, $(Re)_H$=200.

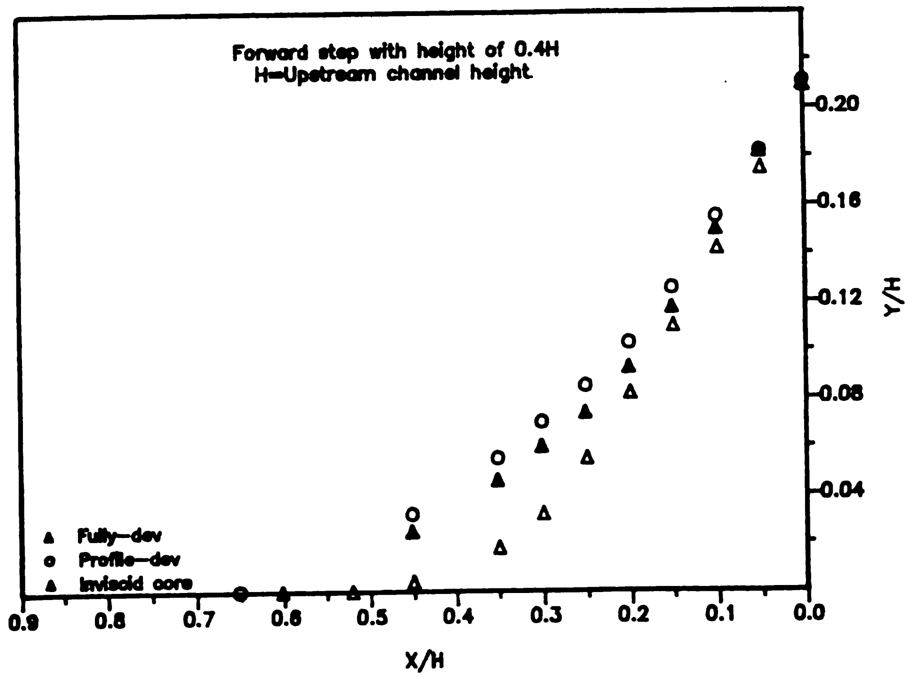

Figure 18. Effect of step position on separation region, $(Re)_H$=2000.

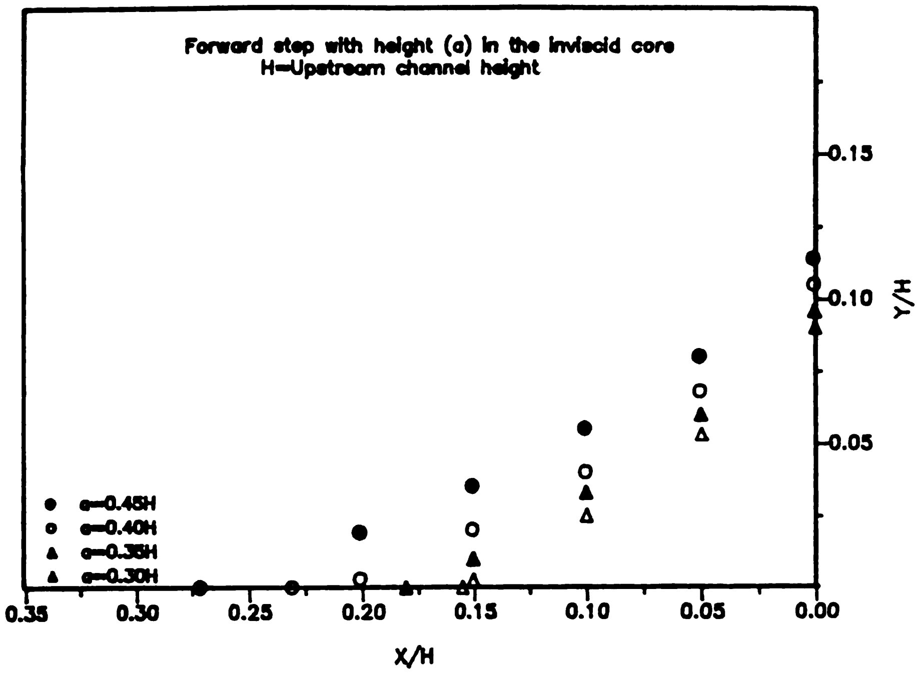

Figure 19. Effect of step height on separation region, $(Re)_H = 200$.

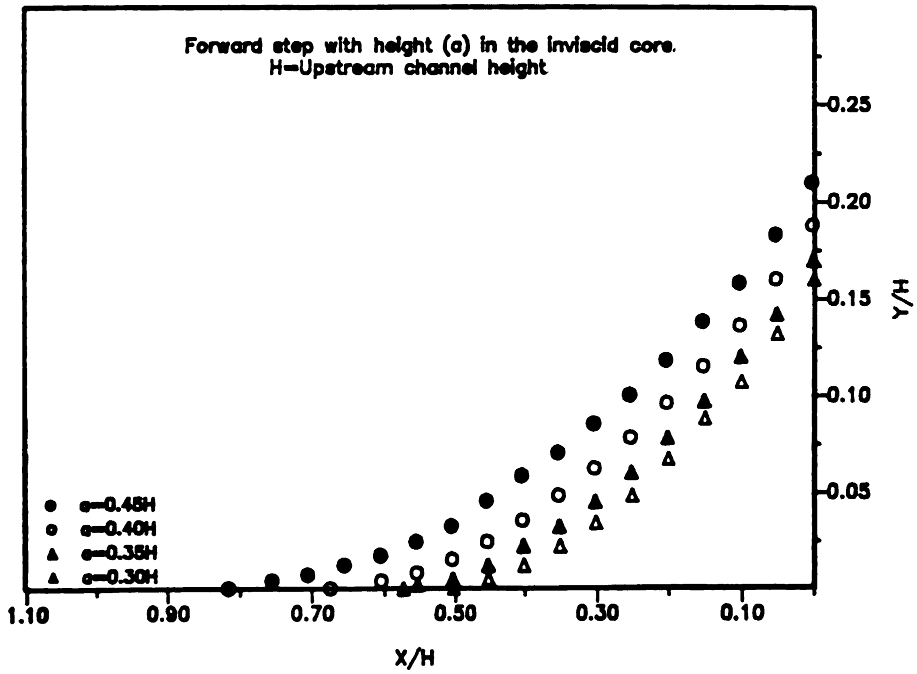

Figure 20. Effect of step height on separation region, $(Re)_H = 1000$.

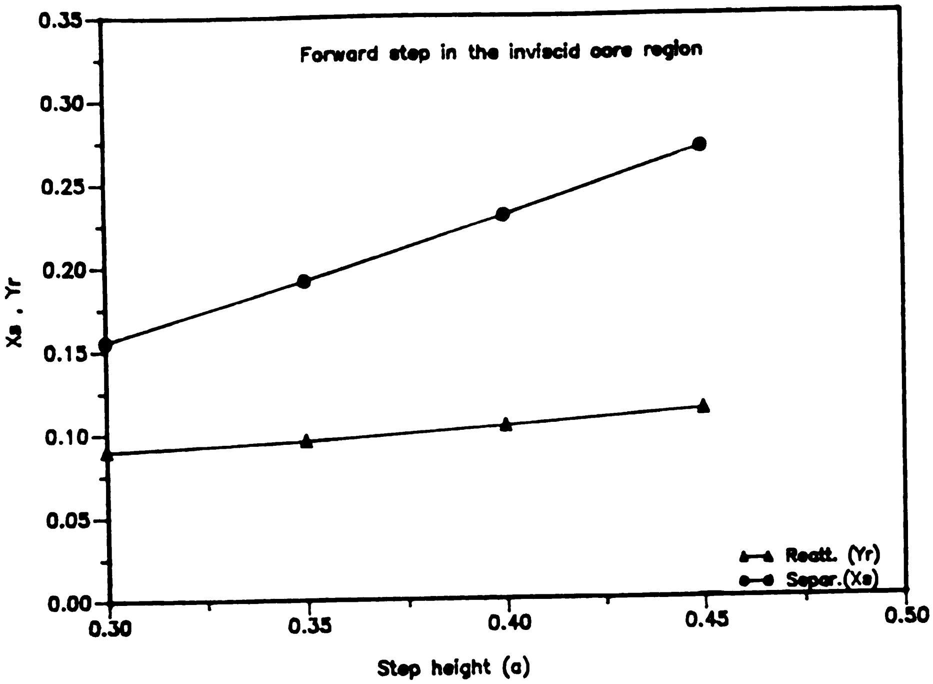

Figure 21. Effect of step height on separation and reattachment points, $(Re)_H=200$.

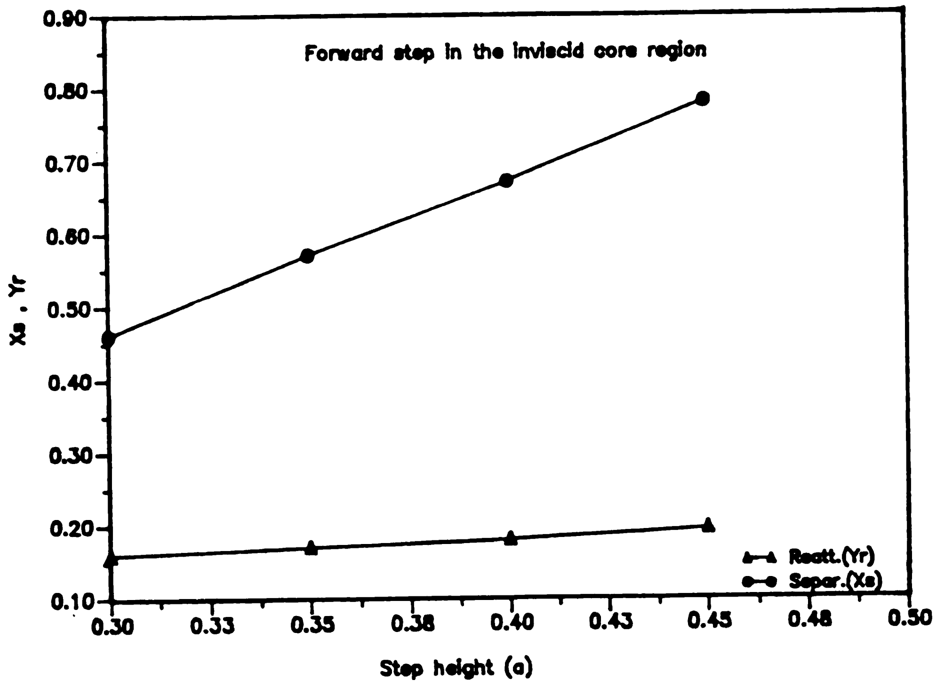

Figure 22. Effect of step height on separation and reattachment points, $(Re)_H=1000$.

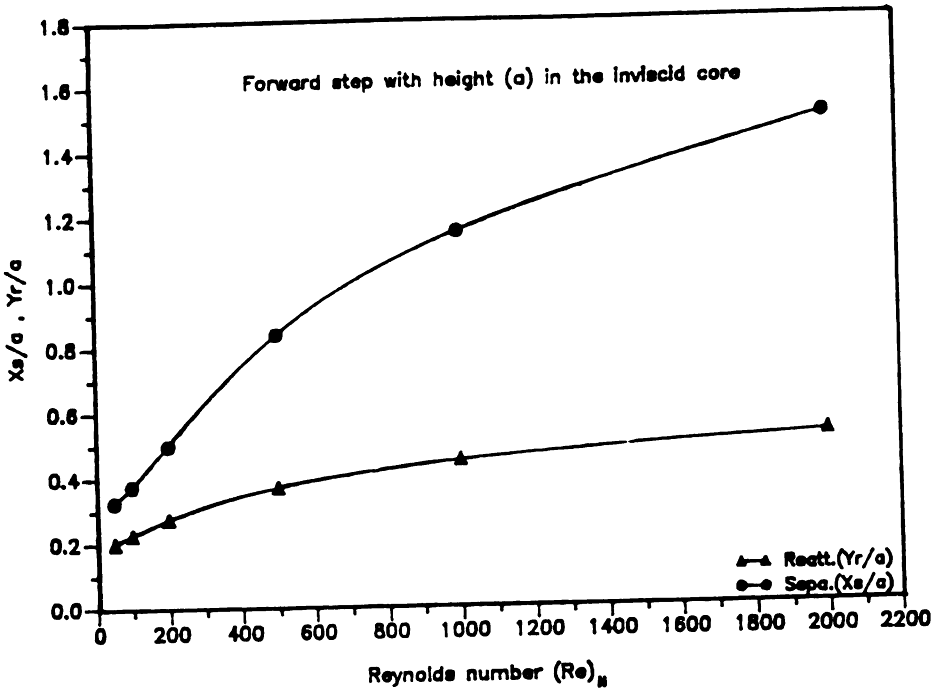

Figure 23. Separation and reattachment points for various Reynolds numbers.

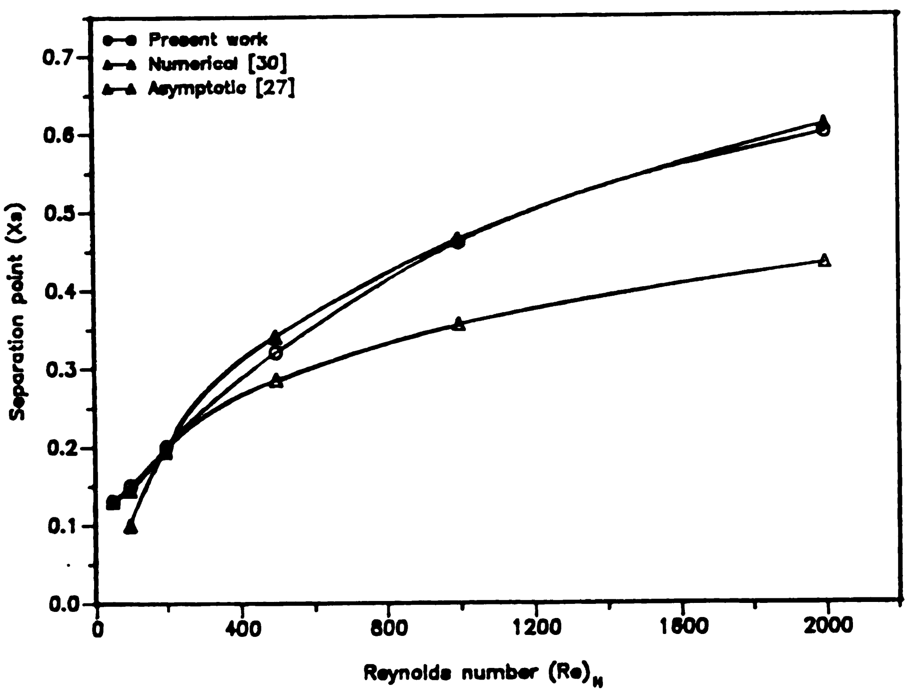

Figure 24. Comparison of separation point for a forward step with numerical results.

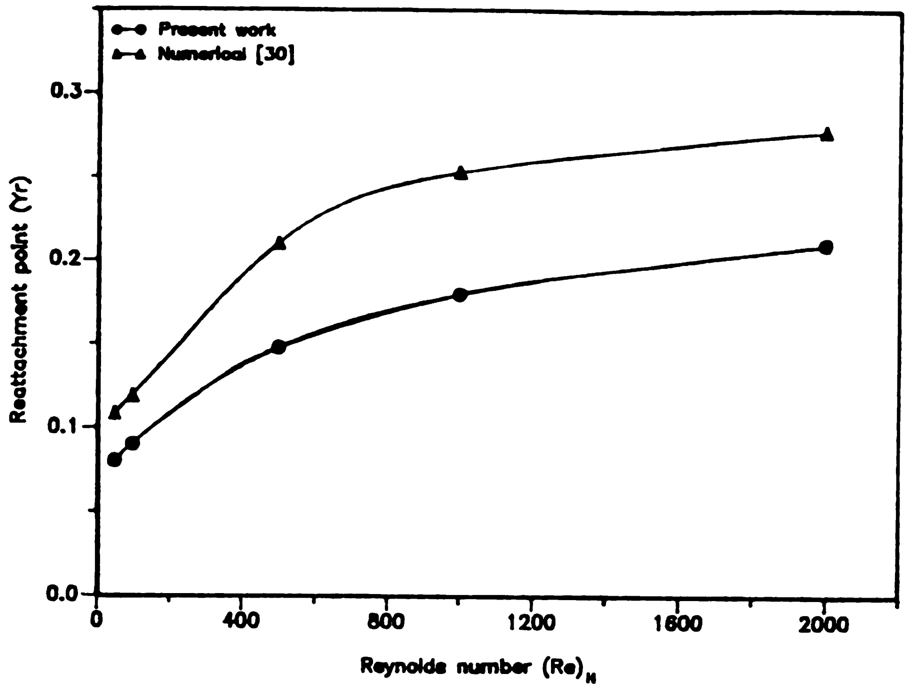

Figure 25. Comparison of reattachment point for a forward step with numerical results.

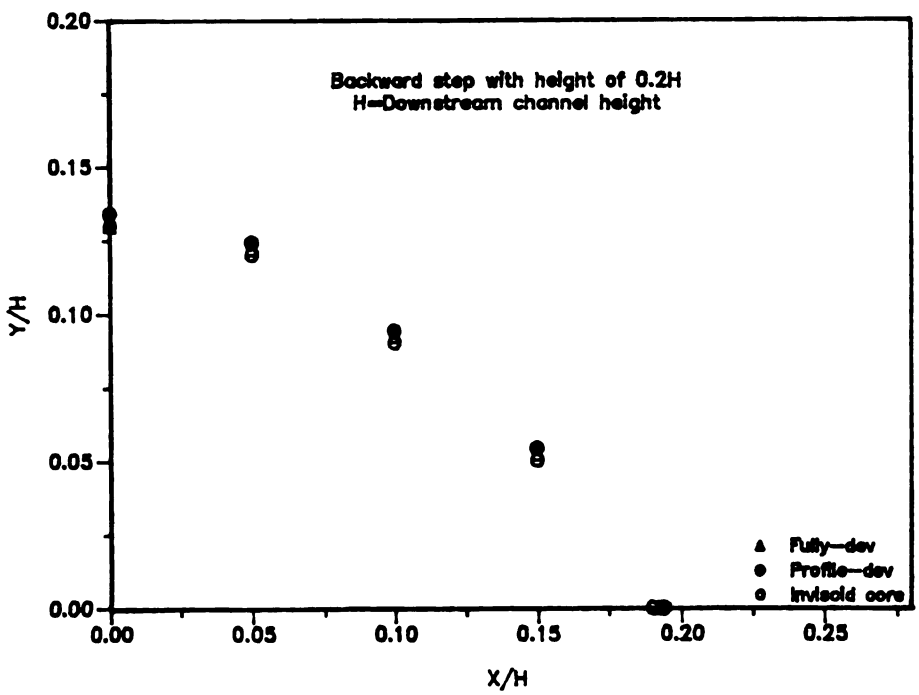

Figure 26. Effect of step position on separation region, $(Re)_H=20$.

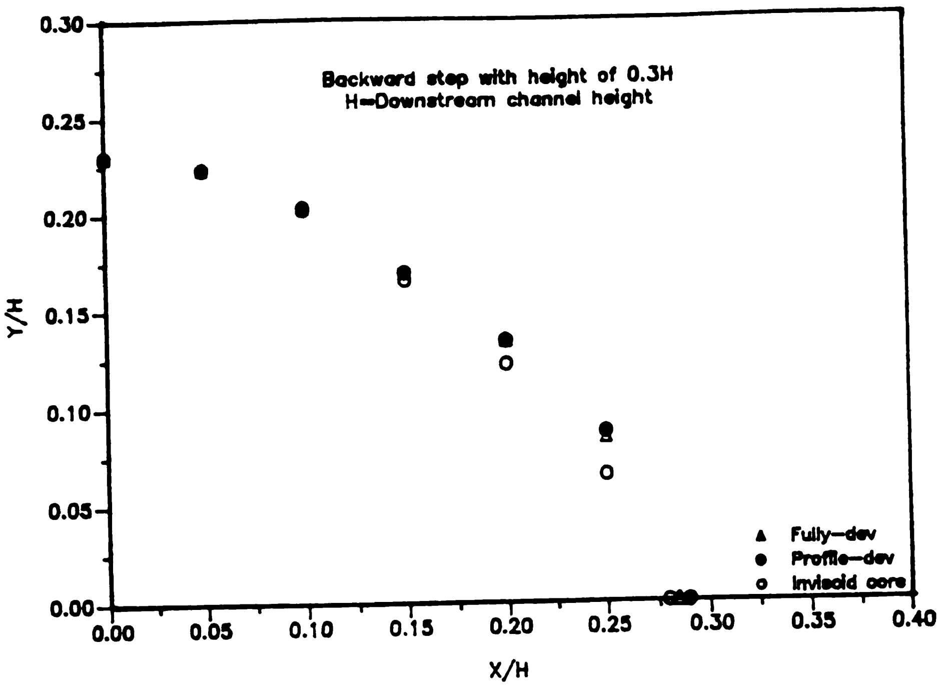

Figure 27. Effect of step position on separation region, $(Re)_H$=20.

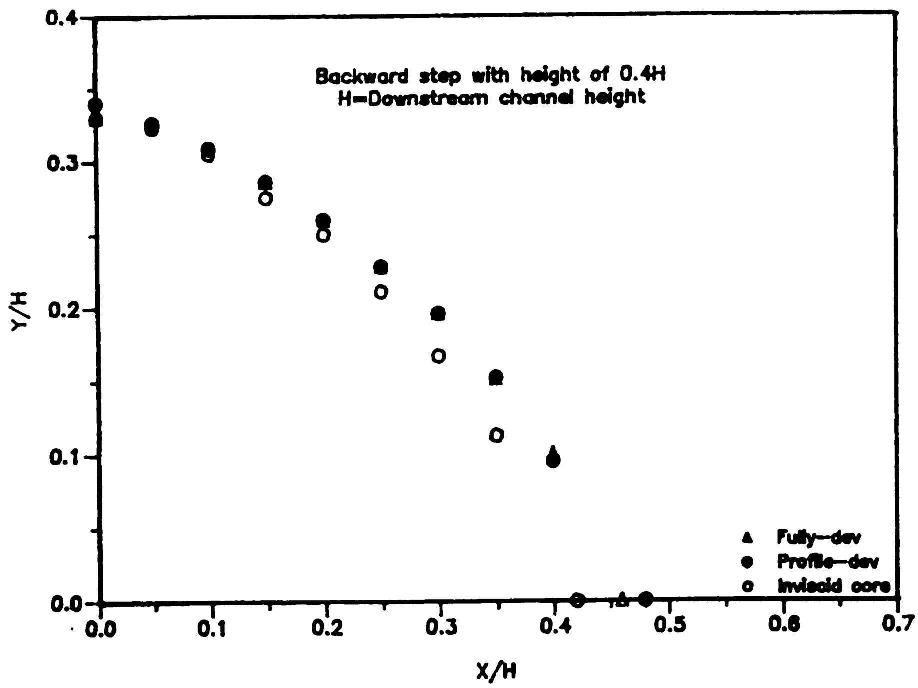

Figure 28. Effect of step position on separation region, $(Re)_H$=20.


Y/H


Y/H

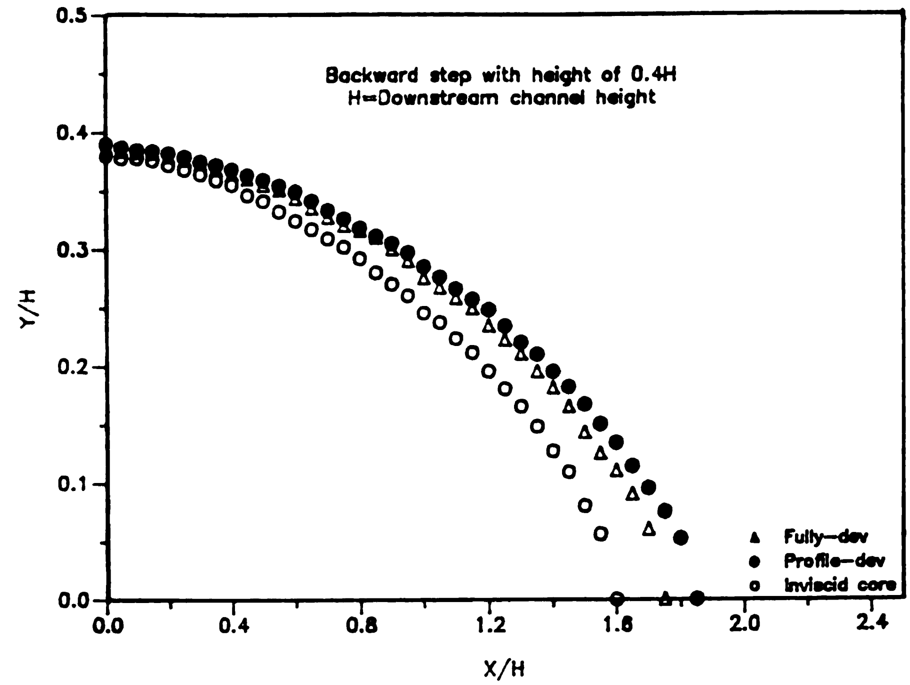

Figure 29. Effect of step position on separation region, $(Re)_H=200$.

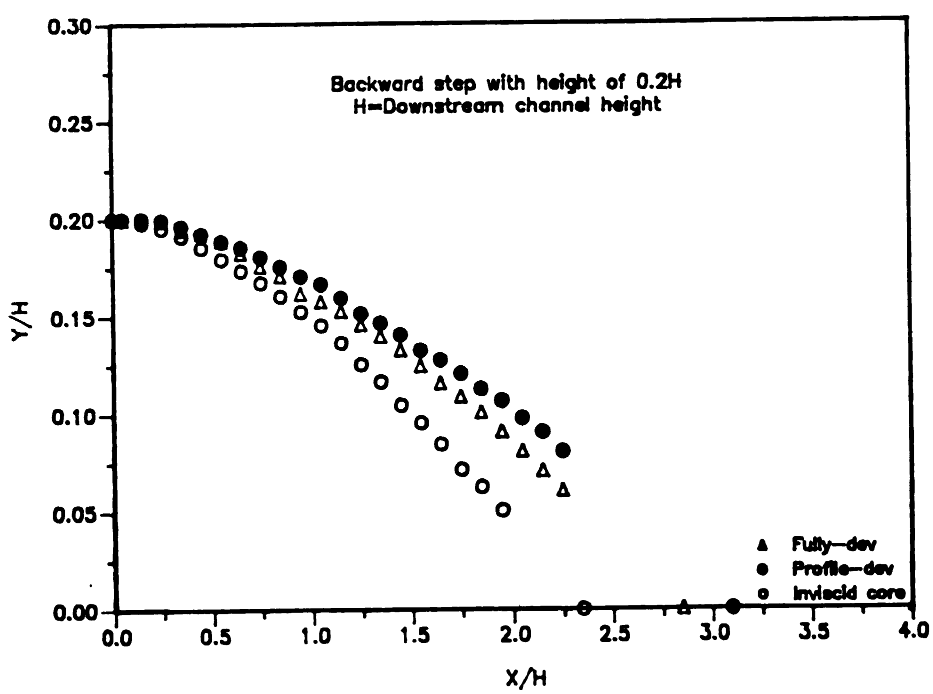

Figure 30. Effect of step position on separation region, $(Re)_H=2000$.

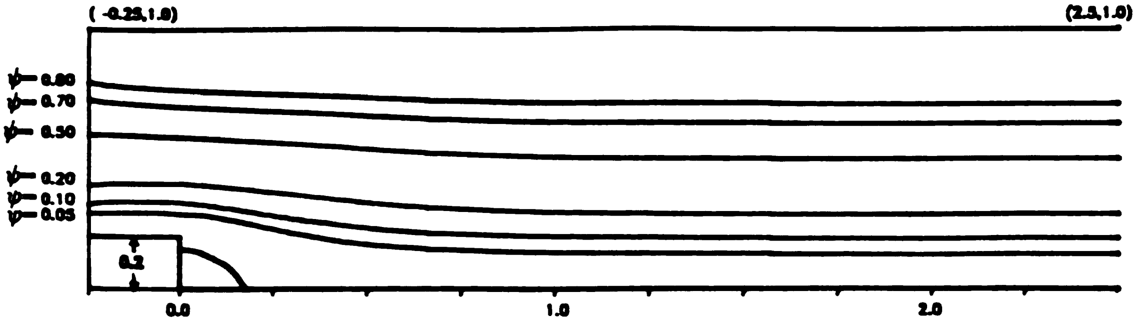

Figure 31. Streamlines in the vicinity of the backward step located in the profile–development region, $(Re)_H=20$.

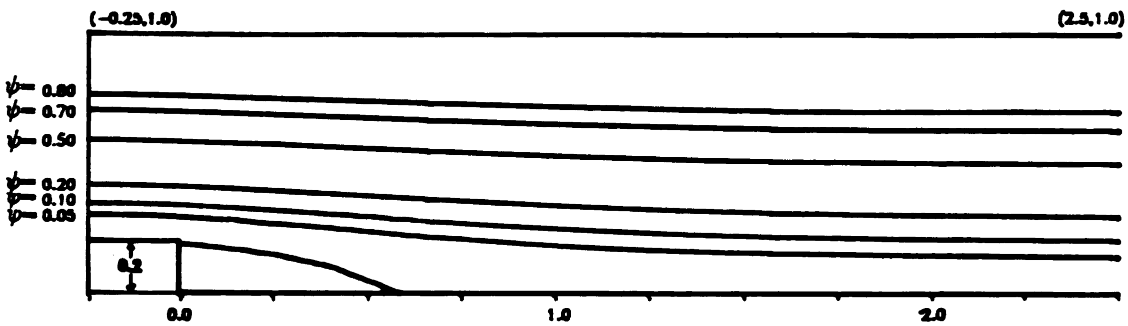

Figure 32. Streamlines in the vicinity of the backward step located in the profile–development region, $(Re)_H=200$.

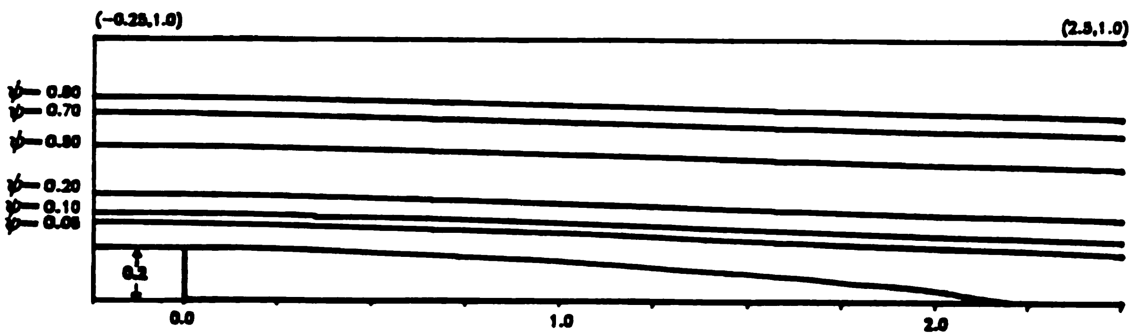

Figure 33. Streamlines in the vicinity of the backward step located in the profile–development region, $(Re)_H=2000$

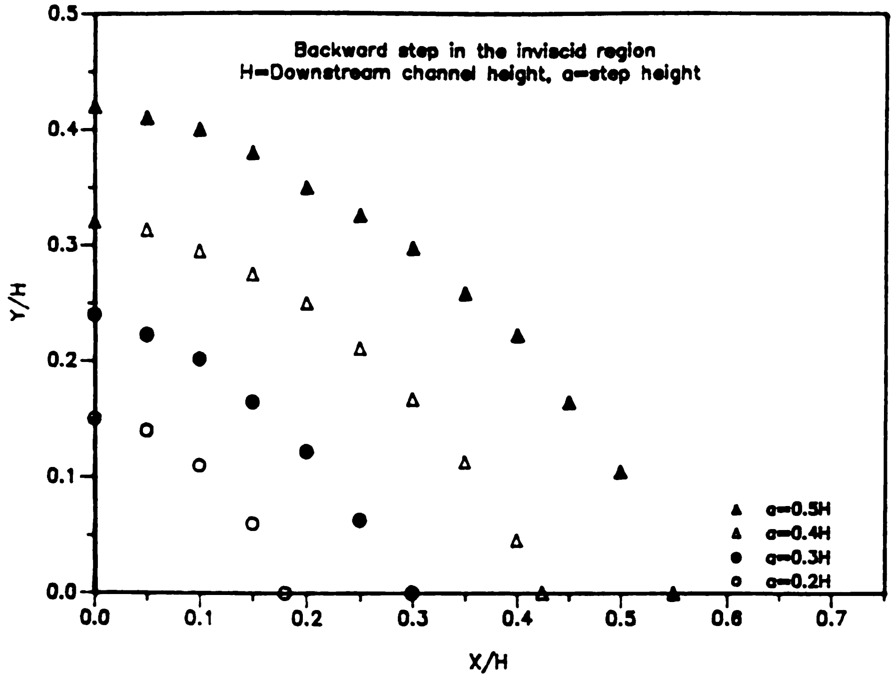

Figure 34. Effect of step height on separation region, $(Re)_H$=20.

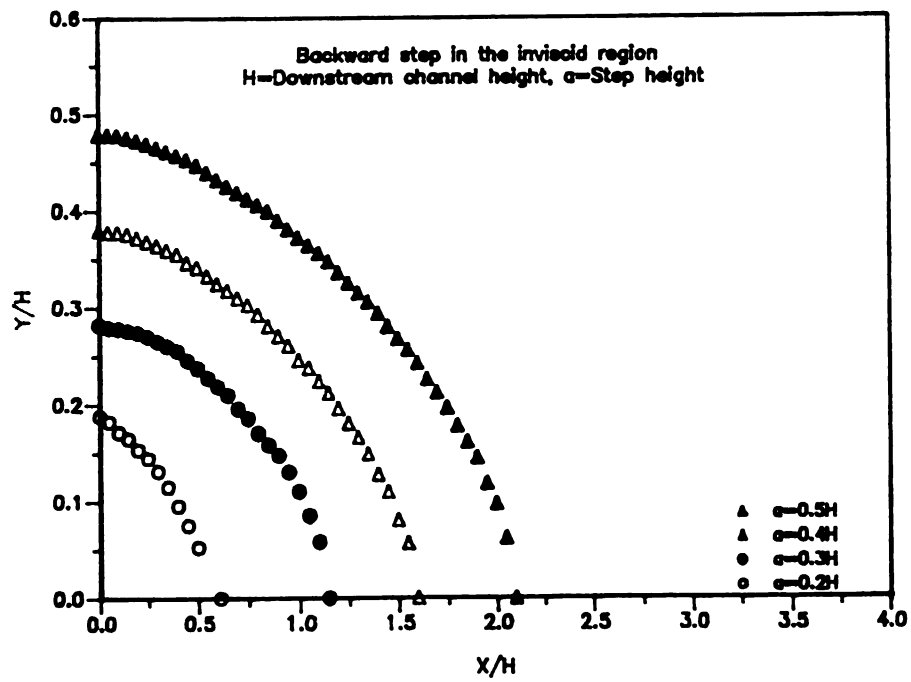

Figure 35. Effect of step height on separation region, $(Re)_H$=200.

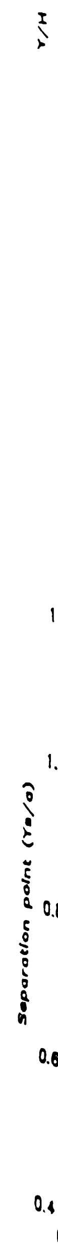
Y/H
Separation point (Ys/a)
1
1.
0.
0.6
0.4

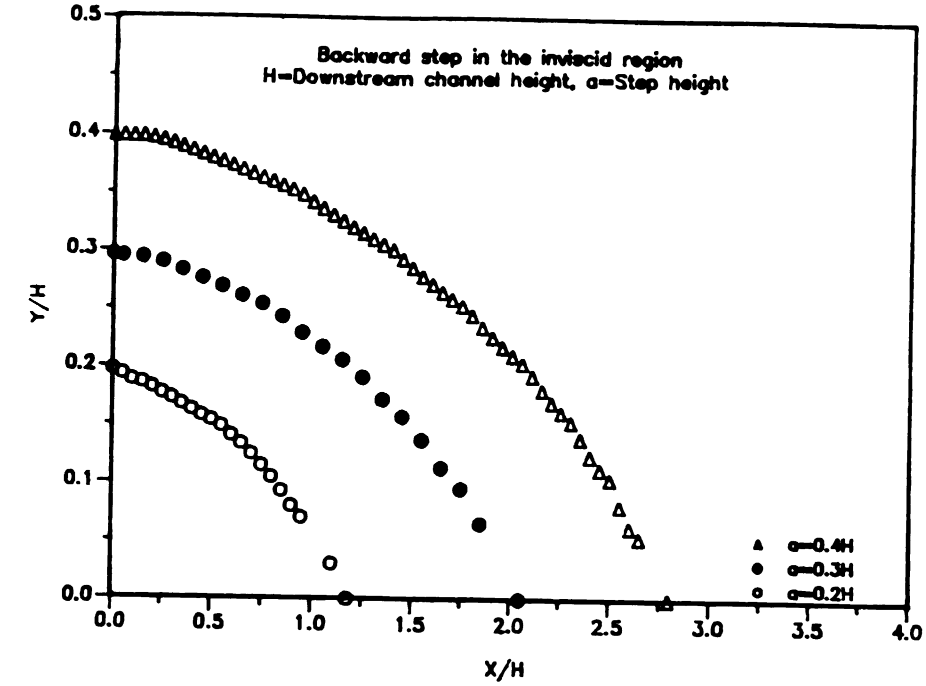

Figure 36. Effect of step height on separation region, $(Re)_H = 500$.

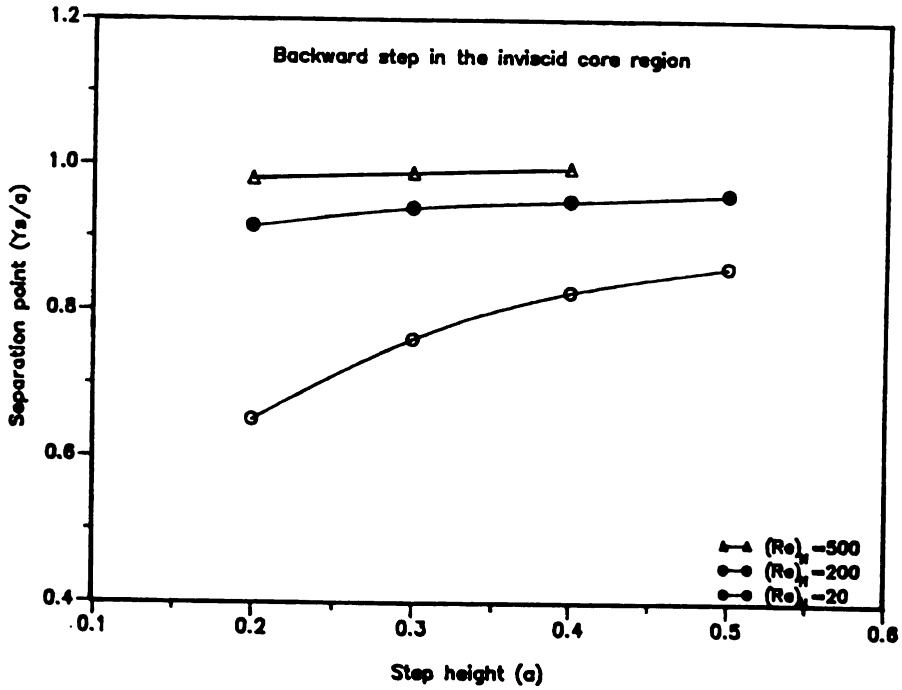

Figure 37. Separation point vs. step height for different Reynolds numbers.

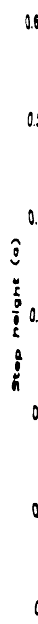
Step height (a)


Y/H

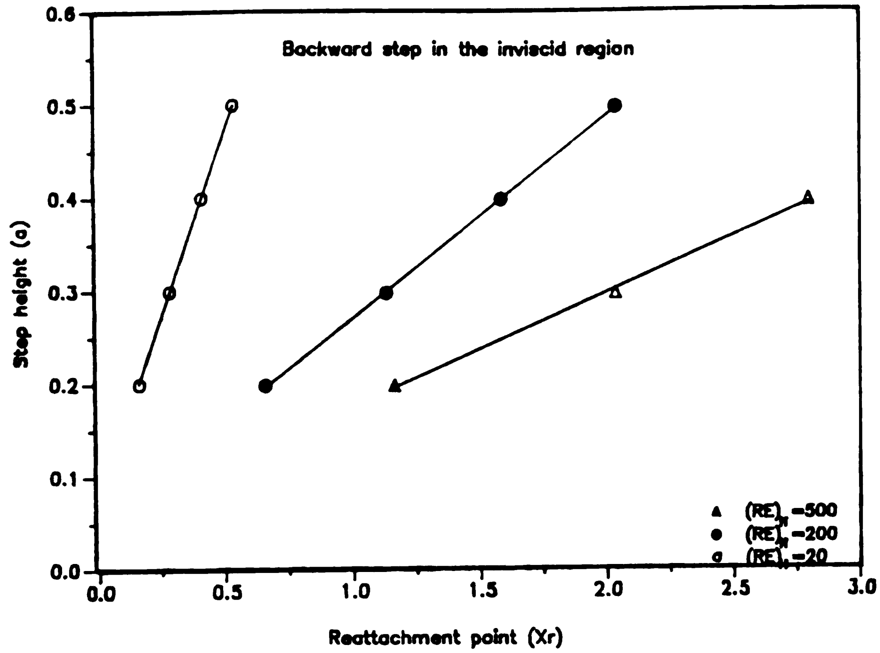

Figure 38. Reattachment point vs. step height for different Reynolds numbers.

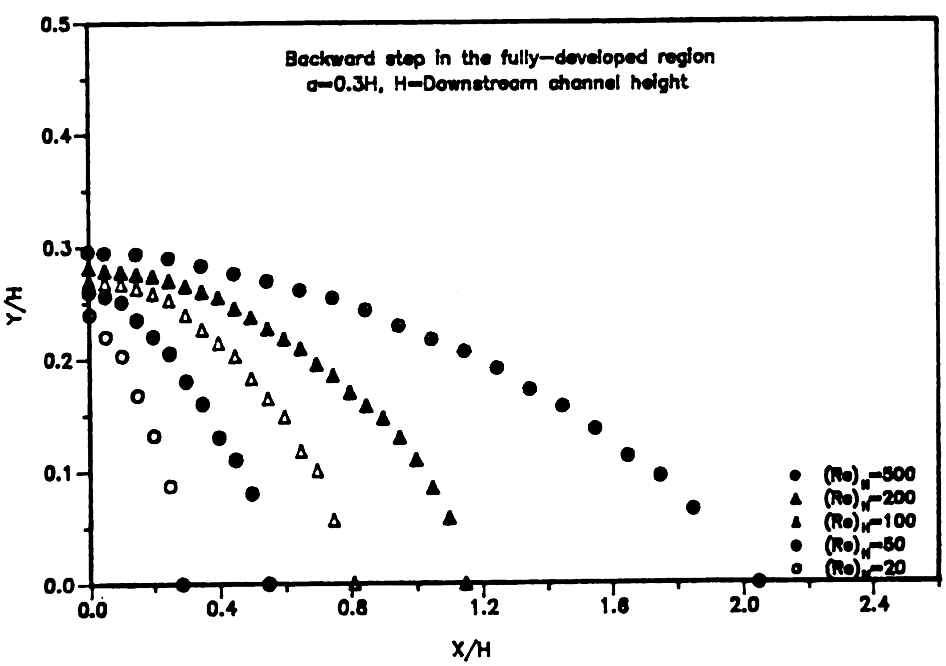

Figure 39. Separation and reattachment points for various Reynolds numbers.

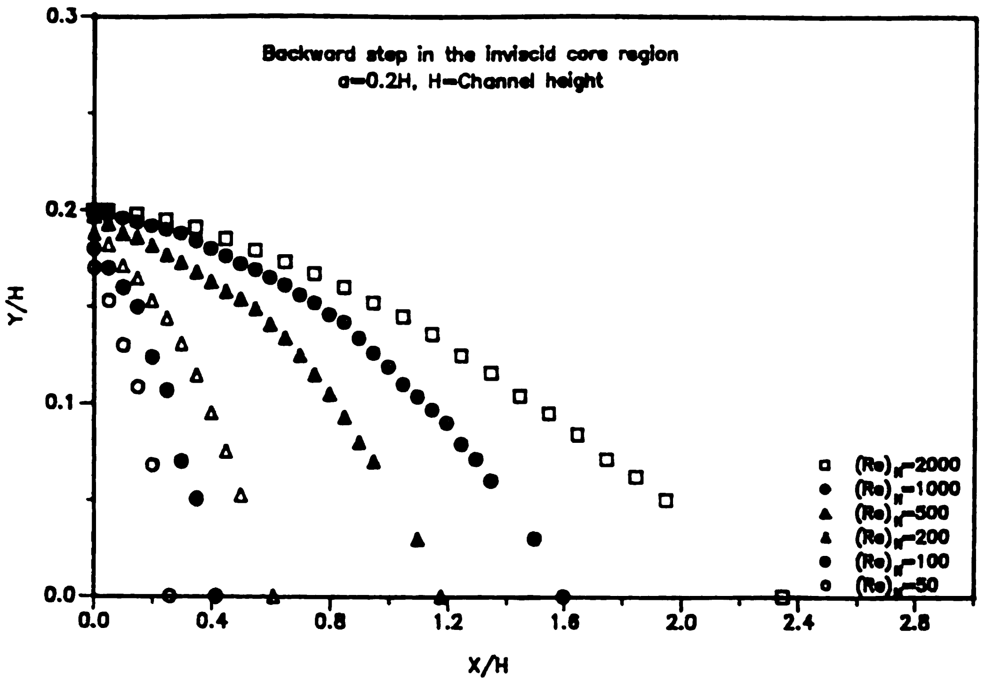

Figure 40. Separation and reattachment points for various Reynolds numbers.

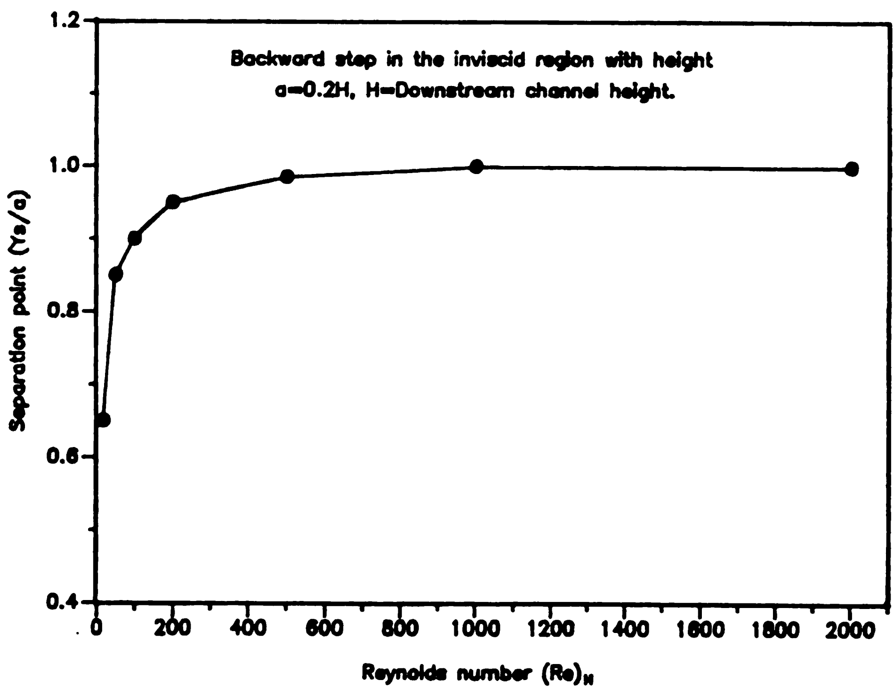

Figure 41. Variation of separation point with Reynolds number.

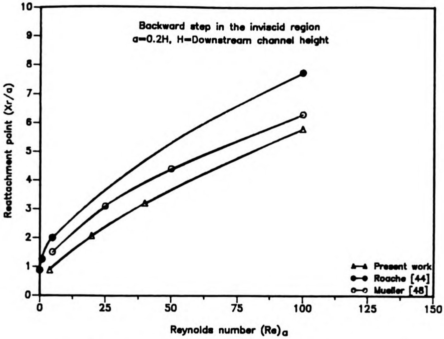

Figure 42. Comparison of reattachment point with theoretical results for Reynolds numbers in the range of (4–100).

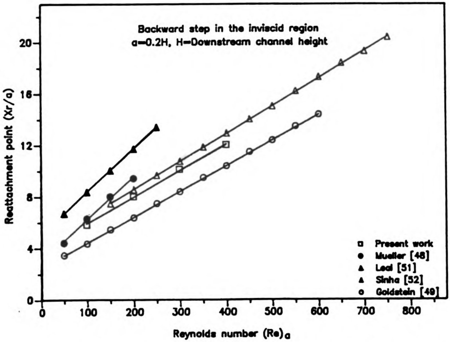

Figure 43. Comparison of reattachment point with experimental data for Reynolds numbers in the range of (100–400).

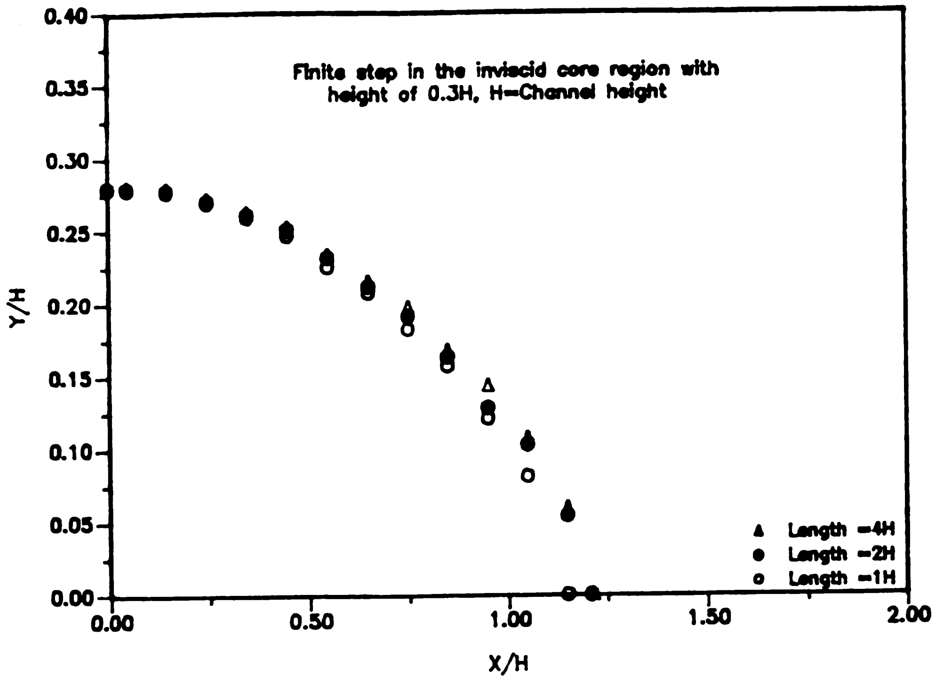

Figure 44. Effect of step length on downstream separation region, $(Re)_H$=200.

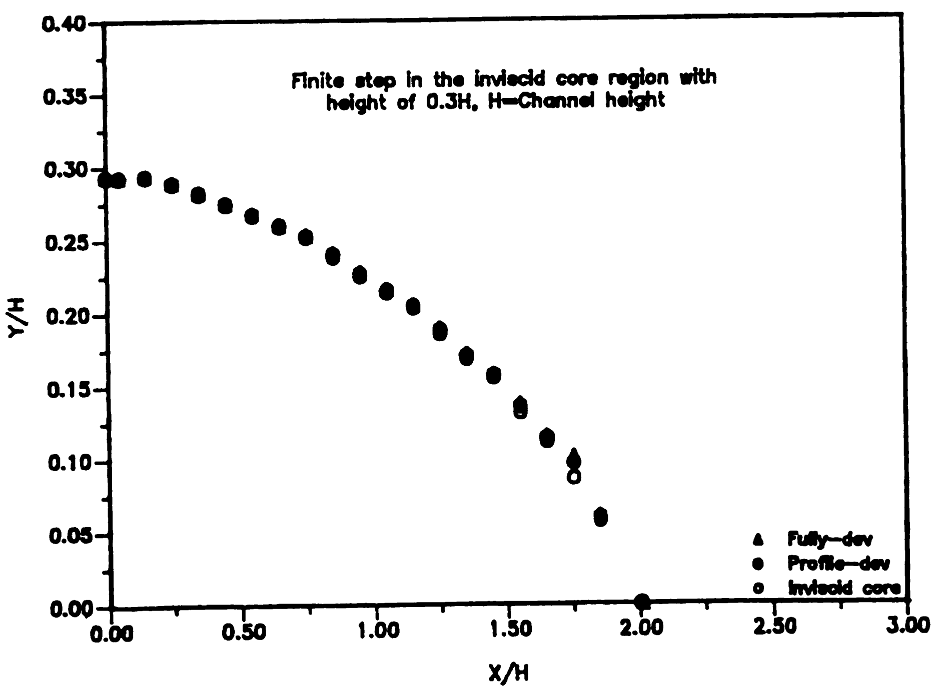

Figure 45. Effect of step position on downstream separation region, $(Re)_H$=500.

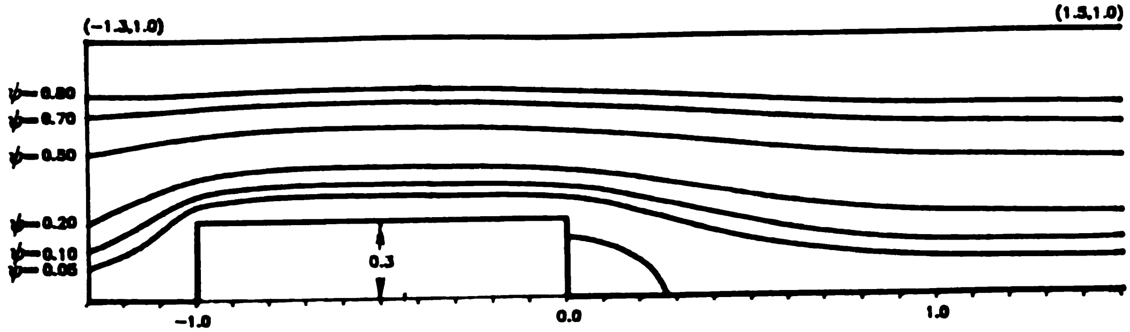

Figure 46. Streamlines in the vicinity of the finite step located in the profile-development region, $(Re)_H=20$.

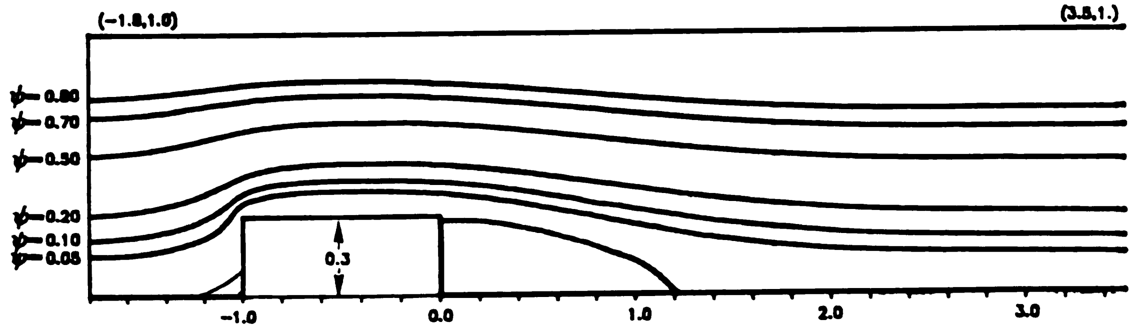

Figure 47. Streamlines in the vicinity of the finite step located in the profile-development region, $(Re)_H=200$.

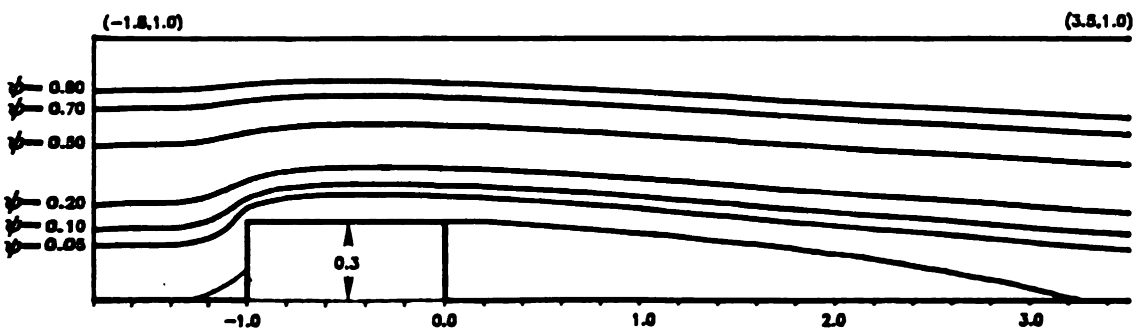

Figure 48. Streamlines in the vicinity of the finite step located in the profile-development region, $(Re)_H=1300$.

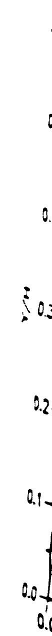
0.2
0.1
0.0

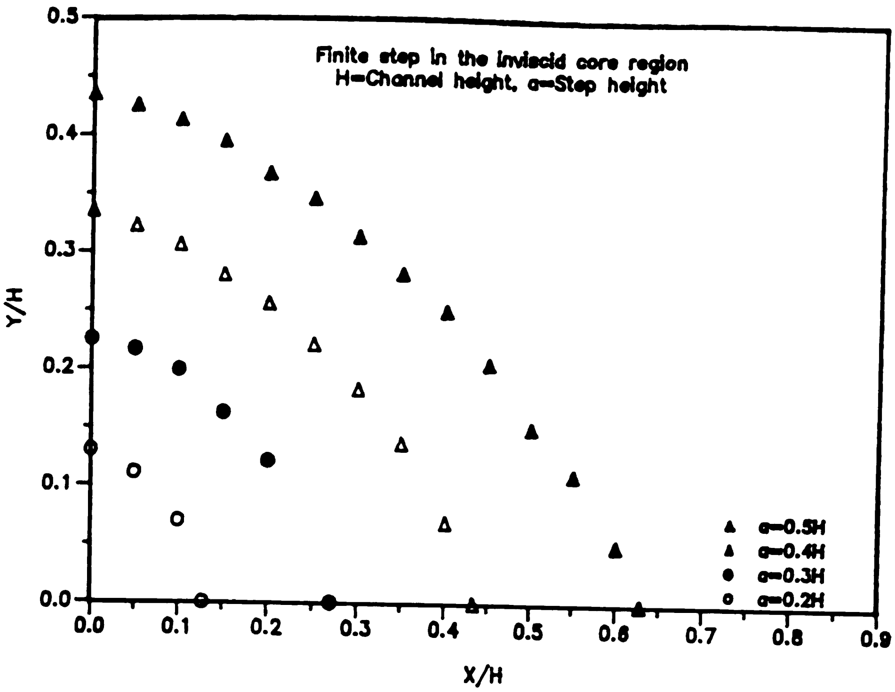

Figure 49. Effect of step height on downstream separation region, $(Re)_H$=20.

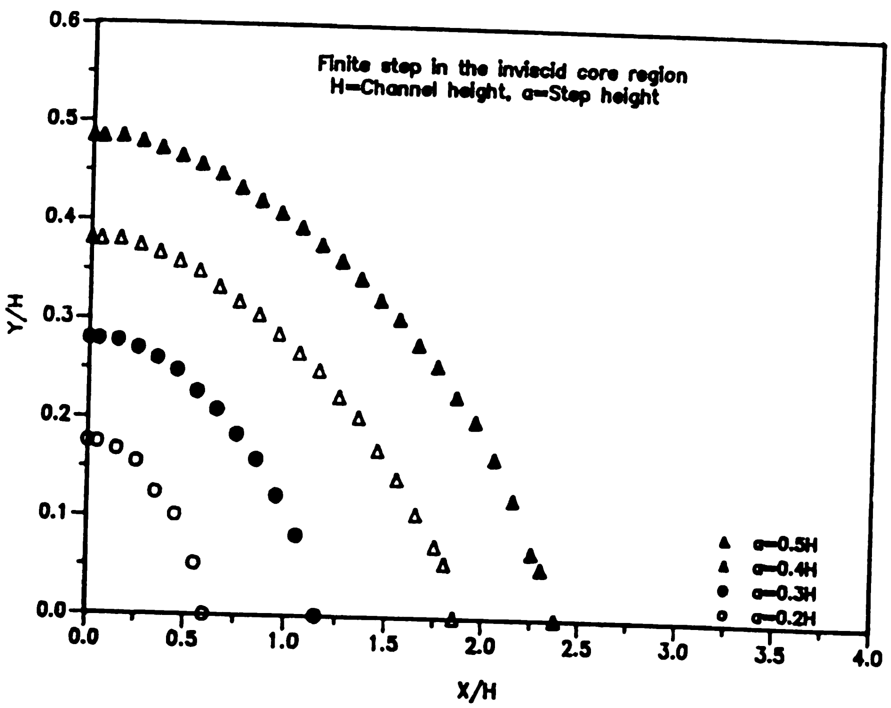

Figure 50. Effect of step height on downstream separation region, $(Re)_H$=200.

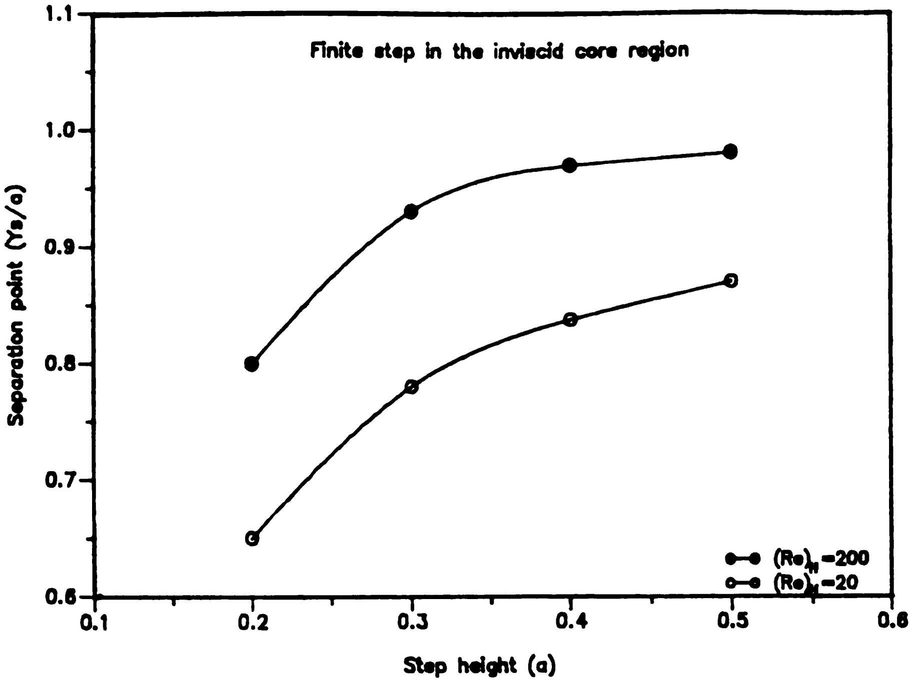

Figure 51. Downstream separation point vs. step height for various Reynolds numbers.

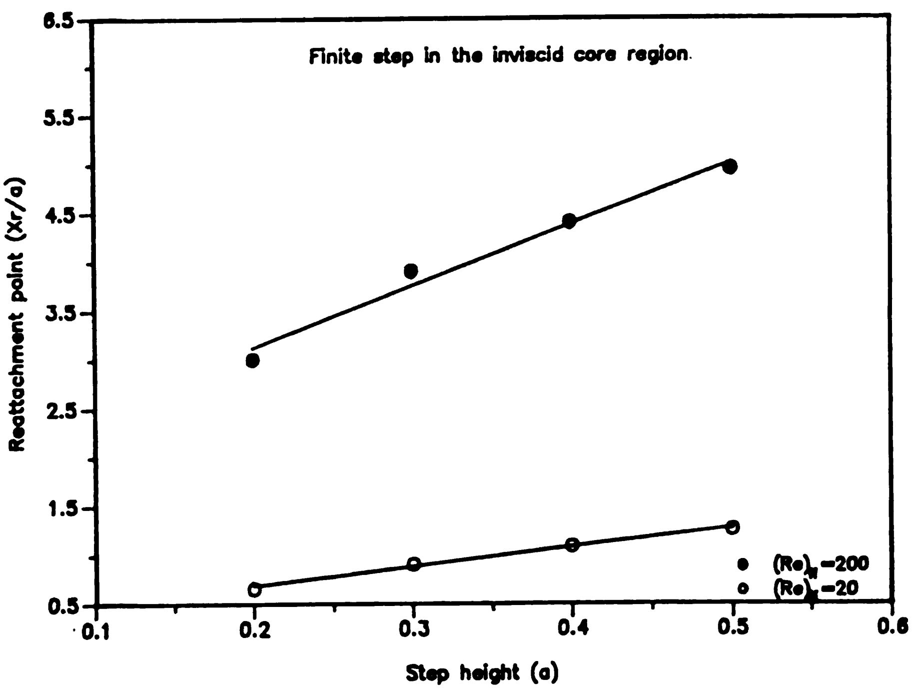

Figure 52. Downstream reattachment point vs. step height for various Reynolds numbers.

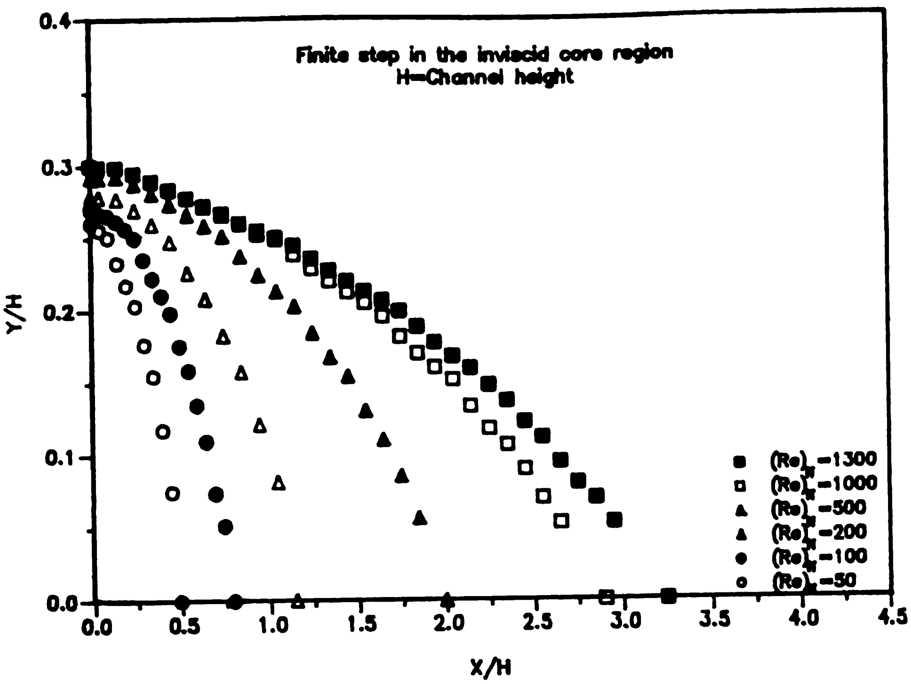

Figure 53. Effect of Reynolds number on downstream separation and reattachment points, a=0.3H.

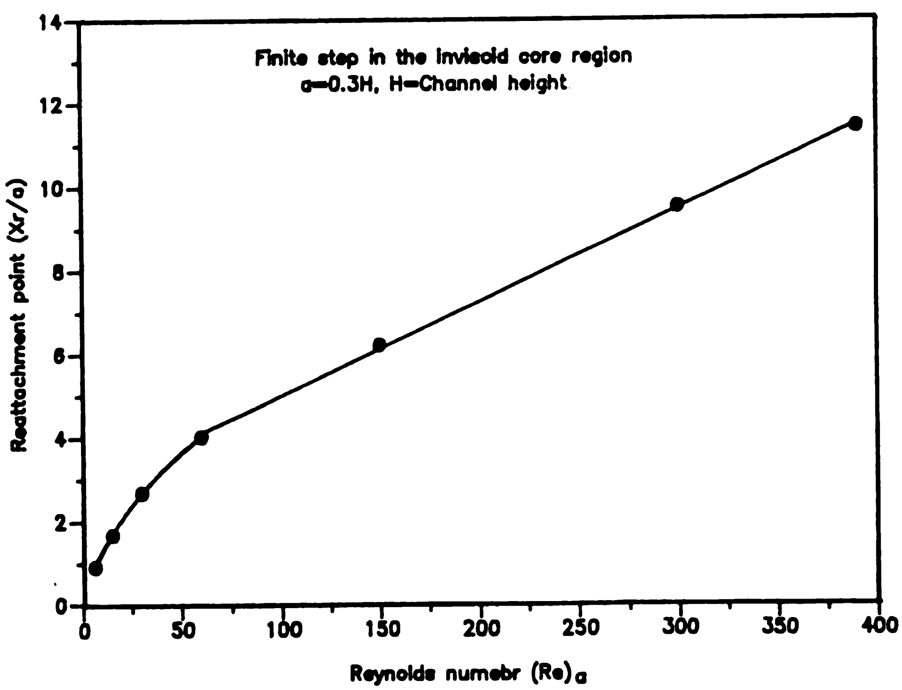

Figure 54. Downstream reattachment point vs. Reynolds number.

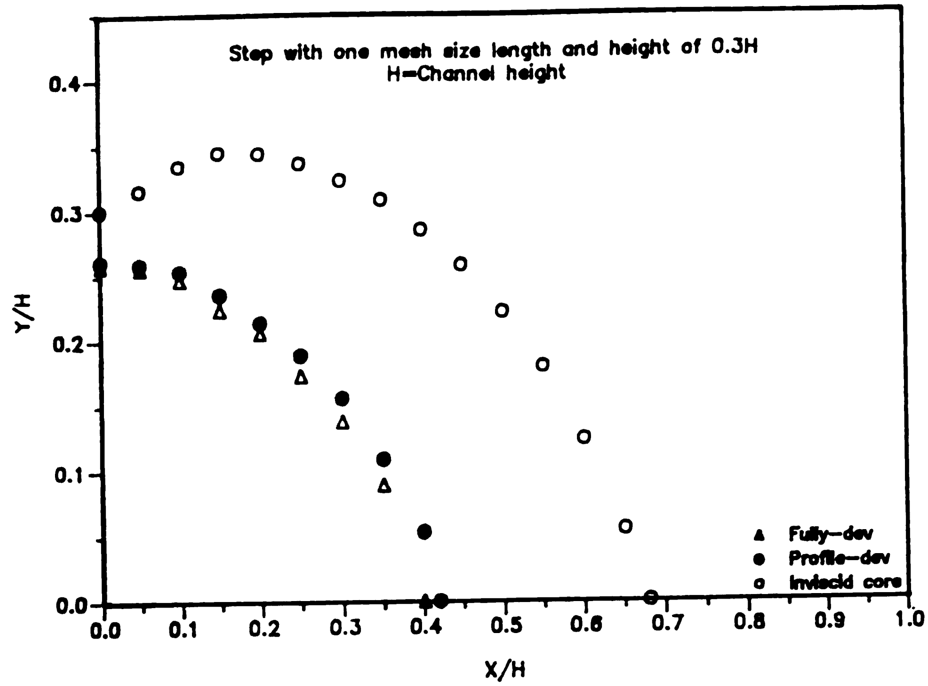

Figure 55. Effect of step position on downstream separation region, $(Re)_H$=20.

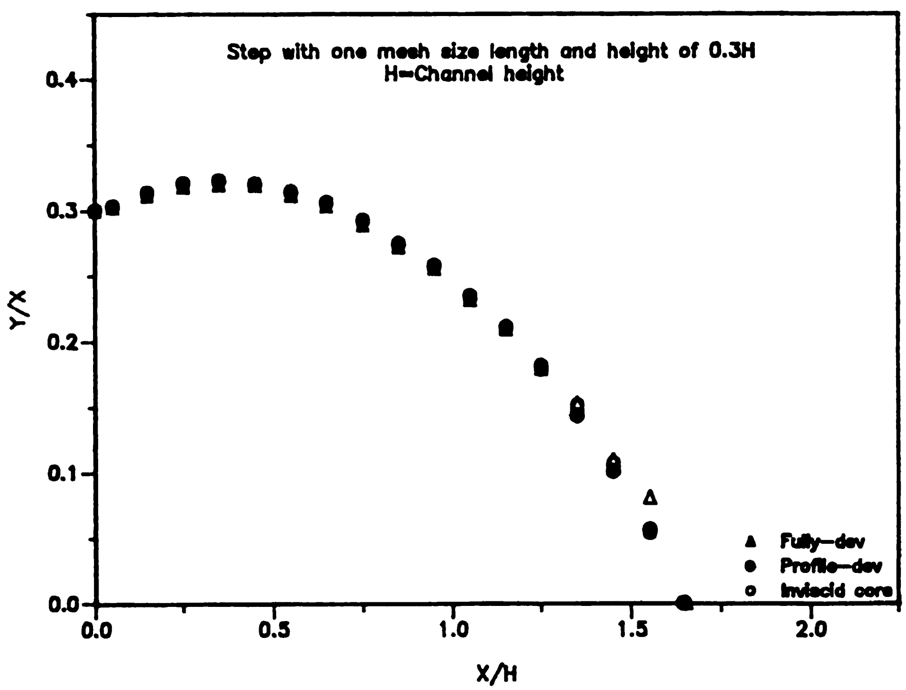

Figure 56. Effect of step position on downstream separation region, $(Re)_H$=200.

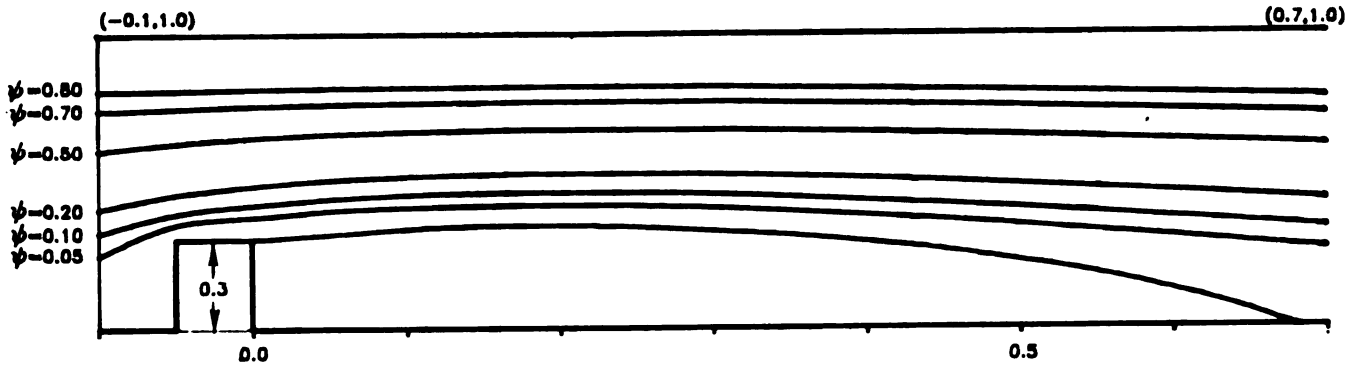

Figure 57. Streamlines in the vicinity of the single step located in the inviscid core region, $(Re)_H=20$.

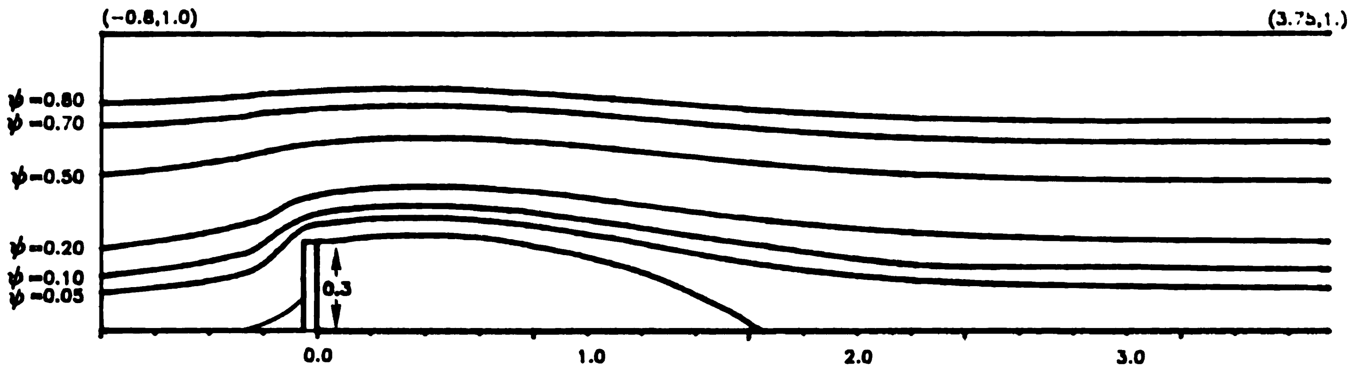

Figure 58. Streamlines in the vicinity of the single step located in the inviscid core region, $(Re)_H=200$.

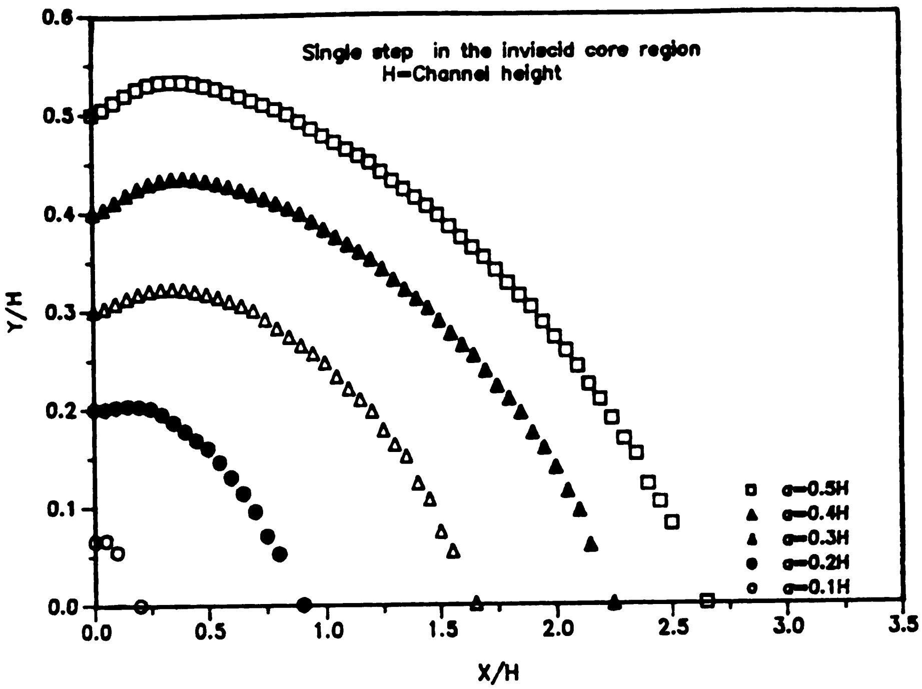

Figure 59. Effect of step height on downstream separation region, $(Re)_H=200$.

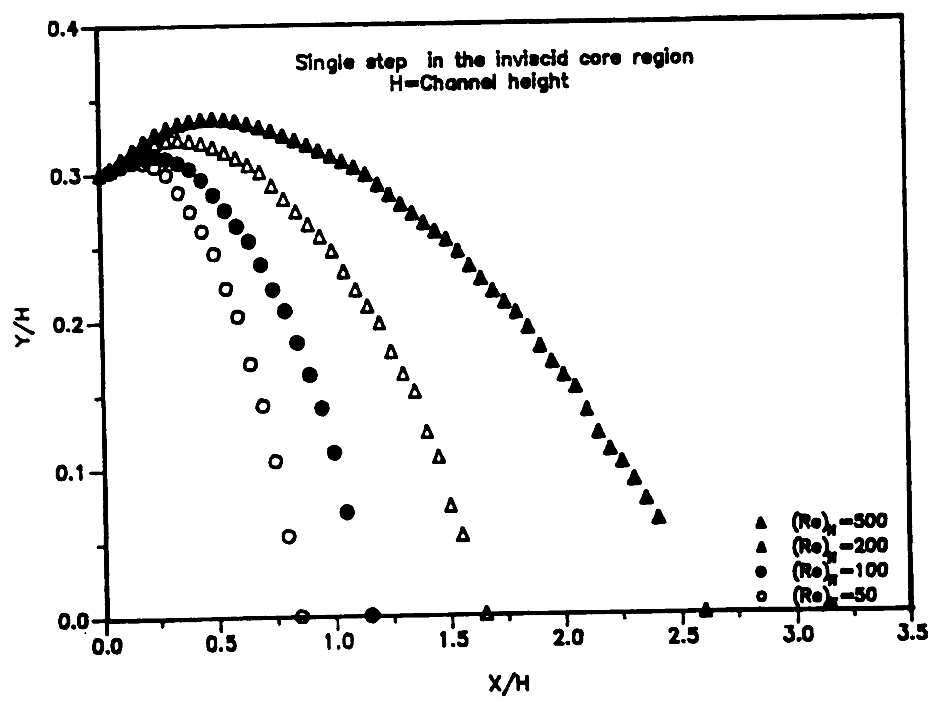

Figure 60. Effect of Reynolds number on downstream separation region, $a=0.3H$.

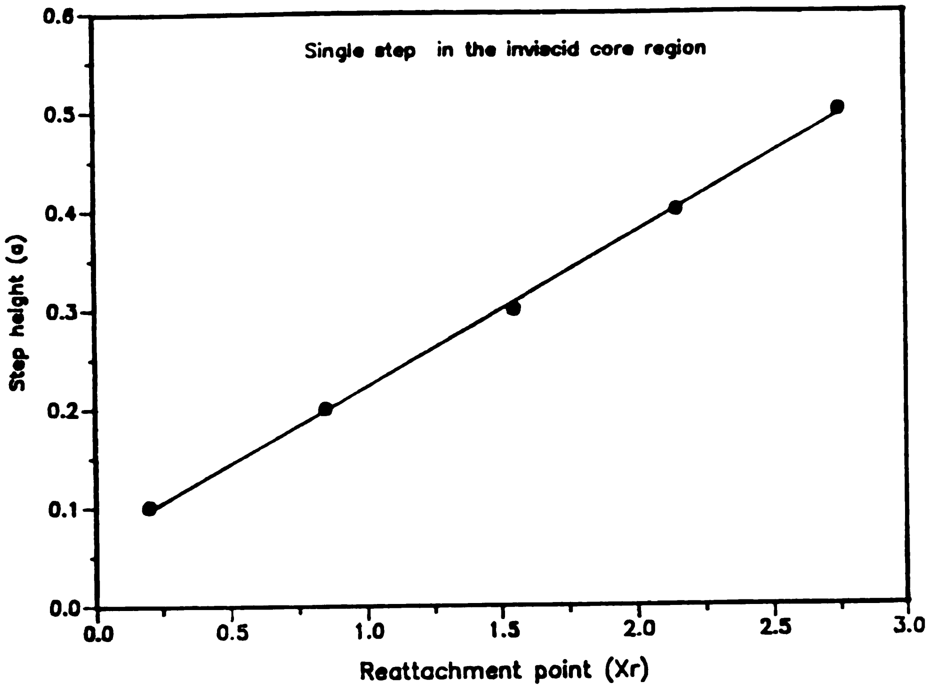

Figure 61. Effect of step height on downstream reattachment point, $(Re)_H$=200.

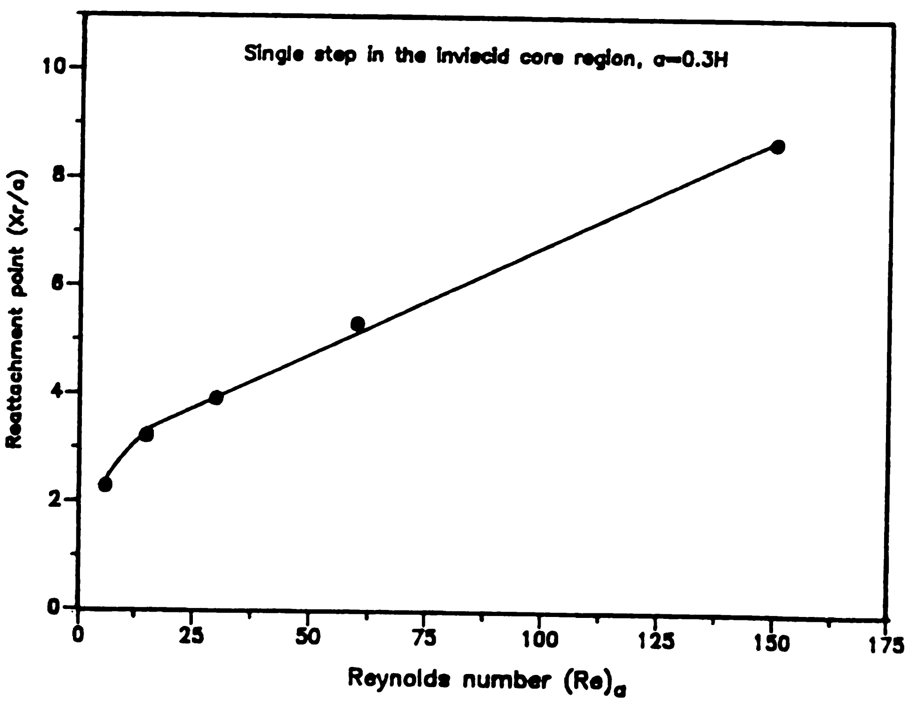

Figure 62. Downstream reattachment point vs. Reynolds number.

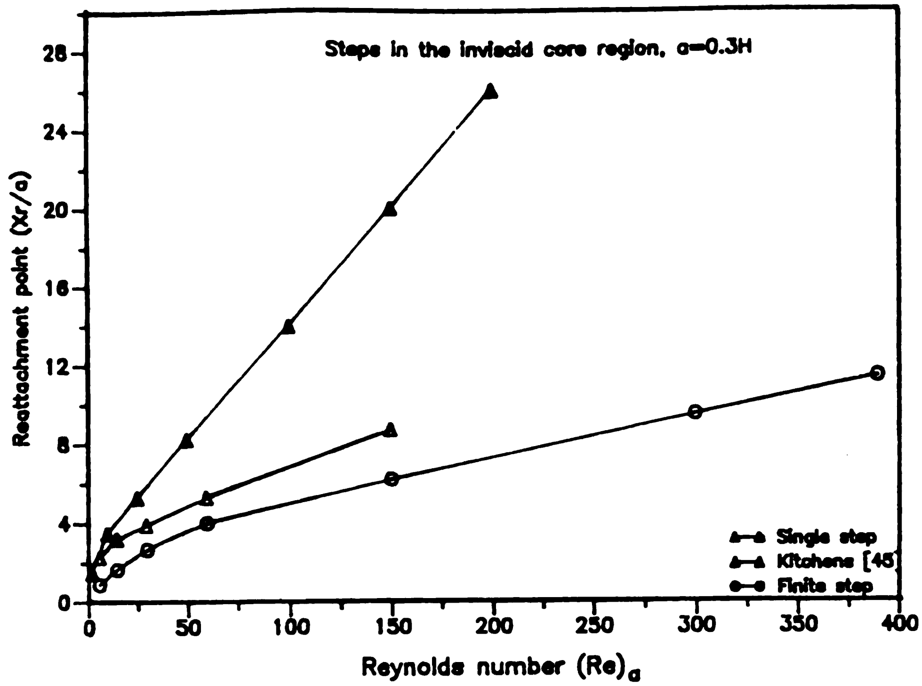

Figure 63. Comparison of downstream reattachment points.

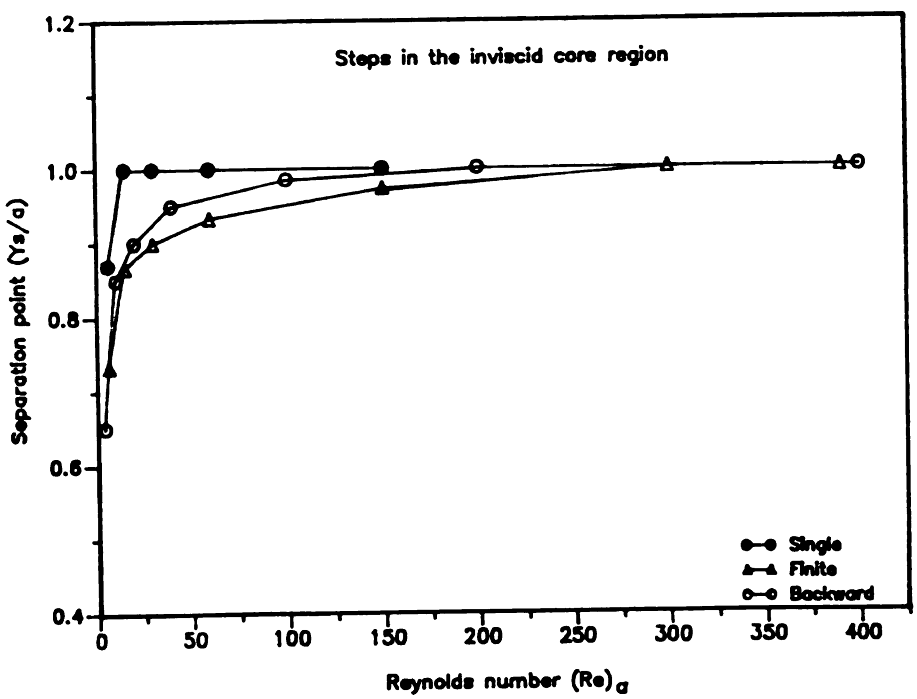

Figure 64. Comparison of downstream separation points for different steps.

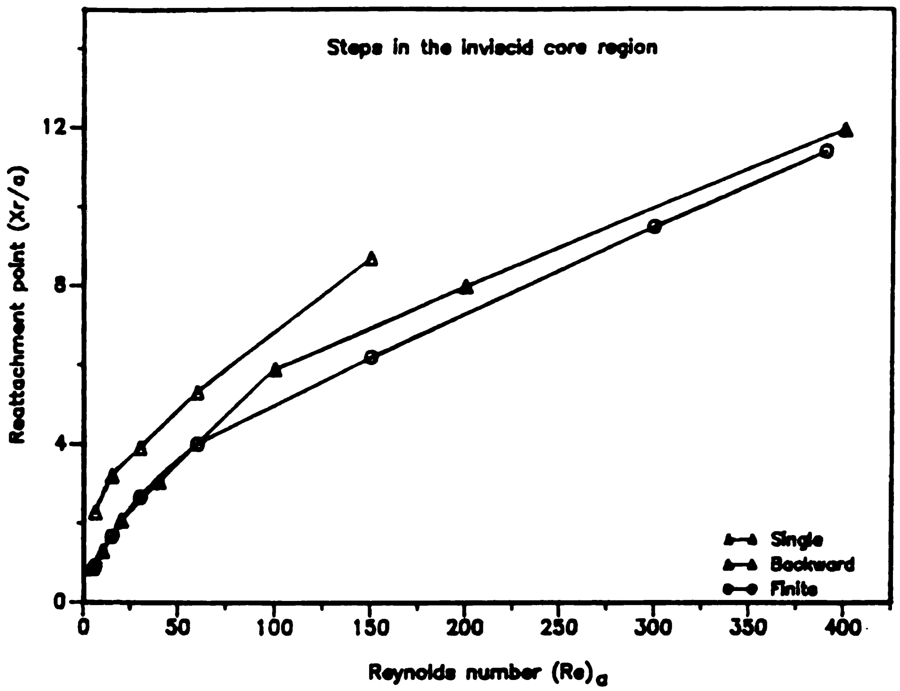

Figure 65. Comparison of downstream reattachment points for different steps.

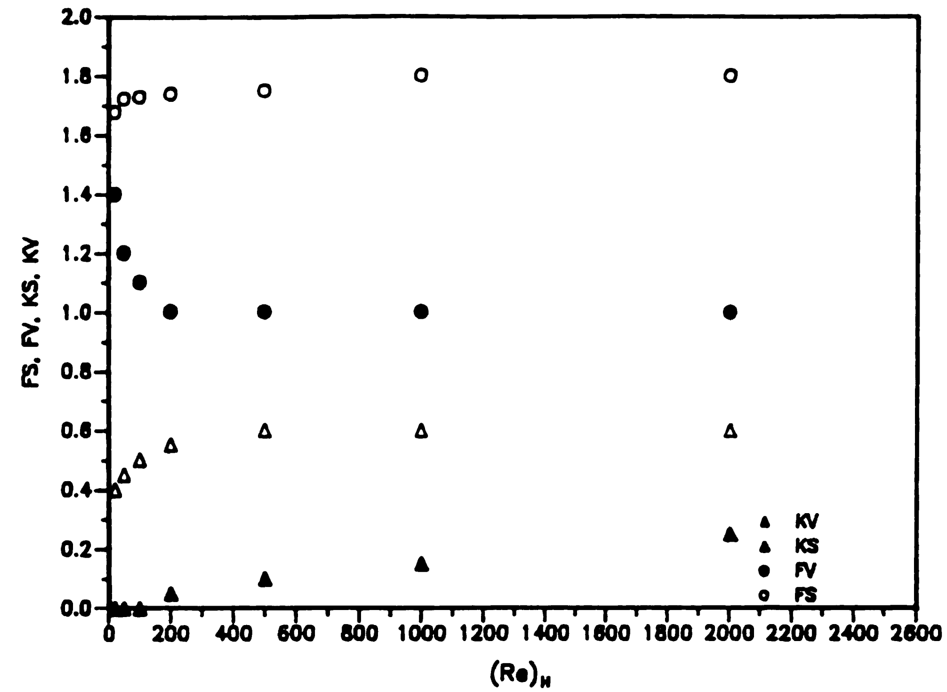

Figure 66. Optimum accelerating parameters vs. Reynolds number, h=1/15.

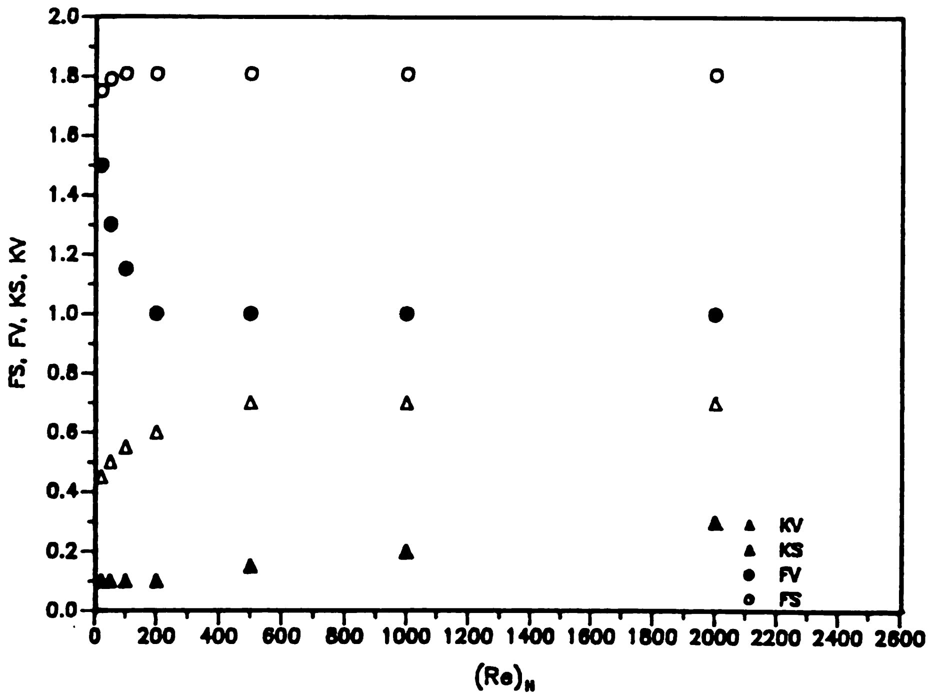

Figure 67. Optimum accelerating parameters vs. Reynolds number, h=1/20.

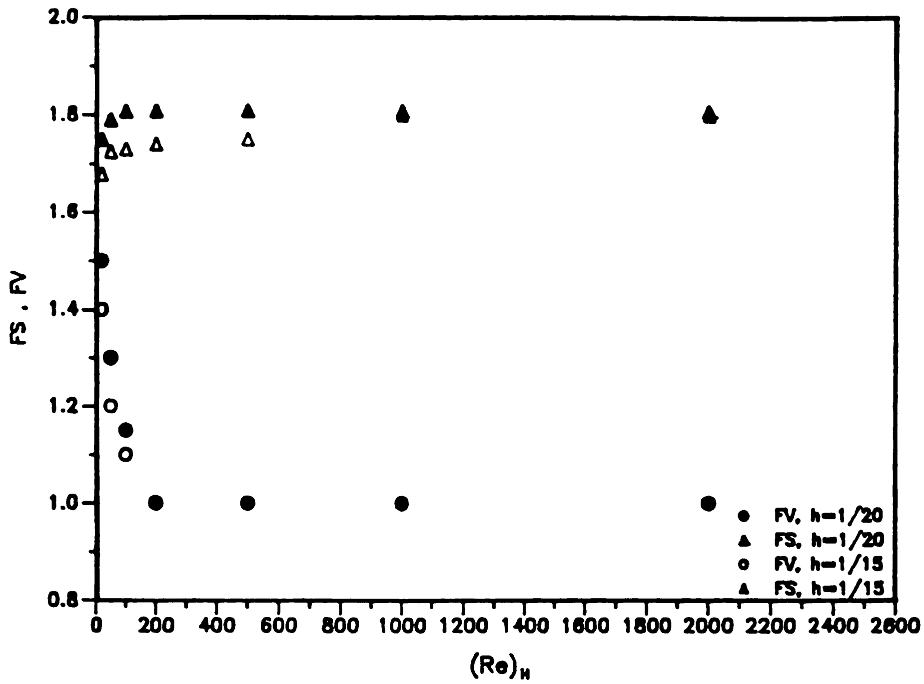

Figure 68. Optimum over–relaxation factors vs. Reynolds number.

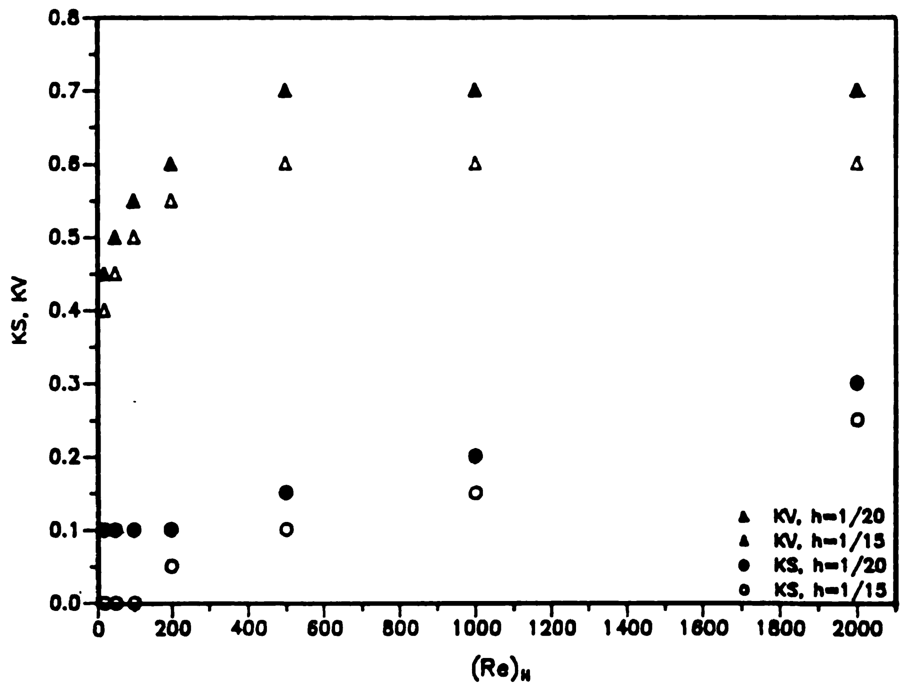

Figure 69. Optimum weighting factors vs. Reynolds number.

BIBLIOGRAPHY

BIBLIOGRAPHY

1. Schiller, L. and Angew, Z., Math. Mech., Vol. 2, P. 96 (1922).

2. Shapiro, A., Siegel, H., and Kline, S.J., Proc. 2nd U.S. Natl. Congr. Appl. Mech., P. 733 (1954).

3. Campbell, W.D. and Slattery, J.C., J. Basic Engg., Vol. 85, P. 41 (1963).

4. Mohannty, A.K. and Asthana, S.B., J. Fluid Mech., Vol. 90, Part 3, P. 433 (1978).

5. Schlichting, H., ZAMM, Vol. 14, P. 368 (1934).

6. Schlichting, H., Boundary Layer Theory, 6th ed. McGraw-Hill Book Company, P. 176 and P. 231 (1968).

7. Van Dyke, M., J. Fluid Mech., Vol. 44, P. 813 (1970).

9. Langhaar, H.L., Trans. ASME J. Appl. Mech., Vol. 64, A-55 (1942).

10. Sparrow, E.M., Lin, S.H. and Lundgren, T.S., Phys. Fluids, Vol. 7, P. 338 (1964).

11. Lundgren, T.S., Sparrow, B.M. and Starr, J.B., ASME J. Basic Engg., Vol. 86, P. 620 (1964).

12. Morihara, H. and Cheng, R.T., J. Computational Phys., Vol. 11, P. 550 (1973).

13. Du Plessis, J.P. and Korger, D.G., J. Appl. Mech., Vol. 51, P. 239 (1984).

14. Christiansen, E.B. and Lemmon, H.E., AICHE J., Vol. 11, P. 995 (1965).

15. Robert, W.H., J. Appl. Sci. Res., Vol. 13, Sec. A, P. 224 (1963).

16. Hwang, C.L. and Fan, L.T., Appl. Sci. Res., Vol. 10, Sec. B, P. 329 (1961).

17. Bodoia, J.R., Osterle, J.F., Appl. Sci. Res., Vol. 10, Sec. A, P. 235 (1961).

18. Vrentas, J.S., Duda, J.L. and Bargeron, K.G., AICHE J., Vol. 12, P. 827 (1968).

19. Friedman, Gillis, J. and Liron, N., Appl. Sci. Res., Vol. 19, Sec. B, P. 426 (1968).

20. Wang, Y.L. and Longwell, P.A., AICHE J., Vol. 10, P. 323 (1964).

21. Smith, F.T., J. Fluid Mech., Vol. 78, P. 709 (1976).

22. Smith, F.T., J. Fluid Mech., Vol. 79, P. 631 (1977).

23. Dennis, S.C. and Chang, G.Z., J. Fluid Mech., Vol. 42, P. 471 (1979).

24. Dimopoulos, H.G. and Hanratty, K., J. Fluid Mech., Vol. 33, P. 303 (1980).

25. Smith, F.T., Proc. Roy. Soc. Lond. A 356, P. 433 (1977).

26. Smith, F.T. and Stewartson, K., Proc. Roy. Soc. Lond. A-332, P. 1 (1973).

27. Smith, F.T., J. Fluid Mech., Vol. 90, Part 4, P. 725 (1979).

28. Smith, F.T. and Duck, P.W., J. Fluid Mech., Vol. 90, Part 4, P. 727 (1980).

29. Blowers, J., Independent Report, Mech. Dept., MSU (1981).

30. Dennis, S.C. and Smith, F.T., Proc. Roy. Soc. Lond., A-372, P. 393 (1980).

31. Hung, T.K. and Macagno, E.O., Houille Blanche, Vol. 21, No. 4, P. 391 (1966).

32. Morihara, H., Ph.D. thesis, State U. of New York at Buffalo (1972).

33. Hurd, A.C. and Peter, A.R., J. Basic Engg., Vol. 92, P. 908 (1970).

34. Nallasamy, M., Ph.D. thesis IIsc Bangalore (1975).

35. Ralph, T.C., J. Phys. of Fluid, Vol. 15, No. 12, P. (1971).

36. Lee, J.S. and Fung, J.L., J. Appl. Mech., Vol. 37, P. 9 (1970).

37. Deshpande, M.D., Giddens, D.P. and Mabon, F.R., J. Biomech., Vol. 9, P. 165 (1976).

38. Gosman, A.D. et. al., Academic Press, N.Y. (1969).

39. Young, D.F. and Tsai, F.Y., J. Biomech., Vol. 6, P. 395 (1973).

40. Greenspan, D., J. of Eng. Math., Vol. 3, P. 21 (1969).

41. Friedman, M., J. of Engg. math., Vol. 6, No. 3, P. 285 (1971).

42. Andreas, A. and Mark, S., Phys. of Fluids, Vol. 25, No. 6, P. 923 (1982).

43. Taylor, T. and Ndefo, E., Proceeding of the Second International Conference on Numerical Methods in Fluid Dynamics, Lecture Notes in Physics, Vol. 8, Springer-Verlag, New York (1971).

44. Roache, P. and Mueller, T., AIAA J., Vol. 8, No. 3, P. 530 (1970).

45. Kitchens Jr., C., AIAA J., Vol. 12, No. 7, P. 1005 (1974).

46. Frank, S. and Andreas, A., Phys. Fluids, Vol. 29, No. 5, P. 1353 (1986).

47. Kwon, D. and Pletcher, R., J. of Fluids Engg., Vol. 108, P. 64 (1986).

48. Mueller, T. and O'Leary, R., AIAA 3rd Fluid and Plasma Dynamics Conference Los Angeles, California June 29-July 1 (1970).

49. Goldstein, et. al., J. of Basic Engg., Ser. D, Vol. 92, P. 732 (1970).

50. Honji, H., J. Fluid Mech., Vol. 69, Part 2, P. 229 (1975).

51. Leal, L. and Acrivos, A., J. Fluid Mech., Vol. 39, Part 4, P. 735 (1969).

52. Sinha, et. al., AIAA J., Vol. 19, No. 12, P. 1527 (1975).

53. Thom, A., Field Computation in Engineering and Physics, P. 125, Van Nostrand, London (1961).

54. Chow, C., An Introduction to Computational Fluid Mechanics, John Wiley and Sons, Inc. (1979).

55. Gillis, J. and Brandt, A., Air Force European Office of Aerospace Research Scientific Report, P. 63 (1964).

56. Brandt, A. and Gillis, J., J. Phys. of Fluid, Vol. 9, P. 690 (1966).

57. Roidt, M. and Cess, R., trans. ASME J. Appl. Mech., Vol. 29, Ser. E, P. 171 (1962).

58. Mohanty, A. and Asthana, S., J. Fluid Mech., Vol. 90, Part 3, P. 433 (1978).

59. Kawaguti, M., Tech. Summary Rept. No. 574, Mathematic Research Center, U. of Wisconsin Madison, Wis. (1965).

60. Nacagno, E. and Hung, T., J. Fluid Mech., Vol. 28, Part 1, P. 43 (1967).

61. Kumar, A. and Yajnik, K., J. Fluid Mech., Vol. 97, Part 1, P. 27 (1980).

62. Schrader, M.L., Ph.D. thesis, Stanford University (1981).

63. Bodoia, J.R., Ph.D. thesis, Carnegie Institute of Technology, July (1959).

APPENDICES

APPENDIX A

Appendix A

Computer program for entrance region of the channel

```
      REAL*8 F(601,51),FS(601,51),Q(601,51),QS(601,51)
     2,U(601,51),Y(51),X(601),PF(601,51),PC(601,51)
      REAL*8 ERF,ERQ,EFF,EQQ
      OPEN(UNIT=1,FILE='OUTPRE',STATUS='NEW',FORM=
     2'FORMATTED')
      OPEN(UNIT=2,NAME=INLET,TYPE='OLD')
C     F,FS ARE THE CALCULATED STREAM FUNCTION AND
C          VORTICITY
C     FS,QS ARE THE STORED STREAM FUNCTION AND
           VORTICITY
C     U IS A STREAMWISE VELOCITY
C     Y IS A NORMAL COORDINATE
C     X IS A STREAMWISE COORDINATE
C     PF IS A STREAMWISE PRESSURE GRADIENT AT THE WALL
C     PC IS A STREAMWISE PRESSURE GRADIENT AT CENTER
C     ERF,ERQ ARE THE MAXIMUM RELATIVE ERRORS
C             IN STREAM FUNCTION AND VORTICITY
C             FOR INNER ITERATIONS
C     EFF,EQQ ARE THE MAXIMUM RELATIVE ERRORS
C             IN STREAM FUNCTION AND VORTICITY
C             FOR OUTER ITERATIONS
      READ(2,15)ITMAX,M,N,H,RE,AKS,AKV
 15   FORMAT(3I10,F5.2,F10.2,2F4.2/)
C     ITMAX IS A PRESELECTED NO. OF ITERATIONS
C     M IS A NO. OF GRID POINTS IN STREAMWISE DIRECTION
C     N IS A NO. OF GRID POINTS IN NORMAL DIRECTION
C     H IS A MESH SIZE EQUAL IN X-AND-Y DIRECTIONS
C     RE IS REYNOLDS NUMBER BASED ON THE CHANNEL HEIGHT
C     FS IS OVER-RELAXATION FACTOR FOR POISSON EQ.
C     FV IS OVER-RELAXATION FACTOR FOR N.S. EQS.
C     AKS IS A WEIGHTING FACTOR FOR STREAM FUNCTION
C     AKV IS A WEIGHTING FACTOR FOR VORTICITY
C     ITERF IS A NO. OF INEER ITER. FOR STREAM FUNCTION
C     ITERQ IS A NO. OF INEER ITER. FOR VORTICITY
C     ITER IS A NO. OF OUTER ITERATIONS FOR STREAM
C          FUNCTION AND VORTICITY
C     COMPUTE OVER-RELAXATION FACTOR
C     ********************************
      PI=4.*ATAN(1.)
      MM1=M-1
      NM1=N-1
      ALPHA=COS(PI/M)+COS(PI/N)
      FS=(8.-4.*SQRT(4.-ALPHA**2))/ALPHA**2
      WRITE(1,534)N,M,FS
 534  FORMAT(10X,'TOTAL GRID Y-DIR.=',I5,10X,
```

```
     2'TOTAL GRID X-DIR.=',I5,'FS=',F10.7/)
C     COMPUTE COORDINATES FOR GRID POINTS
C     **********************************
      X(1)=0.
      DO 1 I=2,M
  1   X(I)=X(I-1)+H
      Y(1)=0.
      DO 2 J=2,N
  2   Y(J)=Y(J-1)+H
C     A. STREAM FUNCTION BOUNDARY CONDITIONS
C     --------------------------------------
C     1. LOWER AND UPPER WALLS CONDITIONS
C     -- --------------------------------
      DO 3 I=1,M
      F(I,1)=0.
  3   F(I,N)=1.
C     2. DOWNSTREAM CONDITION
C     -----------------------
      DO 4 J=2,NM1
  4   F(M,J)=3.*Y(J)**2-2.*Y(J)**3
C     3. UPSTREAM CONDITION (ACTUAL PROFILE)
C     --------------------------------------
      H1=0.055
      Y1(5)=0.17
      F(1,2)=0.03
      F(1,3)=0.0725
      F(1,4)=0.1175
      F(1,5)=Y1(5)
      DO 888 J=6,17
  888 Y1(J)=Y1(J-1)+H1
      DO 814 J=6,17
  814 F(1,J)=Y1(J)
      F(1,18)=0.8825
      F(1,19)=0.9275
      F(1,20)=0.97
      3. UPSTREAM CONDITION (UNIFORM PROFILE)
C     ---------------------------------------
      DO 5 J=2,NM1
   5  F(1,J)=Y(J-1)+H
C     4. INTERIOR REGION (LINEAR INTERPOLATION)
C     -----------------------------------------
      DO 6 I=2,MM1
      DO 6 J=2,NM1
  6   F(I,J)=Y(J)
C     VORTICITY BOUNDARY CONDITIONS
C     -----------------------------
C     1. UPSTREAM CONDITION (ACTUAL PROFILE)
C     --------------------------------------
      Q(1,2)=-0.225
      Q(1,3)=-0.4
      Q(1,4)=-0.5
```

```
      Q(1,5)=-1.5
      DO 331 J=6,16
 331  Q(1,J)=0.
      Q(1,17)=-Q(1,5)
      Q(1,18)=-Q(1,4)
      Q(1,19)=-Q(1,3)
      Q(1,20)=-Q(1,2)
C     1. UPSTREAM CONDITION (UNIFORM PROFILE)
C     --------------------------------------
      DO 34 J=2,NM1
  34  Q(1,J)=0.
C     2. DOWNSTREAM CONDITION
C     ----------------------
      DO 35 J=2,NM1
  34  Q(M,J)=12.*Y(J)-6.
C     3. INTERIOR REGION CONDITION
C     ----------------------------
      DO 400 I=2,MM1
      DO 400 J=2,NM1
 400  Q(I,J)=0.
C     STORING STREAM FUNCTION AND VORTICITY
C     -------------------------------------
      DO 15 I=2,MM1
      DO 15 J=2,NM1
      FS(I,J)=F(I,J)
 15   QS(I,J)=Q(I,J)
C     BEGIN OUTER ITERATION FOR STREAM FUNCTION
C     AND VROTICITY--------------------------
C     -----------
      ITER=0
  18  ITER=ITER+1
C     SOLVING POISSON EQUATION FOR STREAM FUNCTION
C     --------------------------------------------
C     BEGIN INEER ITERATION FOR STREAM FUNCTION
C     -----------------------------------------
      ITERF=0
  80  ITERF=ITERF+1
      ERF=0.
C     COMPUTE STREAM FUNCTION FOR INNER REGION
C     ****************************************
      DO 20 I=2,MM1
      DO 20 J=2,NM1
      FOLDF=F(I,J)
      F(I,J)=F(I,J)+ FS/(2./H**2+2./H**2)*((F(I+1,J)
     2+F(I-1,J))/H**2+(F(I,J+1)+F(I,J-1))/H**2+Q(I,J)
     3-(2./H**2+2./H**2)*F(I,J))
      EEEF=F(I,J)+0.00001
 20   ERF=DMAX1(ERF,DABS((F(I,J)-FOLDF)/EEEF))
C     TEST STREAM FUNCTION FOR CONVERGENCE
C     ------------------------------------
      IF(ERF.LE.0.000001) GO TO 75
```

```
      IF(ITERF.GT.5000 )  GO TO 999
      GO TO 80
C     END OF INNER ITER. FOR STREAM FUNCTION
C     --------------------------------------
C     RECALCULATE F(I,J) USING WEIGHTING FACTOR
C     *****************************************
   75 DO 48 I=2,MM1
      DO 48 J=2,NM1
   48 F(I,J)=AKS*FS(I,J)+(1-AKS)*F(I,J)
C     SOLVING NAVIER-STOKES EQUATIONS FOR VORTICITY
C     ---------------------------------------------
C     BEGIN INNER ITERATION FOR VORTICITY
C     -----------------------------------
      ITERQ=0
  175 ITERQ=ITERQ+1
      ERQ=0.
C     4. LOWER AND UPPER WALLS CONDITIONS
C     -----------------------------------
      DO 32 I=2,MM1
      Q(I,1)=(F(I,1)-F(I,2))*3./H**2-(0.5*Q(I,2))
   32 Q(I,N)=(F(I,N)-F(I,NM1))*3./H**2-(0.5*Q(I,NM1))
      DO 21 I=2,MM1
      DO 21 J=2,NM1
      FOLDQ=Q(I,J)
      A=F(I+1,J)-F(I-1,J)
      B=F(I,J+1)-F(I,J-1)
      REA=0.5*A*RE
      REB=0.5*B*RE
      IF((A.GE.0.).AND.(B.GE.0.)) GO TO 500
      IF((A.GE.0.).AND.(B.LT.0.)) GO TO 600
      IF((A.LT.0.).AND.(B.GE.0.)) GO TO 700
      IF((A.LT.0.).AND.(B.LT.0.)) GO TO 800
  500 Q(I,J)=(1-FV)*Q(I,J)+FV*((Q(I+1,J)+(1.+REB)*
     2Q(I-1,J)+(1.+REA)*Q(I,J+1)+Q(I,J-1))/(4.+REA+REB))
      GO TO 900
  600 Q(I,J)=(1-FV)*Q(I,J)+FV*((Q(I+1,J)*(1.-REB)+
     2Q(I-1,J)+(1.+REA)*Q(I,J+1)+Q(I,J-1))/(4.+REA-REB))
      GO TO 900
  700 Q(I,J)=(1-FV)*Q(I,J)+FV*((Q(I+1,J)+(1.+REB)*
     2Q(I-1,J)+Q(I,J+1)+(1.-REA)*Q(I,J-1))/(4.-REA+REB))
      GO TO 900
  800 Q(I,J)=(1-FV)*Q(I,J)+FV*(((1.-REB)*Q(I+1,J)+
     2Q(I-1,J)+Q(I,J+1)+(1.-REA)*Q(I,J-1))/(4.-REA-REB))
      EEEQ=Q(I,J)+0.00001
  900 ERQ=DMAX1(ERQ,DABS((Q(I,J)-FOLDQ)/EEEQ))
   21 CONTINUE
C     TEST VORTICITY FOR CONVERGENCE
C     ------------------------------
      IF (ERQ.LE.0.000001) GO  TO 85
      IF(ITERQ.GT.5000 )   GO TO 998
      GO TO 175
```

```
C      END OF INNER ITERATION FOR VORTICITY
C      ------------------------------------
C      RECALCULATE Q(I,J) USING WEIGHTING FACTOR
C      *****************************************
  85   DO 111 I=2,MM1
       DO 111 J=2,NM1
 111   Q(I,J)=AKV*QS(I,J)+(1-AKV)*Q(I,J)
       EFF=0.
       EQQ=0.
       DO 93 I=2,MM1
       DO 93 J=2,NM1
       EEEFF=F(I,J)+0.00001
       EEEQQ=Q(I,J)+0.00001
       EFF=DMAX1(EFF,DABS((F(I,J)-FS(I,J))/EEEFF))
 93    EQQ=DMAX1(EQQ,DABS((Q(I,J)-QS(I,J))/EEEQQ))
C      TEST RECALCULATED VALUES FOR CONVERGENCE
C      ----------------------------------------
       ETA=0.000001
       IF((EFF.LE.ETA).AND.(EQQ.LE.ETA)) GO TO 105
       IF(ITER.GT.ITMAX) GO TO 205
       DO 94 I=2,MM1
       DO 94 J=2,NM1
       FS(I,J)=F(I,J)
  94   QS(I,J)=Q(I,J)
       GO TO 18
C      END OF OUTER ITERATION
C      ----------------------
C      COMPUTE STREAMWISE VELOCITY
C      ---------------------------
 105   DO 777 I=2,MM1
       DO 777 J=2,NM1
 777   U(I,J)=(F(I,J+1)-F(I,J-1))/(2.*H)
       WRITE(1,2002)
 2002  FORMAT(3X,'X',5X,'X/RE',6X,'dP/dX(W)',3X,
      2'dP/dX.RE/12',,3X,'dP/dX(C)','dP/dX.RE/12'/)
C      COMPUTE PRESSURE GRADIENT AT THE WALL
C      *************************************
       DO 2101 I=2,MM1
       X(I)=X(I-1)+H
       XF=X(I)
       XD=XF/RE
       RES1=1./(RE*H)
       RES2=1./(RE*H**2)
       RES3=1./(RE*H**3)
       PU(I,1)=RES2*(-U(I,4)+4*U(I,3)-5*U(I,2)+2*U(I,1))
       PDU2=PU(I,1)*RE/12
       PF(I,1)=.5*RES3*(-3*F(I,5)+14*F(I,4)-24*F(I,3)+
      218*F(I,2)-5*F(I,1))
       PDF2=PF(I,1)*RE/12
C      COMPUTE PRESSURE GRADIENT AT THE CENTERLINE
C      *******************************************
```

```
      PC(I,11)=RES2*(-U(I+3,11)+4*U(I+2,11)-5*
     2U(I+1,11)+2*U(I,11))+RES2*(-U(I,14)+
     34*U(I,13)-5.*U(I,12)+2.*U(I,11))-0.5*U(I,11)/H
     4*(-U(I+2,11)+4*U(I+1,11)-3.*U(I,11))
      PDC2=PC(I,11)*RE/12
      WRITE(1,9888)XF,XD,PF2,PDF2,PC2,PDC2
9888  FORMAT(2X,F5.3,2X,F5.3,4F13.4/)
2010  CONTINUE
      WRITE(1,666)ITER,EFF,EQQ,RE
666   FORMAT('NO. OF ITER.=',I5,'EFF=',E14.7,10X,'
     2EQQ=',E14.7,10X,'RE=',F10.2//)
      WRITE(1,808)ITERF,ITERQ
808   FORMAT(10X,'ITERF=',I5,10X,'ITERQ=',I5//)
      WRITE(1,180)
180   FORMAT(10X,' STREAM FUNCTION VALUES'/)
      DO 620 J=1,N
620   WRITE(1,621)(F(I,J),I=1,MM1)
621   FORMAT(1X,'F(I,J)=',12F10.8//)
      WRITE(1,190)
190   FORMAT(10X,'VORTICITY VALUES '/)
      DO 535 J=1,N
535   WRITE(1,536)(Q(I,J),I=1,MM1)
536   FORMAT(1X,'Q(I,J)=',12F10.6//)
      WRITE(1,170)
170   FORMAT(15X,'VELOCITY  DISTRIBUTION ')
      DO 445 J=1,NM1
445   WRITE(1,446)(U(I,J),I=1,MM1)
446   FORMAT(1X,'U(I,J)=',12F10.6//)
      WRITE(1,729)
 729  FORMAT(10X,'CHCEK VELOCITY FROM 99 PER.
     2OF DEVELOPED VELOCITY'//)
      DO 730 I=2,MM1
      IF(U(I,11)-1.485) 731,732,732
732   WRITE(1,733) X(I),U(I,11)
733   FORMAT(10X,'PARABOLIC VELOCITY PROFILE
     2AT DISTANCE =',F10.5//,10X,'VALUE OF
     3CENTERLINE VELOCITY IS =',F10.5//)
731   XXI=0.
730   CONTINUE
      GO TO 333
999   WRITE(1,555)
555   FORMAT(10X,'POISSON EQUATION PROBLEM')
      GO TO 333
998   WRITE(1,656)
656   FORMAT('NAVIER-STOKES EQUATIONS PROBLEM')
205   WRITE(1,767)
767   FORMAT(10X,'OUTER ITERATIONS PROBLEM')
      CLOSE(UNIT=2)
333   CLOSE(UNIT=1)
      STOP
      END
```


SET

FLOW CHART FOR ITERATIVE PROCEDURE

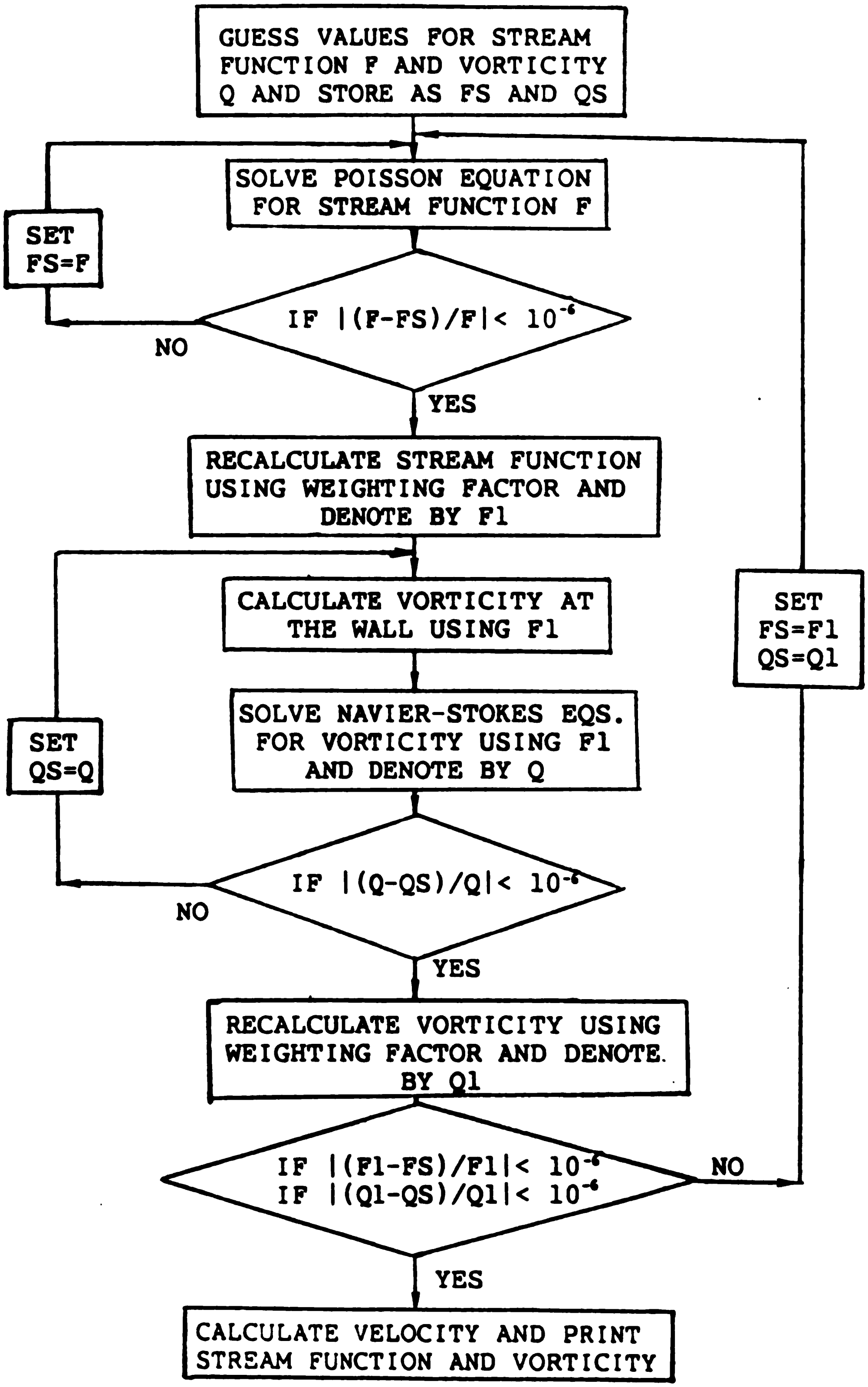

APPENDIX B

```
2

.
C
C
C
C
C
C
C
C
C
C
C
C
C
C

88
C
C
C
C
C
C
C
C
C
C
C
C
C
C
C
```

Appendix B

Computer program for the forward step

```
      REAL*8 F(2601,21),FS(2601,21),Q(2601,21),
     2QS(2601,21),U(2601,21),Y(21),X(2601),Z(21)
      REAL*8 ERF,ERQ,EFF,EQQ
      OPEN(UNIT=1,FILE='OUTCON',STATUS='NEW',FORM=
     2'FORMATTED')
      OPEN(UNIT=2,NAME=CONDATA,TYPE='OLD')
C     F,Q ARE THE CALCULATED STREAM FUNCTION
C         AND VORTICITY
C     FS,QS ARE THE STORED STREAM FUNCTION
C           AND VORTICITY
C     ERF,ERQ ARE THE MAXIMUM RELATIVE ERRORS IN
C             STREAM FUNCTION AND VORTICITY
C             FOR INNER ITERATION
C     EFF ARE THE  MAXIMUM RELATIVE ERRORS IN
C             STREAM FUNCTION AND VORTICITY
C             FOR OUTER ITERATION
C     U IS A STREAMWISE VELOCITY
C     X IS A STREAMWISE DIRECTION
C     Y IS A NORMAL DIRECTION
C     Z IS A DISTANCE FROM THE TOP OF THE STEP
      READ (2,88) ITMAX,M,N,L,MA,H,RE,AKS,AKV
   88 FORMAT (5I5,4F10.5)
C     ITMAX IS A PRESELECTED NO. OF ITERATIONS
C     M IS A NO. OF GRID POINTS IN STREAMWISE DIRECTION
C     N IS A NO. OF GRID POINTS IN NORMAL DIRECTION
C     L IS A STEP POSITION
C     MA IS A STEP HEIGHT
C     H IS A MESH SIZE EQUAL IN X-AND Y-DIRECTION
C     RE IS REYNOLDS NUMBER BASED ON CHANNEL HEIGHT
C     AKS IS A WEIGHTING FACTOR FOR STREAM FUNCTION
C     AKV IS A WEIGHTING FACTOR FOR VORTICITY
C     FS IS AN OVER-RELAXATION FACTOR FOR POISSON EQ.
C     FV IS AN OVER-RELAXATION FACTOR FOR N.S.EQS.
C     ITERF IS A NO. OF INNER ITER. FOR STREAM FUNCTION
C     ITERQ IS A NO. OF INNER ITER. FOR VORTICITY
C     INER IS A NO. OF OUTER ITER. FOR STREAM
C           FUNCTION AND VORTICITY
      NM1=N-1
      MM1=M-1
      LL=L-1
      LR=L+1
      MA1=MA+1
      MA2=MA-1
```

```
C
C
534
3333
C
C
1
2
3
C
C
C
C
4
C
C
C
C
```

```
C      COMPUTE OVER-RELAXATION FACTOR
C      ******************************
       PI=4.*ATAN(1.)
       ALPHA=COS(PI/M)+COS(PI/N)
       FS=(8.-4.*SQRT(4.-ALPHA**2))/ALPHA**2
       PRINT 534,N,M,FS
 534   FORMAT(10X,'TOTAL GRID Y-DIR.=',I5,10X,
      2'TOTAL GRID X-DIR.=',I5,'FS=',F10.7/)
       PRINT 3333,L,MA,RE
 3333  FORMAT('L=',I3,'MA=',I2,10X,'RE=',F8.1//)
C      COMPUTE COORDINATE FOR GRID POINTS
C      **********************************
       X(1)=0.
       DO 1 I=2,M
   1   X(I)=X(I-1)+H
       Y(1)=0.
       DO 2 J=2,N
   2   Y(J)=Y(J-1)+H
       Z(MA)=0.
       DO 3 J=MA1,N
   3   Z(J)=Z(J-1)+1./(N-MA)
C      A. STREAM FUNCTION BOUNDARY CONDITIONS
C      --------------------------------------
C      1. LOWER WALLS CONDITIONS
C      -------------------------
       DO 4 I=1,L
   4   F(I,1)=0.
       DO 5 J=2,MA
   5   F(L,J)=0.
       DO 40 I=LR,M
  40   F(I,MA)=0.
C      2. UPPER WALL CONDITION
C      -----------------------
       DO 6 I=1,M
   6   F(I,N)=1.
C      3. UPSTREAM CONDITION
C      ---------------------
       DO 7 J=2,NM1
   7   F(1,J)=Y(J-1)+H
C      4. INTERIOR REGION CONDITION
C      ----------------------------
       DO 8 I=2,LL
       DO 8 J=2,NM1
   8   F(I,J)=Y(J)
       DO 9 I=L,MM1
       DO 9 J=MA1,NM1
   9   F(I,J)=Z(J)
C      5. DOWNSTREAM CONDITION
C      -----------------------
       DO 10 J=MA1,NM1
  10    F(M,J)=3.*Z(J)**2-2.*Z(J)**3
```

```
C     B. VORTICITY BOUNDARY CONDITIONS
C     --------------------------------
C     1. INTERIOR REGION CONDITION
C     ----------------------------
      DO 11 I=2,LL
      DO 11 J=2,NM1
   11 Q(I,J)=0.
      DO 12 I=L,MM1
      DO 12 J=MA1,NM1
   12 Q(I,J)=0.
C     2. UPSTERAM CONDITION
C     ---------------------
      DO 13 J=2,NM1
   13 Q(1,J)=0.
C     3. DOWNSTREAM CONDITION
C     -----------------------
      DO 14 J=MA1,NM1
   14 Q(M,J)=12.*Z(J)-6.
C     STORING STREAM FUNCTION AND VORTICITY
C     -------------------------------------
      DO 15 I=2,LL
      DO 15 J=2,NM1
      FS(I,J)=F(I,J)
   15 QS(I,J)=Q(I,J)
      DO 16 I=L,MM1
      DO 16 J=MA1,NM1
      FS(I,J)=F(I,J)
   16 QS(I,J)=Q(I,J)
C     BEGIN OUTER ITERATIONS FOR STREAM FUNCTION
C     AND VORTICITY-------------------------------
C     -----------
      ITER=0
  300 ITER=ITER+1
C     BEGIN INNER ITERATION FOR STREAM FUNCTION
C     -----------------------------------------
      ITERF=0
   80 ITERF=ITERF+1
      ERF=0.
C     SOLVING POISSON EQUATION FOR STREAM FUNCTION
C     --------------------------------------------
C     COMPUTE STREAM FUNCTION ON THE LEFT OF STEP
C     *******************************************
      DO 17 I=2,LL
      DO 17 J=2,NM1
      FOLDF=F(I,J)
      F(I,J)=F(I,J)+0.25*FS*(F(I-1,J)+F(I+1,J)+
     2F(I,J-1)+F(I,J+1)-4.*F(I,J)+H*H*Q(I,J))
      EEEF=F(I,J)+0.00001)
   17 ERF=DMAX1(ERF,DABS((F(I,J)-FOLDF)/EEEF))
C     COMPUTE STREAM FUNCTIONS ON THE TOP OF STEP
C     *******************************************
```

```
    D
    I
    E
    I
   2
    I
18
C
C
C
C
 75
 19
 20
C
C
 175
C
C
 21
C
C
  23
  24
  24.
C
C
```

```
      DO 18 I=L,MM1
      DO 18 J=MA1,NM1
      FOLDF=F(I,J)
      F(I,J)=F(I,J)+0.25*FS*(F(I-1,J)+F(I+1,J)+
     2F(I,J-1)+F(I,J+1)-4.*F(I,J)+H*H*Q(I,J))
      EEEF=F(I,J)+0.00001
 18   ERF=DMAX1(ERF,DABS((F(I,J)-FOLDF)/EEEF))
C     CHECK STREAM FUNCTION FOR CONVERGENCE
C     -------------------------------------
      IF(ERF.LE.0.00001) GO TO 75
      IF(ITERF.GT.2000 ) GO TO 999
      GO TO 80
C     END OF INNER ITERATION FOR STREAM FUNCTION
C     ------------------------------------------
  75  DO 19 I=2,LL
      DO 19 J=2,NM1
 19   F(I,J)=AKS*FS(I,J)+(1-AKS)*F(I,J)
      DO 20 I=L,MM1
      DO 20 J=MA1,NM1
 20   F(I,J)=AKS*FS(I,J)+(1-AKS)*F(I,J)
C     BEGIN INNER ITERATION FOR VROTICITY
C     -----------------------------------
      ITERQ=0
 175  ITERQ=ITERQ+1
      ERQ=0.
C     4. UPPER WALL CONDITION
C     -----------------------
      DO 21 I=2,MM1
 21   Q(I,N)=(F(I,N)-F(I,NM1))*3./H**2-(0.5*Q(I,NM1))
C     5. LOWER WALLS CONDITIONS
C     -------------------------
      DO 23 J=2,MA2
  23  Q(L,J)=(F(L,J)-F(LL,J))*3./H**2-(0.5*Q(LL,J))
      DO 24 I=LR,MM1
  24  Q(I,MA)=(F(I,MA)-F(I,MA1))*3./H**2-(0.5*Q(I,MA1))
      Q(L,1)=0.
      DO 244 I=2,LL
 244  Q(I,1)=(F(I,1)-F(I,2))*3./H**2-(0.5*Q(I,2))
      Q(L,MA)=-(1/H**2)*(F(L,MA1)+F(LL,MA))
C     COMPUTE VORTICITY ON THE LEFT OF THE STEP
C     *****************************************
      DO 26 I=2,LL
      DO 26 J=2,NM1
      FOLDQ=Q(I,J)
      A=F(I+1,J)-F(I-1,J)
      B=F(I,J+1)-F(I,J-1)
      REA=0.5*A*RE
      REB=0.5*B*RE
      IF((A.GE.0.).AND.(B.GE.0.))  GO TO 500
      IF((A.GE.0.).AND.(B.LT.0.))  GO TO 600
      IF((A.LT.0.).AND.(B.GE.0.))  GO TO 700
```

```
      IF((A.LT.0.).AND.(B.LT.0.))  GO TO 800
 500  Q(I,J)=(1-FV)*Q(I,J)+FV*((Q(I+1,J)+(1.+REB)*
     2Q(I-1,J)+(1.+REA)*Q(I,J+1)+Q(I,J-1))/(4.+REA+REB))
      GO TO 900
 600  Q(I,J)=(1-FV)*Q(I,J)+FV*((Q(I+1,J)*(1.-REB)+
     2Q(I-1,J)+(1.+REA)*Q(I,J+1)+Q(I,J-1))/(4.+REA-REB))
      GO TO 900
 700  Q(I,J)=(1-FV)*Q(I,J)+FV*((Q(I+1,J)+(1.+REB)*
     2Q(I-1,J)+Q(I,J+1)+(1.-REA)*Q(I,J-1))/(4.-REA+REB))
      GO TO 900
 800  Q(I,J)=(1-FV)*Q(I,J)+FV*(((1.-REB)*Q(I+1,J)+
     2Q(I-1,J)+Q(I,J+1)+(1.-REA)*Q(I,J-1))/(4.-REA-REB))
 900  EEEQ=Q(I,J)+0.00001
      ERQ=DMAX1(ERQ,DABS((Q(I,J)-FOLDQ)/EEEQ))
 26   CONTINUE
C     COMPUTE VORTICITY ON THE TOP  OF THE STEP
C     ****************************************
      DO 27 I=L,MM1
      DO 27 J=MA1,NM1
      FOLDQ=Q(I,J)
      A=F(I+1,J)-F(I-1,J)
      B=F(I,J+1)-F(I,J-1)
      REA=0.5*A*RE
      REB=0.5*B*RE
      IF((A.GE.0.).AND.(B.GE.0.))  GO TO 5000
      IF((A.GE.0.).AND.(B.LT.0.))  GO TO 6000
      IF((A.LT.0.).AND.(B.GE.0.))  GO TO 7000
      IF((A.LT.0.).AND.(B.LT.0.))  GO TO 8000
 5000 Q(I,J)=(1-FV)*Q(I,J)+FV*((Q(I+1,J)+(1.+REB)*
     2Q(I-1,J)+(1.+REA)*Q(I,J+1)+Q(I,J-1))/(4.+REA+REB))
       GO TO 1900
 6000 Q(I,J)=(1-FV)*Q(I,J)+FV*((Q(I+1,J)*(1.-REB)+
     2Q(I-1,J)+(1.+REA)*Q(I,J+1)+Q(I,J-1))/(4.+REA-REB))
      GO TO 1900
 7000 Q(I,J)=(1-FV)*Q(I,J)+FV*((Q(I+1,J)+(1.+REB)*
     2Q(I-1,J)+Q(I,J+1)+(1.-REA)*Q(I,J-1))/(4.-REA+REB))
      GO TO 1900
 8000 Q(I,J)=(1-FV)*Q(I,J)+FV*(((1.-REB)*Q(I+1,J)+
     2Q(I-1,J)+Q(I,J+1)+(1.-REA)*Q(I,J-1))/(4.-REA-REB))
 1900 EEEQ=Q(I,J)+0.00001
      ERQ=DMAX1(ERQ,DABS((Q(I,J)-FOLDQ)/EEEQ))
  27  CONTINUE
C     CHECK VORTICITY FOR CONVERGENCE
C     ------------------------------
      IF (ERQ.LE.0.000001) GO TO 85
      IF(ITERQ.GT.5000  )  GO TO 998
      GO TO 175
C     END OF INNER ITERATION FOR VORTICITY
C     ------------------------------------
 85   DO 28 I=2,LL
      DO 28 J=2,NM1
```

```
 28   Q(I,J)=AKV*QS(I,J)+(1-AKV)*F(I,J)
      DO 29 I=L,MM1
      DO 29 J=MA1,NM1
  29  Q(I,J)=AKV*QS(I,J)+(1-AKV)*F(I,J)
      EFF=0.
      EQQ=0.
      DO 30 I=2,LL
      DO 30 J=2,NM1
      EEEFF=F(I,J)+0.00001
      EEEQQ=Q(I,J)+0.00001
      EFF=DMAX1(EFF,DABS((F(I,J)-FS(I,J))/EEEFF))
 30   EQQ=DMAX1(EQQ,DABS((Q(I,J)-QS(I,J))/EEEQQ))
      DO 31 I=L,MM1
      DO 31 J=MA1,NM1
      EEEFF=F(I,J)+0.00001
      EEEQQ=Q(I,J)+0.00001
      EFF=DMAX1(EFF,DABS((F(I,J)-FS(I,J))/EEEFF))
  31  EQQ=DMAX1(EQQ,DABS((Q(I,J)-QS(I,J))/EEEQQ))
C     CHECK FOR OUTER CONVERGANCE
C     --------------------------
      ETA=0.000001
      IF((EFF.LE.ETA).AND.(EQQ.LE.ETA)) GO TO 105
      IF(ITER.GT.ITMAX) GO TO 205
      DO 32 I=2,LL
      DO 32 J=2,NM1
      FS(I,J)=F(I,J)
  32  QS(I,J)=Q(I,J)
      DO 33 I=L,MM1
      DO 33 J=MA1,NM1
      FS(I,J)=F(I,J)
  33  QS(I,J)=Q(I,J)
      GO TO 300
C     END OF OUTER ITERATION
C     ----------------------
 105  DO 38 I=2,LL
      DO 38 J=2,NM1
 38   U(I,J)=(F(I,J+1)-F(I,J-1))/(2.*H)
      DO 39 I=L,MM1
      DO 39 J=MA1,NM1
 39   U(I,J)=(F(I,J+1)-F(I,J-1))/(2.*H)
      WRITE(1,666)ITER,EFF,EQQ
 666  FORMAT(10X,'NO. OF ITER.=',I5,10X,'EFF=',E14.7,
     2'EQQ=',E14.7//)
      WRITE(1,170)
 170  FORMAT(15X,'VELOCITY  DISTRIBUTION ')
      DO 445 I=2,LL
 445  WRITE(1,446)(U(I,J),J=2,NM1)
 446  FORMAT(1X,'U(I,J)=',10F11.8//)
      DO 447 I=L,MM1
 447  WRITE(1,448)(U(I,J),J=MA1,NM1)
 448  FORMAT(1X,'U(I,J)=',15F7.4//)
```

```
      WRITE(1,180)
180   FORMAT(10X,' STREAM FUNCTION VALUES'/)
      DO 620 I=2,LL
620   WRITE(1,621)(F(I,J),J=2,NM1)
621   FORMAT(1X,'F(I,J)=',10F11.8//)
      DO 622 I=L,MM1
622   WRITE(1,623)(F(I,J),J=MA1,NM1)
623   FORMAT(1X,'F(I,J)=',10F11.8//)
      WRITE(1,190)
190   FORMAT(10X,'VORTICITY VALUES '/)
      DO 533 I=2,LL
533   WRITE(1,538)(Q(I,J),J=1,N)
538   FORMAT(1X,'Q(I,J)=',10F11.5//)
      DO 535 I=L,MM1
535   WRITE(1,536)(Q(I,J),J=MA,N)
536   FORMAT(1X,'Q(I,J)=',10F11.5//)
      GO TO 333
999   WRITE(1,555)
555   FORMAT(10X,'POISSON EQUATION PROBLEM')
      GO TO 333
998   WRITE(1,656)
656   FORMAT(10X,'NAVIER-STOKES EQUATIONS PROBLEM')
205   WRITE(1,767)
767   FORMAT(10X,'OUTER ITERATIONS PROBLEM')
      CLOSE(UNIT=2)
333   CLOSE(UNIT=1)
      STOP
      END
```

APPENDIX C

Appendix C

Computer program for the backward step

```
      REAL*8 F(3201,21),FS(3201,21),Q(3201,21),
     2QS(3201,21),U(3201,21),Y(21),X(3201),Z(21)
      REAL*8 ERF,ERQ,EFF,EQQ
      OPEN(UNIT=1,FILE='OUTMOD',STATUS='NEW',FORM=
     2'FORMATTED')
      OPEN(UNIT=2,NAME=MODDATA,TYPE='OLD')
C     ALL PARAMETERS HAVE THE SAME DEFINATIONS AS
C     IN FORWARD STEP PROGRAM
      READ (2,88)ITMAX,M,N,,MA,L,RE,H,AKS,AKV
 88   FORMAT(5I10,4F10.4/)
      NM1=N-1
      MM1=M-1
      LL=L-1
      LR=L+1
      MA1=MA+1
      MA2=MA-1
C     COMPUTE OVER-RELAXATION FACTOR
C     ******************************
      PI=4.*ATAN(1.)
      ALPHA=COS(PI/M)+COS(PI/N)
      FS=(8.-4.*SQRT(4.-ALPHA**2))/ALPHA**2
      PRINT 534,N,M,FS
 534  FORMAT(10X,'TOTAL GRID Y-DIR.=',I5,10X,
     2'TOTAL GRID X-DIR.=',I5,'FS=',F10.7/)
C     COMPUTE COORDINATE FOR GRID POINTS
C     **********************************
      X(1)=0.
      DO 1 I=2,M
  1   X(I)=X(I-1)+H
      Y(1)=0.
      DO 2 J=2,N
  2   Y(J)=Y(J-1)+H
      Z(MA)=0.
      DO 3 J=MA1,N
  3   Z(J)=Z(J-1)+1./(N-MA)
C     A. STREAM FUNCTION BOUNDARY CONDITIONS
C     --------------------------------------
C     1. LOWER WALLS CONDITIONS
C     -------------------------
      DO 4 I=1,L
  4   F(I,MA)=0.
      DO 5 J=2,MA
  5   F(L,J)=0.
      DO 40 I=LR,M
 40   F(I,1)=0.
```

```
C       2. UPPER WALL CONDITION
C       -----------------------
        DO 6 I=1,M
    6   F(I,N)=1.
C       3. UPSTREAM CONDITION
C       ---------------------
        DO 7 J=MA1,NM1
    7   F(1,J)=Z(J)
C       4. INTERIOR REGION CONDITION
C       ----------------------------
        DO 8 I=2,L
        DO 8 J=MA1,NM1
    8   F(I,J)=Z(J)
        DO 9 I=LR,MM1
        DO 9 J=2,NM1
    9   F(I,J)=Y(J)
C       5. DOWNSTREAM CONDITION
C       -----------------------
        DO 10 J=2,NM1
   10   F(M,J)=3.*Y(J)**2-2.*Y(J)**3
C       B.VORTICITY BOUNDARY CONDITIONS
C       -------------------------------
C       1. INTERIOR REGION CONDITION
C       ----------------------------
        DO 11 I=2,L
        DO 11 J=MA1,NM1
   11   Q(I,J)=0.
        DO 12 I=LR,MM1
        DO 12 J=2,NM1
   12   Q(I,J)=0.
C       2. UPSTERAM CONDITION
C       ---------------------
        DO 13 J=MA1,NM1
   13   Q(1,J)=0.
C       3. DOWNSTREAM CONDITION
C       -----------------------
        DO 14 J=2,NM1
   14   Q(M,J)=12.*Y(J)-6.
C       STORING THE VALUES
C       ------------------
        DO 15 I=2,L
        DO 15 J=MA1,NM1
        FS(I,J)=F(I,J)
   15   QS(I,J)=Q(I,J)
        DO 16 I=LR,MM1
        DO 16 J=2,NM1
        FS(I,J)=F(I,J)
   16   QS(I,J)=Q(I,J)
C       BEGIN OUTER ITERATION FOR STREAM FUNCTION
C       AND VORTICITY-----------------------------
C       -------------
```

```
      ITER=0
300   ITER=ITER+1
C     SOLVING POISSON EQUATION FOR STREAM FUNCTION
C     --------------------------------------------
C     BEGIN INNER ITERATION FOR STREAM FUNCTION
C     -----------------------------------------
      ITERF=0
 80   ITERF=ITERF+1
      ERF=0.
C     COMPUTE STREAM FUNCTION ON THE TOP OF STEP
C     ******************************************
      DO 17 I=2,L
      DO 17 J=MA1,NM1
      FOLDF=F(I,J)
      F(I,J)=F(I,J)+0.25*FS*(F(I-1,J)+F(I+1,J)
     2+F(I,J-1)+F(I,J+1)-4.*F(I,J)+H*H*Q(I,J))
      EEEF=F(I,J)+0.00001
 17   ERF=DMAX1(ERF,DABS((F(I,J)-FOLDF)/EEEF))
C     COMPUTE STREAM FUNCTIONS ON THE RIGHT OF STEP
C     *********************************************
      DO 18 I=LR,MM1
      DO 18 J=2,NM1
      FOLDF=F(I,J)
      F(I,J)=F(I,J)+0.25*FS*(F(I-1,J)+F(I+1,J)+
     2F(I,J-1)+F(I,J+1)-4.*F(I,J)+H*H*Q(I,J))
      EEEF=F(I,J)+0.00001
 18   ERF=DMAX1(ERF,DABS((F(I,J)-FOLDF)/EEEF))
C     CHECK STREAM FUNCTION FOR CONVERGENCE
C     -------------------------------------
      IF(ERF.LE.0.0001) GO TO 75
      IF(ITERF.GT.5000) GO TO 999
      GO TO 80
C     END OF INNER ITERATION FOR STREAM FUNCTION
C     ------------------------------------------
 75   DO 19 I=2,L
      DO 19 J=MA1,NM1
 19   F(I,J)=AKS*FS(I,J)+(1-AKS)*F(I,J)
      DO 20 I=LR,MM1
      DO 20 J=2,NM1
 20   F(I,J)=AKS*FS(I,J)+(1-AKS)*F(I,J)
C     SOLVING NAVIER STOKES EQUATIONS FOR VORTICITY
C     ---------------------------------------------
C     BEGIN INEER ITERATION FOR VORTICITY
C     -----------------------------------
      ITERQ=0
175   ITERQ=ITERQ+1
      ERQ=0.
C     4. UPPER WALL CONDITION
C     -----------------------
      DO 21 I=2,MM1
 21   Q(I,N)=(F(I,N)-F(I,NM1))*3./H**2-(0.5*Q(I,NM1))
```

```
C      5. LOWER WALLS CONDITIONS
C      ------------------------
       DO 23 J=2,MA2
  23   Q(L,J)=(F(L,J)-F(LR,J))*3./H**2-(0.5*Q(LR,J))
       DO 24 I=LR,MM1
  24   Q(I,1)=(F(I,1)-F(I,2))*3./H**2-(0.5*Q(I,2))
       Q(L,1)=0.
       DO 244 I=2,LL
 244   Q(I,MA)=(F(I,MA)-F(I,MA1))*3./H**2-(0.5*Q(I,MA1))
       Q(L,MA)=-(1/H**2)*(F(L,MA1)+F(LR,MA))
C      COMPUTE VORTICITY ON THE TOP OF THE STEP
C      ****************************************
       DO 26 I=2,L
       DO 26 J=MA1,NM1
       FOLDQ=Q(I,J)
       A=F(I+1,J)-F(I-1,J)
       B=F(I,J+1)-F(I,J-1)
       REA=0.5*A*RE
       REB=0.5*B*RE
       IF((A.GE.0.).AND.(B.GE.0.))  GO TO 500
       IF((A.GE.0.).AND.(B.LT.0.))  GO TO 600
       IF((A.LT.0.).AND.(B.GE.0.))  GO TO 700
       IF((A.LT.0.).AND.(B.LT.0.))  GO TO 800
 500   Q(I,J)=(1-FV)*Q(I,J)+FV*((Q(I+1,J)+(1.+REB)*
      2Q(I-1,J)+(1.+REA)*Q(I,J+1)+Q(I,J-1))/(4.+REA+REB))
       GO TO 900
 600   Q(I,J)=(1-FV)*Q(I,J)+FV*((Q(I+1,J)*(1.-REB)+
      2Q(I-1,J)+(1.+REA)*Q(I,J+1)+Q(I,J-1))/(4.+REA-REB))
       GO TO 900
 700   Q(I,J)=(1-FV)*Q(I,J)+FV*((Q(I+1,J)+(1.+REB)*
      2Q(I-1,J)+Q(I,J+1)+(1.-REA)*Q(I,J-1))/(4.-REA+REB))
       GO TO 900
 800   Q(I,J)=(1-FV)*Q(I,J)+FV*(((1.-REB)*Q(I+1,J)+
      2Q(I-1,J)+Q(I,J+1)+(1.-REA)*Q(I,J-1))/(4.-REA-REB))
 900   EEEQ=Q(I,J)+0.00001
       ERQ=DMAX1(ERQ,DABS((Q(I,J)-FOLDQ)/EEEQ))
  26   CONTINUE
C      COMPUTE VORTICITY ON THE RIGHT  OF THE STEP
C      *******************************************
       DO 27 I=LR,MM1
       DO 27 J=2,NM1
       FOLDQ=Q(I,J)
       A=F(I+1,J)-F(I-1,J)
       B=F(I,J+1)-F(I,J-1)
       REA=0.5*A*RE
       REB=0.5*B*RE
       IF((A.GE.0.).AND.(B.GE.0.))  GO TO 5000
       IF((A.GE.0.).AND.(B.LT.0.))  GO TO 6000
       IF((A.LT.0.).AND.(B.GE.0.))  GO TO 7000
       IF((A.LT.0.).AND.(B.LT.0.))  GO TO 8000
5000   Q(I,J)=(1-FV)*Q(I,J)+FV*((Q(I+1,J)+(1.+REB)*
```

```
     2Q(I-1,J)+(1.+REA)*Q(I,J+1)+Q(I,J-1))/(4.+REA+REB))
       GO TO 1900
 6000 Q(I,J)=(1-FV)*Q(I,J)+FV*((Q(I+1,J)*(1.-REB)+
     2Q(I-1,J)+(1.+REA)*Q(I,J+1)+Q(I,J-1))/(4.+REA-REB))
      GO TO 1900
 7000 Q(I,J)=(1-FV)*Q(I,J)+FV*((Q(I+1,J)+(1.+REB)*
     2Q(I-1,J)+Q(I,J+1)+(1.-REA)*Q(I,J-1))/(4.-REA+REB))
      GO TO 1900
 8000 Q(I,J)=(1-FV)*Q(I,J)+FV*(((1.-REB)*Q(I+1,J)+
     2Q(I-1,J)+Q(I,J+1)+(1.-REA)*Q(I,J-1))/(4.-REA-REB))
1900  EEEQ=F(I,J)+0.00001
      ERQ=DMAX1(ERQ,DABS((Q(I,J)-FOLDQ)/EEEQ))
  27  CONTINUE
C     CHECK VORTICITY FOR CONVERGENCE
C     ------------------------------
      IF (ERQ.LE.0.00001) GO TO 85
      IF(ITERQ.GT.5000 )  GO TO 998
      GO TO 175
C     END OF INNER ITERATION FOR VORTICITY
C     -----------------------------------
 85   DO 28 I=2,L
      DO 28 J=MA1,NM1
 28   Q(I,J)=AKV*QS(I,J)+(1-AKV)*F(I,J)
      DO 29 I=LR,MM1
      DO 29 J=2,NM1
  29  Q(I,J)=AKV*FS(I,J)+(1-AKV)*Q(I,J)
      EFF=0.
      EQQ=0.
      DO 30 I=2,L
      DO 30 J=MA1,NM1
      EEEFF=F(I,J)+0.00001
      EEEQQ=Q(I,J)+0.00001
      EFF=DMAX1(EFF,DABS((F(I,J)-FS(I,J))/EEEFF))
 30   EQQ=DMAX1(EQQ,DABS((Q(I,J)-QS(I,J))/EEEQQ))
      DO 31 I=LR,MM1
      DO 31 J=2,NM1
      EEEFF=F(I,J)+0.00001
      EEEQQ=Q(I,J)+0.00001
      EFF=DMAX1(EFF,DABS((F(I,J)-FS(I,J))/EEEFF))
  31  EQQ=DMAX1(EQQ,DABS((Q(I,J)-QS(I,J))/EEEQQ))
C     CHECK OUTER ITERATION FOR CONVERGANCE
C     -----------------------------------
      ETA=0.000001
      IF((EFF.LE.ETA).AND.(EQQ.LE.ETA)) GO TO 105
      IF(ITER.GT.ITMAX) GO TO 205
      DO 32 I=2,L
      DO 32 J=MA1,NM1
      FS(I,J)=F(I,J)
  32  QS(I,J)=Q(I,J)
      DO 33 I=LR,MM1
      DO 33 J=2,NM1
```

```
      FS(I,J)=F(I,J)
   33 QS(I,J)=Q(I,J)
      GO TO 300
C     END OF OUTER ITERATION
C     ----------------------
  105 DO 38 I=2,L
      DO 38 J=MA1,NM1
   38 U(I,J)=(F(I,J+1)-F(I,J-1))/(2.*H)
      DO 39 I=LR,MM1
      DO 39 J=2,NM1
   39 U(I,J)=(F(I,J+1)-F(I,J-1))/(2.*H)
      WRITE(1,666)ITER,EFF,EQQ,RE,AKS,AKV,L
  666 FORMAT('NO.OF ITER.=',I5,'EFF=',E14.7,'EQQ=',E1
     24.7,'RE=',F10.2,'AKS='F4.2,'AKV=',F4.2,I5//)
      WRITE(1,170)
  170 FORMAT(15X,'VELOCITY  DISTRIBUTION ')
      DO 445 I=2,L
  445 WRITE(1,446)(U(I,J),J=MA1,NM1)
  446 FORMAT(1X,'U(I,J)=',12F8.4//)
      DO 447 I=LR,M
  447 WRITE(1,448)(U(I,J),J=2,NM1)
  448 FORMAT(1X,'U(I,J)=',10F10.4//)
      WRITE(1,180)
  180 FORMAT(10X,' STREAM FUNCTION VALUES'/)
      DO 620 I=1,L
  620 WRITE(1,621)(F(I,J),J=MA,NM1)
  621 FORMAT(1X,'F(I,J)=',13F8.4//)
      DO 622 I=LR,M
  622 WRITE(1,623)(F(I,J),J=2,NM1)
  623 FORMAT(1X,'F(I,J)=',10F10.4//)
      WRITE(1,190)
  190 FORMAT(10X,'VORTICITY VALUES '/)
      DO 533 I=1,L
  533 WRITE(1,538)(Q(I,J),J=MA,N)
  538 FORMAT(1X,'Q(I,J)=',13F9.4//)
      DO 535 I=LR,M
  535 WRITE(1,536)(Q(I,J),J=1,N)
  536 FORMAT(1X,'Q(I,J)=',10F10.4//)
      GO TO 333
  999 WRITE(1,555)
  555 FORMAT('POISSON EQUATION PROBLEM')
      GO TO 333
  998 WRITE(1,656)
  656 FORMAT('NAVIER-STOKES EQUATIONS PROBLEM')
  205 WRITE(1,767)
  767 FORMAT(10X,'OUTER ITERATION PROBLEM')
      CLOSE(UNIT=2)
  333 CLOSE(UNIT=1)
      STOP
      END
```

APPENDIX D

Appendix D

Computer program for the finite step

```
      REAL*8 F(1580,21),FS(1580,21),Q(1580,21),
     2QS(1580,21),U(1580,21),X(1580),Y(21),Z(21)
      REAL*8 ERF,ERQ,EFF,EQQ
      OPEN(UNIT=1,FILE='OUTSTEP',STATUS='NEW',
     2FORM='FORMATTED')
      OPEN(UNIT=2,NAME=STEPDATA,TYPE='OLD')
      READ(2,88)ITMAX,M,N,L,K,MA,RE,H,AKS,AKV
   88 FORMAT(6I6,4F10.5/)
C     K IS THE END OF THE STEP
C     ALL OTHER PARAMETERS HAVE THE SAME
C     DEFINATINS AS IN FORWARD STEP PROGRAM
      MM1=M-1
      NM1=N-1
      LL=L-1
      LR=L+1
      KL=K-1
      KR=K+1
      MA1=MA+1
      MA2=MA-1
C     COMPUTE OVER-RELAXATION FACTOR
C     ******************************
      PI=4.*ATAN(1.)
      ALPHA=COS(PI/M)+COS(PI/N)
      FS=(8.-4.*SQRT(4.-ALPHA**2))/ALPHA**2
      PRINT 4444,RE,L,K,MA
 4444 FORMAT('RE=',F5.1,'L=',I3,'K=',I5,'MA=',I2/)
      PRINT 4445,AKS,AKV
 4445 FORMAT(10X,'AKS=',F10.4,'AKV=',F10.4/)
      WRITE(1,534)N,M,FS
  534 FORMAT(10X,'TOTAL GRID Y-DIR.=',I5,10X,
     2'TOTAL GRID X-DIR.=',I5,'FS=',F10.7/)
C     COMPUTE COORDINATES FOR GRID POINTS
C     ***********************************
      X(1)=0.
      DO 1 I=2,M
    1 X(I)=X(I-1)+H
      Y(1)=0.
      DO 2 J=2,N
    2 Y(J)=Y(J-1)+H
      Z(MA)=0.
      DO 3 J=MA1,N
    3 Z(J)=Z(J-1)+1./(N-MA)
C     A. STREAM FUNCTION BOUNDARY CONDITIONS
C     --------------------------------------
```

```
C      1. LOWER WALLS CONDITIONS
C      -------------------------
       DO 4 I=1,L
  4    F(I,1)=0.
       DO 5 J=2,MA
  5    F(L,J)=0.
       DO 40 I=LR,KL
 40    F(I,MA)=0.
       DO 41 J=2,MA
 41    F(K,J)=0.
       DO 42 I=KR,M
 42    F(I,1)=0.
C      2. UPPER WALL CONDITION
C      -----------------------
       DO 6 I=1,M
  6    F(I,N)=1.
C      3. UPSTREAM CONDITION
C      ---------------------
       DO 7 J=2,NM1
  7    F(1,J)=Y(J-1)+H
C      4. INTERIOR REGION CONDITION
C      ----------------------------
       DO 8 I=2,LL
       DO 8 J=2,NM1
  8    F(I,J)=Y(J)
       DO 9 I=L,K
       DO 9 J=MA1,NM1
  9    F(I,J)=Z(J)
       DO 91 I=KR,MM1
       DO 91 J=2,NM1
 91    F(I,J)=Y(J-1)+H
C      5. DOWNSTREAM CONDITION
C      -----------------------
       DO 10 J=2,NM1
 10    F(M,J)=3.*Y(J)**2-2.*Y(J)**3
C      B. VORTICITY BOUNDARY CONDITIONS
C      --------------------------------
C      1. INTERIOR REGION CONDITION
C      ----------------------------
       DO 11 I=2,LL
       DO 11 J=2,NM1
 11    Q(I,J)=0.
       DO 12 I=L,K
       DO 12 J=MA1,NM1
 12    Q(I,J)=0.
       DO 121 I=KR,MM1
       DO 121 J=2,NM1
121    Q(I,J)=0.
C      2. UPSTERAM CONDITION
C      ---------------------
```

```
      DO 13 J=2,NM1
   13 Q(1,J)=0.0
C     3. DOWNSTREAM CONDITION
C     ----------------------
      DO 14 J=2,NM1
   14 Q(M,J)=12.*Y(J)-6
C     STORING STREAM FUNCTION AND VORTICITY
C     -------------------------------------
      DO 15 I=2,LL
      DO 15 J=2,NM1
      FS(I,J)=F(I,J)
   15 QS(I,J)=Q(I,J)
      DO 16 I=L,K
      DO 16 J=MA1,NM1
      FS(I,J)=F(I,J)
   16 QS(I,J)=Q(I,J)
      DO 161 I=KR,MM1
      DO 161 J=2,NM1
      FS(I,J)=F(I,J)
  161 QS(I,J)=Q(I,J)
C     BEGIN OUTER ITERATION FOR STREAM FUNCTION
C     AND VORTICITY---------------------------
C     ----------------------------------------
      ITER=0
  300 ITER=ITER+1
C     SOLVING POSSISON EQUATION FOR STREAM FUNCTION
C     ---------------------------------------------
C     BEGIN INNER ITERATION FOR STREAM FUNCTION
C     -----------------------------------------
      ITERF=0
   80 ITERF=ITERF+1
      ERF=0.
C     COMPUTE STREAM FUNCTION ON THE LEFT OF STEP
C     *******************************************
      DO 17 I=2,LL
      DO 17 J=2,NM1
      FOLDF=F(I,J)
      F(I,J)=F(I,J)+0.25*FS*(F(I-1,J)+F(I+1,J)+
     2F(I,J-1)+F(I,J+1)-4.*F(I,J)+H*H*Q(I,J))
      EEEF=F(I,J)+0.00001
   17 ERF=DMAX1(ERF,DABS((F(I,J)-FOLDF)/EEEF))
C     COMPUTE STREAM FUNCTION ON THE TOP OF THE STEP
C     **********************************************
      DO 18 I=L,K
      DO 18 J=MA1,NM1
      FOLDF=F(I,J)
      F(I,J)=F(I,J)+0.25*FS*(F(I-1,J)+F(I+1,J)+
     2F(I,J-1)+F(I,J+1)-4.*F(I,J)+H*H*Q(I,J))
      EEEF=F(I,J)+0.00001
   18 ERF=DMAX1(ERF,DABS((F(I,J)-FOLDF)/EEEF))
```

```
C      COMPUTE STREAM FUNCTION ON THE RIGHT OF THE STEP
C      ***********************************************
       DO 181 I=KR,MM1
       DO 181 J=2,NM1
       FOLDF=F(I,J)
       F(I,J)=F(I,J)+0.25*FS*(F(I-1,J)+F(I+1,J)+
      2F(I,J-1)+F(I,J+1)-4.*F(I,J)+H*H*Q(I,J))
       EEEF=F(I,J)+0.00001
 181   ERF=DMAX1(ERF,DABS((F(I,J)-FOLDF)/EEEF))
C      CHECK STREAM FUNCTION FOR CONVERGENCE
C      ------------------------------------
       IF(ERF.LE.0.000001) GO TO 75
       IF(ITERF.GT.5000  ) GO TO 999
       GO TO 80
C      END OF INNER ITERATION FOR STREAM FUNCTION
C      ------------------------------------------
C      RECALCULATE F(I,J) USING WEIGHTING FACTOR
C      ******************************************
 75    DO 19 I=2,LL
       DO 19 J=2,NM1
 19    F(I,J)=AKS*FS(I,J)+(1-AKS)*F(I,J)
       DO 20 I=L,K
       DO 20 J=MA1,NM1
 20    F(I,J)=AKS*FS(I,J)+(1-AKS)*F(I,J)
       DO 120 I=KR,MM1
       DO 120 J=2,NM1
 120   F(I,J)=AKS*FS(I,J)+(1-AKS)*F(I,J)
C      BEGIN INNER ITERATION FOR VORTICITY
C      -----------------------------------
       ITERQ=0
 175   ITERQ=ITERQ+1
       ERQ=0.
C      4. UPPER WALL CONDITION
C      -----------------------
       DO 21 I=2,MM1
 21    Q(I,N)=(F(I,N)-F(I,NM1))*3./H**2-(0.5*Q(I,NM1))
C      5. LOWER WALLS CONDITIONS
C      -------------------------
       DO 23 J=2,MA2
  23   Q(L,J)=(F(L,J)-F(LL,J))*3./H**2-(0.5*Q(LL,J))
       Q(K,1)=0.
       Q(L,1)=0.
       DO 24 I=LR,KL
 24    Q(I,MA)=(F(I,MA)-F(I,MA1))*3./H**2-(0.5*Q(I,MA1))
       DO 244 I=2,LL
 244   Q(I,1)=(F(I,1)-F(I,2))*3.0/H**2-(0.5*Q(I,2))
       DO 242 J=2,MA2
 242   Q(K,J)=(F(K,J)-F(KR,J))*3./H**2-(0.5*Q(KR,J))
       DO 245 I=KR,MM1
 245   Q(I,1)=((F(I,1)-F(I,2))*3./H**2-(0.5*Q(I,2))
```

```
      Q(L,MA)=-(1./H**2)*(F(L,MA1)+F(LL,MA))
      Q(K,MA)=-(1./H**2)*(F(K,MA1)+F(KR,MA))
C     COMPUTE VORTICITY ON THE LEFT OF THE STEP
C     ****************************************
      DO 26 I=2,LL
      DO 26 J=2,NM1
      FOLDQ=Q(I,J)
      A=F(I+1,J)-F(I-1,J)
      B=F(I,J+1)-F(I,J-1)
      REA=0.5*A*RE
      REB=0.5*B*RE
      IF((A.GE.0.).AND.(B.GE.0.))  GO TO 500
      IF((A.GE.0.).AND.(B.LT.0.))  GO TO 600
      IF((A.LT.0.).AND.(B.GE.0.))  GO TO 700
      IF((A.LT.0.).AND.(B.LT.0.))  GO TO 800
 500  Q(I,J)=(1-FV)*Q(I,J)+FV*((Q(I+1,J)+(1.+REB)*
     2Q(I-1,J)+(1.+REA)*Q(I,J+1)+Q(I,J-1))/(4.+REA+REB))
      GO TO 900
 600  Q(I,J)=(1-FV)*Q(I,J)+FV*((Q(I+1,J)*(1.-REB)+
     2Q(I-1,J)+(1.+REA)*Q(I,J+1)+Q(I,J-1))/(4.+REA-REB))
      GO TO 900
 700  Q(I,J)=(1-FV)*Q(I,J)+FV*((Q(I+1,J)+(1.+REB)*
     2Q(I-1,J)+Q(I,J+1)+(1.-REA)*Q(I,J-1))/(4.-REA+REB)
      GO TO 900
 800  Q(I,J)=(1-FV)*Q(I,J)+FV*(((1.-REB)*Q(I+1,J)+
     2Q(I-1,J)+Q(I,J+1)+(1.-REA)*Q(I,J-1))/(4.-REA-REB))
      EEEQ=Q(I,J)+0.00001
 900  ERQ=DMAX1(ERQ,DABS((Q(I,J)-FOLDQ)/EEEQ))
 26   CONTINUE
C     COMPUTE VORTICITY ON THE TOP  OF THE STEP
C     ****************************************
      DO 27 I=L,K
      DO 27 J=MA1,NM1
      FOLDQ=Q(I,J)
      A=F(I+1,J)-F(I-1,J)
      B=F(I,J+1)-F(I,J-1)
      REA=0.5*A*RE
      REB=0.5*B*RE
      IF((A.GE.0.).AND.(B.GE.0.))  GO TO 5000
      IF((A.GE.0.).AND.(B.LT.0.))  GO TO 6000
      IF((A.LT.0.).AND.(B.GE.0.))  GO TO 7000
      IF((A.LT.0.).AND.(B.LT.0.))  GO TO 8000
 5000 Q(I,J)=(1-FV)*Q(I,J)+FV*((Q(I+1,J)+(1.+REB)*
     2Q(I-1,J)+(1.+REA)*Q(I,J+1)+Q(I,J-1))/(4.+REA+REB))
      GO TO 1900
 6000 Q(I,J)=(1-FV)*Q(I,J)+FV*((Q(I+1,J)*(1.-REB)+
     2Q(I-1,J)+(1.+REA)*Q(I,J+1)+Q(I,J-1))/(4.+REA-REB))
      GO TO 1900
 7000 Q(I,J)=(1-FV)*Q(I,J)+FV*((Q(I+1,J)+(1.+REB)*
     2Q(I-1,J)+Q(I,J+1)+(1.-REA)*Q(I,J-1))/(4.-REA+REB))
```

```
      GO TO 1900
 8000 Q(I,J)=(1-FV)*Q(I,J)+FV*(((1.-REB)*Q(I+1,J)+
     2Q(I-1,J)+Q(I,J+1)+(1.-REA)*Q(I,J-1))/(4.-REA-REB))
      EEEQ=Q(I,J)+0.00001
1900  ERQ=DMAX1(ERQ,DABS((Q(I,J)-FOLDQ)/EEEQ))
  27  CONTINUE
C     COMPUTE VORTICITY ON THE RIGHT OF THE STEP
C     ******************************************
      DO 272 I=MER,MM1
      DO 272 J=2,NM1
      FOLDQ=Q(I,J)
      A=F(I+1,J)-F(I-1,J)
      B=F(I,J+1)-F(I,J-1)
      REA=0.5*A*RE
      REB=0.5*B*RE
      IF((A.GE.0.).AND.(B.GE.0.))  GO TO 5001
      IF((A.GE.0.).AND.(B.LT.0.))  GO TO 6001
      IF((A.LT.0.).AND.(B.GE.0.))  GO TO 7001
      IF((A.LT.0.).AND.(B.LT.0.))  GO TO 8001
 5001 Q(I,J)=(1-FV)*Q(I,J)+FV*((Q(I+1,J)+(1.+REB)*
     2Q(I-1,J)+(1.+REA)*Q(I,J+1)+Q(I,J-1))/(4.+REA+REB))
      GO TO 2900
 6001 Q(I,J)=(1-FV)*Q(I,J)+FV*((Q(I+1,J)*(1.-REB)+
     2Q(I-1,J)+(1.+REA)*Q(I,J+1)+Q(I,J-1))/(4.+REA-REB))
      GO TO 2900
 7001 Q(I,J)=(1-FV)*Q(I,J)+FV*((Q(I+1,J)+(1.+REB)*
     2Q(I-1,J)+Q(I,J+1)+(1.-REA)*Q(I,J-1))/(4.-REA+REB))
      GO TO 2900
 8001 Q(I,J)=(1-FV)*Q(I,J)+FV*(((1.-REB)*Q(I+1,J)+
     2Q(I-1,J)+Q(I,J+1)+(1.-REA)*Q(I,J-1))/(4.-REA-REB))
      EEEQ=Q(I,J)+0.00001
2900  ERQ=DMAX1(ERQ,DABS((Q(I,J)-FOLDQ)/EEEQ))
 272  CONTINUE
C     CHECK VORTICITY FOR CONVERGENCE
C     -----------------------------
      IF (ERQ.LE.0.00001)  GO TO 85
      IF(ITERQ.GT.5000 )   GO TO 998
      GO TO 175
C     END OF INNER ITERATION FOR VORTICITY
C     -----------------------------------
C     RECALCULATE Q(I,J) USING WEIGHTING FACTOR
C     ****************************************
 85   DO 28 I=2,LL
      DO 28 J=2,NM1
 28   Q(I,J)=AKV*QS(I,J)+(1-AKV)*Q(I,J)
      DO 29 I=L,K
      DO 29 J=MA1,NM1
  29  Q(I,J)=AKV*QS(I,J)+(1-AKV)*Q(I,J)
      DO 129 I=KR,MM1
      DO 129 J=2,NM1
```

```
  129   Q(I,J)=AKV*QS(I,J)+(1-AKV)*Q(I,J)
        EFF=0.
        EQQ=0.
        DO 30 I=2,LL
        DO 30 J=2,NM1
        EEEFF=F(I,J)+0.00001
        EEEQQ=Q(I,J)+0.00001
        EFF=DMAX1(EFF,DABS((F(I,J)-FS(I,J))/EEEFF))
  30    EQQ=DMAX1(EQQ,DABS((Q(I,J)-QS(I,J))/EEEQQ))
        DO 31 I=L,K
        DO 31 J=MA1,NM1
        EEEFF=F(I,J)+0.00001
        EEEQQ=Q(I,J)+0.00001
        EFF=DMAX1(EFF,DABS((F(I,J)-FS(I,J))/EEEFF))
   31   EQQ=DMAX1(EQQ,DABS((Q(I,J)-QS(I,J))/EEEQQ))
        DO 131 I=KR,MM1
        DO 131 J=2,NM1
        EEEFF=F(I,J)+0.00001
        EEEQQ=Q(I,J)+0.00001
        EFF=DMAX1(EFF,DABS((F(I,J)-FS(I,J))/EEEFF))
  131   EQQ=DMAX1(EQQ,DABS((Q(I,J)-QS(I,J))/EEEQQ))
C       CHECK OUTER ITERATION FOR CONVERGENCE
C       -------------------------------------
        ETA=0.000001
        IF((EFF.LE.ETA).AND.(EQQ.LE.ETA)) GO TO 105
        IF(ITER.GT.ITMAX) GO TO 205
        DO 32 I=2,LL
        DO 32 J=2,NM1
        FS(I,J)=F(I,J)
   32   QS(I,J)=Q(I,J)
        DO 33 I=L,K
        DO 33 J=MA1,NM1
        FS(I,J)=F(I,J)
   33   QS(I,J)=Q(I,J)
        DO 133 I=KR,MM1
        DO 133 J=2,NM1
        FS(I,J)=F(I,J)
  133   QS(I,J)=Q(I,J)
        GO TO 300
C       END OF OUTER ITERATION
C       ----------------------
C       COMPUTE STREAMWISE VELOCITY
C       ***************************
  105   DO 38 I=2,LL
        DO 38 J=2,NM1
  38    U(I,J)=(F(I,J+1)-F(I,J-1))/(2.*H)
        DO 39 I=L,K
        DO 39 J=MA1,NM1
  39    U(I,J)=(F(I,J+1)-F(I,J-1))/(2.*H)
        DO 139 I=KR,MM1
```

```
      DO 139 J=2,NM1
139   U(I,J)=(F(I,J+1)-F(I,J-1))/(2.*H)
      WRITE(1,666)ITER,EFF,EQQ,RE
666   FORMAT(10X,'NO. OF ITER.=',I5,10X,'EFF=',E14.7
     2,10X,'EQQ=',E14.7,10X,'RE=',F10.2//)
      WRITE(1,170)
170   FORMAT(15X,'VELOCITY  DISTRIBUTION ')
      DO 445 I=2,LL
445   WRITE(1,446)(U(I,J),J=2,NM1)
446   FORMAT(1X,'U(I,J)=',10F10.3//)
      DO 447 I=L,K
447   WRITE(1,448)(U(I,J),J=MA1,NM1)
448   FORMAT(1X,'U(I,J)=',10F10.4//)
      DO 449 I=KR,MM1
449   WRITE(1,450)(U(I,J),J=2,NM1)
450   FORMAT(1X,'U(I,J)=',10F10.3//)
      WRITE(1,180)
180   FORMAT(10X,' STREAM FUNCTION VALUES'/)
      DO 620 I=2,LL
620   WRITE(1,621)(F(I,J),J=2,N)
621   FORMAT(1X,'F(I,J)=',10F10.6//)
      DO 622 I=L,K
622   WRITE(1,623)(F(I,J),J=MA,N)
623   FORMAT(1X,'F (I,J)=',11F9.6//)
      DO 664 I=KR,M
664   WRITE(1,665)(F(I,J),J=2,N)
665   FORMAT(1X,'F(I,J)=',10F10.6//)
      WRITE(1,190)
190   FORMAT(10X,'VORTICITY VALUES'/)
      DO 533 I=1,LL
533   WRITE(1,681)(Q(I,J),J=1,N)
681   FORMAT(1X,'Q(I,J)=',10F10.3//)
      DO 535 I=L,K
535   WRITE(1,536)(Q(I,J),J=MA,N)
536   FORMAT(1X,'Q(I,J)=',11F9.3//)
      DO 537 I=KR,M
537   WRITE(1,538)(Q(I,J),J=1,N)
538   FORMAT(1X,'Q(I,J)=',10F10.3)
      GO TO 333
999   WRITE(1,555)
555   FORMAT('POISSON EQUATION PROBLEM')
      GO TO 333
998   WRITE(1,656)
656   FORMAT('NAVIER-STOKES EQUATIONS PROBLEM')
205   WRITE(1,767)
767   FORMAT(10X,'OUTER ITERATION PROBLEM')
      CLOSE(UNIT=2)
333   CLOSE(UNIT=1)
      STOP
      END
```